Three Generations, One Future: A Systematic Analysis on Nicotine's Effect across generations in *C. elegans*.

by

Faten Ahmad Taki

July, 2013

Director of Thesis: Dr. Baohong Zhang

Department of Biology

Tobacco smoking is a worldwide epidemic that is responsible for diseases and death rates that surpass those attributed to a combination of other causes (e.g. cancer, HIV, accidents). A major mediator of tobacco-smoke related negative consequences is nicotine. Nicotine is an addictive poison that entraps users in a vicious cycle of constant drug seeking and reinforcement. Despite the public health policies and laws enforced to decrease the habitual smoking, it is still prevalent, especially among adolescents. According to WHO, 40% of children and up to 60% of teenagers are passively and actively exposed to tobacco smoke. Early life stages are more vulnerable and sensitive to environmental and life experienced stresses. At that stage, stresses can have enduring effects that not only persist until adulthood, but are also inherited to the subsequent generations. With respect to nicotine, a wealth of studies have investigated the dose and time-dependent effects of this chemical on multiple systems including cell lines and model organisms. However, the transgenerational effect of nicotine exposed during post-embryonic stages has not been reported. On the molecular level, an increasing number of popular findings that show the involvements of certain microRNAs in physiological processes have expanded to

include response to nicotine. Nevertheless, a systematic profiling of microRNA expression levels is yet to be determined. In our study, we employed *C. elegans* as our model to investigate the transgenerational effect of nicotine exposure limited to the post-embryonic larval stages of the parent F0 generation. Two concentrations (20µM and 20mM) were chosen based on previous studies. We investigated the effect of nicotine on the behavior of L4 *C. elegans* (N2) across three generations (F0, F1, and F2). Here we report that nicotine altered the sinusoidal locomotion, body bends, and forward and backward speeds across three generations. Such represented an enduring and heritable addiction initiated by parental post-embryonic nicotine exposure. In addition our qRT-PCR results showed that direct nicotine exposure throughout the larval stages (30 hours), altered the systematic miRNA expression profiles in L4 *C. elegans* in a dose-dependent manner. Through target prediction analyses coupled with background research, fos-1 was predicted to be a key mediator of the addiction-like behavior in *C. elegans* larvae. Conclusively, our results offer novel insights on the sensitivity of early developmental stages to nicotine exposure. The behavioral transgenerational effect as well as the parental altered miRNA profiles will set the basis for future miRNA transgenerational analyses coupled with target and pathway validation. With this in mind, the need for suitable reference genes for normalization and reliable interpretations is necessary. We dedicated our last objective to identify reference gene candidates to serve this purpose. Based on results from five statistical approaches (geNorm, NormFinder, BestKeeper, dCt method, and RefFinder), we report that the expression levels of tba-1 and cdc-42 were the most stable among all of sixteen compiled genes. Taken together, our work is preliminary for a new research direction concerned with nicotine that would help support public health policies and awareness campaigns to further stress on the risks and dangers of tobacco addiction.

Title

A Thesis presented to

The Faculty of Department of Biology

East Carolina University

In Partial Fulfillment

of the Requirements for the Degree

Masters of Science in Molecular Biology and Biotechnology

by

Faten Ahmad Taki

July, 2013

Title: Three Generations, One Future: A Systematic Analysis on Nicotine's Effect across generations in *C. elegans*.

By

Faten A. Taki

APPROVED BY:

DIRECTOR OF THESIS: ----------

Baohong Zhang, PhD

COMMITTEE MEMBER: ----------

Xiaoping Pan, PhD

COMMITTEE MEMBER: ----------

Mary Farwell, PhD

COMMITTEE MEMBER: ----------

Shouquan Huo, PhD

CHAIR OF DEPARTMENT OF BIOLOGY: ----------

Jeff McKinnon, PhD

DEAN OF THE GRADYATE SCHOOL: ----------

Paul J. Gemperline, PhD

DEDICATION

I dedicate this thesis to the memory of my beloved aunt ‘عمہ تو’ Nadia Taki. Despite being thousands of miles away, she made sure I felt her sincere love and *dua*. I love and miss her a lot and she will always be with me no matter where I am.

ACKNOWLEDGEMENTS

I wish I was a better writer to be able to really express my upmost appreciation and respect to my advisor Dr. Baohong Zhang for all his support and true mentorship. Mainly, stress or pressure was never the trigger to do more work, but it was always his encouragement and confidence that triggered me to be more productive. With his eclectic research skills, hard work and commitment, Dr. Zhang helped me learn how to conduct research and to understand the importance of patience and "trial and error" to progress in the field. These two years have been a transforming experience for me. This is mainly attributed to the many opportunities introduced to me by Dr. Zhang. I have been and will be lucky to be a member of his lab, and I look forward to continue my research under his supervision for my Phd studies.

Special thanks to my committee members Dr. Pan, Dr. Farwell and Dr. Huo for all their support and advice. Without their help, my thesis would not have been finalized. Their suggestions, experiences and scientific perspective have been the basis of wonderful ideas not only for my current thesis, but also for more future research approaches and plans. For these points and more, I am very thankful to having them on my committee.

My lab members, who are also my close friends, have been a source of great support, help, laughter and joy for me throughout this process. A whole-hearted thank you goes to Fuliang Xie, Yanqiong Zhang, Brandon Winfrey, Dorothy Dobbins, Hongmei Wu and Ryan Polli. I am very happy to be part of this group, I wish them all the very best with their bright futures, and truly hope that our team spirit remains a part of our next life stages.

My sincere gratitude goes to the Fulbright program funded by the US DOS. Research and graduate school were and would have remained only a dream to me. Being a part of the Graduate School at ECU sparked enthusiasm in me to have more academic, research, and cultural experiences and aspirations. Complimentarily, Fulbright helped me realize that they are not impossible…

Perhaps the acknowledgements for my mom and dad Lana and Ahmad Taki and my family need a chapter by itself. In spite of their worries, their unlimited love coupled with their ability to give me freedom to take my own decisions and go after my dreams even when I was much younger, will always be cherished by me. I hope I grow up to be as wonderful as they are to their family, friends, and community.

الحمدلله Always…

TABLE OF CONTENTS

LIST OF TABLES

LIST OF FIGURES

LIST OF ABBREVIATIONS

ACR (acr-5; acr-15)	AcetylCholine Receptor
Ago	Argonaute
AGS	Gastric carcinoma cell sublines
AVA	Ventral cord interneuron
AVB	Ventral cord interneuron
AVD	Ventral cord interneuron
AVE	Ventral cord interneuron
BBB	Blood Brain Barrier
C. elegans	Caenorhabditis elegans
cDNA	Complementary DNA
Ct	Threshold cycle (Ct) values
DAVID	Database for Annotation, Visualization and Integrated Discovery
DGCR8	DiGeorge syndrome critical region gene 8
dNTP	Deoxyribonucleotide triphosphates
EDD	E3 isolated by differential display (Ubiquitin-ligase)
eIF4E	Eukaryotic translation initiation factor 4E
eIF6	Eukaryotic translation initiation factor 6
eRF3	Eukaryotic polypeptide chain release factor
GOrilla	Gene Ontology enRIchment anaLysis and visuaLizAtion tool
GW182	Protein family with multiple glycine–tryptophan repeats (GW repeats)
MeV	MultiExperiment Viewer
MFC	Mean Fold Change
MID	Middle
mir/ miR	MicroRNA
miRNA*	“passenger strand” (read miRNA star)
OP50	Uracil auxotroph E. coli strain which has limited growth on NGM plates.
ORF	Open Reading Frame
PABC	A peptide-binding domain on the C terminus of PABPs
PABP	Poly(A)-binding proteins
PAIP1	Polyadenylate-binding protein-interacting protein 1
PAIP2	PABP-interacting protein 2
PAN	Poly-A nuclease
PAZ	Piwi-Argonaute-Zwilli
PC12	Cell line derived from a pheochromocytoma of the rat adrenal medulla
PDLSC	Multipotent stem cells derived from periodontal ligaments
PVC	Ventral cord interneuron
qRT-PCR	Quantitative real time polymerase chain reaction
RISC	RNA-induced Silencing Complex
RIV	Ring interneuron
SD	Standard deviation
SMB	Ring motor neuron/interneuron
SMD	Ring motor neuron/interneuron
SPSS	Statistical Package for the Social Sciences

TFI	Tobacco free initiative
TOP	Transducer of ERBB2
TRBP	TAR RNA-binding protein
TRPC	TRP (transient receptor potential) channel family
UTR	Untranslated region
WHO	World Health Organization

LIST OF RECIPES

Protocol and Recipes for *C. elegans* Research (Adapted from (Stiernagle 2006))

NGM agar	Final Volume (1L)
NaCl	3g
Peptone	2.5g
Agar	17g
Distilled water	975ml
Autoclave at 121oC for 20 minutes	
Cool till 55^{o}C	
Cholesterol (5mg/ml)	1ml
CaCl2 (1M)	1ml
MgSo4 (1M)	1ml
Potassium Phosphate (1M)	25ml
Mix well and pour into petri plates	

M9	Final Volume (1L)
NaHPO4.7H2O	11.32g
KH2PO4	3g
NaCl	5g
MgSO4.7H2)	0.25g
Distilled water	up to 1L
Autoclave	

CaCl2(1M)	Final Volume (100ml)
CaCl2.2H2O	14.7g
Distilled water	up to 100ml
Autoclave	

MgSO4(1M)	Final Volume (100ml)
MgSO4.7H2O	24.6g
Distilled water	up to 100ml
Autoclave	

Potassium phosphate (1M)	Final volume (1L)
KH2PO4(1M)	118.3g
K2HPO4(1M)	23g
Distilled water	up to 1L
Autoclave	

Cholesterol solution	Final Volume (10ml)
Cholesterol	50mg
Ethyl alcohol	10ml

Synchronization solution	Final volume (25ml)
Water	17.5ml
NaOH(5M)	2.5ml
Chlorox bleach	5ml

The bleach is always added last. The synchronization solution was always prepared freshly before use

Luria Broth (LB)	Final volume (1L)
Tryptone	10g
Yeast extract	5g
NaCl	5g
Distilled water	up to 1L

Autoclave
Cool down before OP50 inoculation

OP50 stock (food)

- Inoculate prepared 300ml LB medium with 1 OP50 frozen pellet.
- Incubate on shaker for 12-24 hours at 37^{o}C.
- Transfer 10ml of OP50 solution into a 15ml falcon tube.
- Spin for 20 minutes at 3000 rpm.
- Discard supernatant and store the OP50 pellet in 20^{o}C as food stock.
- Before use, dilute with M9 buffer and measure bacterial concentration using spectrophotometer (Thermoscientific) at λ=600nm for final Absorbance value=2

Stiernagle, T.

2006 Maintenance of *C. elegans*. WormBook, ed. The *C. elegans* Research Community.

Chapter 1: Overview on Nicotine, *C. elegans*, and MicroRNAs

Nicotine

Tobacco Smoking: a global habit

Efforts to set policies (e.g. TFI: tobacco free initiative) to optimize human health conditions have been continuously adopted to reduce and prevent diseases and health deterioration. According to WHO, tobacco-smoking is responsible for the death of nearly 6 million individuals per year. This group represents half of the tobacco-exposed individuals, 600,000 of which are second-hand smokers. As reported by CDC, the weight of the dangers of tobacco-smoking can be underscored by the death percentage that overrides deaths caused by HIV, alcohol, illegal drugs, murders, suicide, and vehicle-related injuries, combined (CDC 2000–2004). Of the facts listed by WHO, the circle of second-hand smoking includes about 40% of children at home, a situation that doubles the likelihood of them growing up to be smokers. Unfortunately, tobacco smoking negatively affects every organ. The consequential health deterioration (e.g. cardiovascular, respiratory and reproductive diseases, cancer) and premature death constitutes a major economic burden as productivity decreases (USDHHS 2004). Among the 4000 chemicals that constitute tobacco, we will focus on nicotine as it is of the major contributors to tobacco's effects.

Nicotine chemistry and mechanism of action

The pharmacological activity of nicotine from tobacco is not limited to its S-potent form. It peaks at the end of a cigarette smoking and is distributed in the human body within 20 minutes to reach tissues and organs (e.g. lungs, brain (with high efficiency), liver, kidney, spleen, skeletal muscle, placenta, amniotic fluid). With blood PH of about 7.4, nicotine is both ionized, non-

ionized (membrane permeable), and bound to plasma proteins (Benowitz 1988; Matta, et al. 2007). In humans, nicotine is primarily metabolized by the liver CYP2A6. As a result, its half-life varies from two to eight hours depending on the smoking regularity with elimination time increasing even more (20 hours) in chronic heavy smokers.

Nicotine is known to be psychoactive. Consequently, its target cells include, but are not restricted to, the mesolimbic reward pathways (Wada, et al. 1989). Nicotine-induced effects are complex as they appear to be dose-dependent, but not monotonic. A biphasic response has been reported where lower doses caused stimulation, while higher doses were associated with a depressant-like effect on the nervous system (Benowitz 1988) (Table 1.1; Figure 1.1). Nicotine generally binds to nicotinic AchR (ligand gated ion channels). The general model includes sensitization of the latter receptors after acute nicotine treatment, followed by desensitization after prolonged exposure. Depending on the cell type, the response to chronic nicotine treatment involves a decrease or increase in the concentration of these receptors resulting from the transcriptional or post-transcriptional modifications (Changeux 1991; Peng, et al. 1994; Waggoner, et al. 2000). The acetylcholine receptors will shift from resting, to short-term desensitized, to long-term inactivated states. The rate of becoming sensitized again depends on the receptor and the nicotine concentration. Generally, as the nicotine concentration decreases (after abstinence), the more receptors will become sensitized again. The more the receptors are altered on the surface of a variety of cells, which include but are not restricted to the brain reward system, the more the nicotine is needed for satisfaction from the pathological status (Dani and Heinemann 1996) (Figure 1.2). Such background information was used to form a basis for our hypothetical model to explain the phenotype observed in L4 N2 worms as a result of nicotine treatment as will be seen in the results section.

Nicotine addiction is a complex trait that is mediated by several factors (e.g. environment, genetics) (CDC 2010). Addiction is considered a maladaptive form of neuroplasticity (Sartor, et al. 2012). The fastest route to attain high nicotine blood peaks is through inhalation (e.g. cigarette smoke) (Benowitz 1988). Then, within 8-10 seconds, high nicotine arterial levels reach the brain (Matta, et al. 2007). This relatively easy route of administration only inflates the proportion of individuals affected. Several criteria act as a prerequisite for addictive behavior, but we focused on two extrapolatable features that are mostly relevant to -and were observed in- the behavior of our model organism. One state is known as "tolerance" and can be described as desensitization and adaptation to the stressor (i.e. nicotine), in which the initial repetitive dose produces a lesser effect (e.g. ligand concentration at the receptor site). A more reliable index of addiction is the "withdrawal" (CDC 2010; Shiffman 1989), whose symptoms are similar to those resulting from the chemical-induced chronic toxicity, possibly persisting even after its removal. Therefore, "withdrawal"-related phenotypes should be interpreted with caution to avoid analytical confounds (Mitchell, et al. 2010). Meanwhile, other addiction-related behaviors are usually tested in higher organism such as the ability of the chemical (e.g. nicotine) to cause positive (pleasurable effects) or negative (reduction of withdrawal symptoms) reinforcement. Such remains relatively ambiguous in the case of nicotine (Benowitz 1988; CDC 2010) and are less likely to be easily modeled by *C. elegans*.

***Caenorhabditis elegans*: a biological model**

It was only 60 years from *C. elegans*'s isolation that its appreciation as a biological model was established (Brenner 1974; Maupus 1990). The latter is attributed to its ease of maintenance with *E.coli* (OP50) as food source on temperatures ranging between 15 and 25^{o}C in

liquid or on solid media (Brenner 1974; Wilson , et al. 2010). Its short generation time of 2-3 days at 20^{o}C and lifecycle of 2-3 weeks (Figure 1.3) makes it relatively convenient for lifespan as well as trans-generational studies. To reach adulthood, the embryo has to pass through four larval stages, the second (L2) of which can be interrupted by stressful conditions (e.g. starvation, overcrowding) (Altun and Hall 2009). The worm enters a resistant dauer stage which can live to several months and returns to L4 following favorable conditions. "Deceptively simple, but simply deceptive" -a term used by Gruber et al. (Gruber, et al. 2009)- is a suitable description of a simple multicellular transparent organism that allows ethical investigations from cellular (e.g. apoptosis) (Kirienko, et al. 2010; Kokel, et al. 2006) to holistic organism level phenomena (e.g. ageing) (Greer, et al. 2011; Hamilton, et al. 2005). Interestingly, normally arising from a 0.1-0.2% mutation rate (Ward and Carrel 1979), the males -distinguished by their fan shaped tail (Emmons 2005)- can be further induced and are useful for genetic cross-linking experiments (McGraw-Hill-Higher-Education 2011). The number of offsprings produced by a self -fertile hermaphrodite increases from 300 to 1000 in case of mating (Riddle, et al. 1997).

C. elegans is ideal for biotechnological manipulations (fluorescence-tags) which can be visualized by a simple microscope, high-throughput drug design (Geary and Thompson 2001; Giacomotto and Segalat 2010; Kaletta and Hengartner 2006; Markaki and Tavernarakis 2010) as well as research in cancer (Kirienko, et al. 2010) and other diseases like Alzheimer's, and Huntington (Ewald and Li 2009; Kaletta and Hengartner 2006; Siddiqui, et al. 2008; Voisine, et al. 2007). In order to understand certain phenotypes, critical pathways and mechanisms (Hulme and Whitesides 2011; Schulz, et al. 2007), researchers took advantage of the worm's anatomy, its differentiated tissue (e.g. neurons, muscles) as well as its fully sequenced 100 MB genome. The latter shares 80% homology with the human genome (e.g. CEP-1/p53, let-60/RAS (Beitel, et al.

1990) (Lai, et al. 2000; Pinkston, et al. 2006; Sonnhammer and Durbin 1997), but at the same time has less redundancies in coding and noncoding genes (Consortium 1998; Kazazian 2004). This allowed extrapolations to be done with relative ease as will be further discussed in the following paragraphs.

As for the toxicological and biomedical fields, *C. elegans* has a lot to offer. It has been used to test and study the mechanism of action of many chemicals, heavy metals and drugs (Kaletta and Hengartner 2006; Leung, et al. 2008; Markaki and Tavernarakis 2010; Mitchell, et al. 2010; Wang and Xing 2008). Its contributions extended to include neuroscience. Among the 959 cells, the *C. elegans* adult hermaphrodite has 302 (one third) of which are neurons, 20 of which are pharyngeal, 32 (10%) of which are involved in chemosensation, and the rest being somatic (Hart and Chao 2010). The command interneurons (AVA, AVB, AVD, AVE, and PVC) act as mediators. They perceive the signal from the chemosensory neurons, transmit it to the motor neurons, and therefore allow the control body muscle contraction (Von Stetina, et al. 2006). As shown by Leung et al. (Leung, et al. 2008), neurostudies on *C. elegans* offer an in depth analysis down to a single-neuron resolution. This is based on delineated systems, including but not restricted to the nervous system (Brenner 1974; Sulston 1983; Sulston, et al. 1983; White, et al. 1986) coupled with technologies allowing single cell laser ablation (Feng, et al. 2006) and is promoted by the relative ease of establishing mutant strains (Antoshechkin and Sternberg 2007). The worm's simple nervous system includes features conserved and common to higher organisms neurotransmitters (acetylcholine, serotonin, dopamine, glutamate, gamma-aminobutyric acid, octopamine, tyramine) (Leung, et al. 2008; Loer 2010) as well as other proteins that play a major role in neuro-signaling (e.g. 29 AchR subunits) (Jones, et al. 2007). Consequentially, an observable phenotype is reflective of the net inner interactions and

processes, a relationship that is often used by researchers when attempting to understand the mechanism of action of treated chemicals or particular environmental conditions.

In our study, we took advantage of the behavior of the worms. *C. elegans*'s locomotion is a result of rhythmic undulatory movements. The simple anatomy coupled with its well defined nervous system allows the study of neural circuits in response to different conditions. Briefly, the worms' locomotion is dependent on the motor circuitry that triggers sinusoidal waves. The latter drives alternating muscle excitation/relaxation along the dorso-ventral axes. Consequently, the worms move forward or backward as a result of posteriorly or anteriorly-directed-wave-propagation, respectively. The AVA and AVD command interneurons drive backward movement (reversals), while the PVC and AVB neurons drive the forward movement. An example of the complexity provided by this system is the movement decision. The latter is not restricted to the interaction of these distinct inter-neural circuits, but also is due to the involvement of each circuit in the regulation of the opposing movement (Chalfie, et al. 1985; Von Stetina, et al. 2006; Zheng, et al. 1999). All of the above details provide a rationale for selecting *C. elegans* as our ideal simple organism to study complex nicotine-associated behavior and molecular alterations.

Nicotine and *C. elegans*

In *C. elegans*, nicotine alters some behavior such as egg laying, pharyngeal pumping, muscle contraction, and male spicule ejection (Matta, et al. 2007). In addition, the emergence of *C. elegans* as a model for nicotine addiction was also reported (Feng, et al. 2006). In fact, depending on the experimental design for nicotine treatment, *C. elegans* exhibited acute response, tolerance, withdrawal, and sensitization (Feng, et al. 2006). Unlike other models (e.g.

rats), the half-life of nicotine in *C. elegans* is not known. Therefore, nicotine is constantly, rather than intermittently, supplied during the experimental period. In addition, the presence of a cuticle acts as a barrier to many chemicals. Based on the previous reports, it is assumed that the internal concentration of any chemical is much less than the supplied dose (Matta, et al. 2007). Accordingly, all of the mentioned points were taken into account when designing our experimental methods and material for optimal investigations on the behavioral level, complimented by molecular assays mainly focusing on, but not restricted to, our main area of interest: miRNAs.

MicroRNAs

Introduction to epigenetics and miRNA

The genome encodes all physiological functions, but its expression is tightly regulated in response to a network of factors. Extensive research has been devoted to dissect the factors involved in gene regulation and has provided clues concerned with the environmental contribution in shaping physiological phenotypes. Interestingly, such environmentally-induced changes are mainly mediated by diverse epigenetic processes which in most cases result in heritable changes that do not involve changes in the DNA (Bird 2007; Goldberg, et al. 2007). Recently, epigenetics has been considered to be the link between the environment and the genome that contribute to emergent cellular processes. As mentioned before, we are mainly interested in one of the epigenetic regulators known as miRNAs (Zhang and Ho 2011).

In the last decade, the discovery of a master gene regulator emerged. It was in 1993 in *C. elegans* that lin-4 was involved in regulation via an RNA-RNA antisense interaction (Lee, et al. 1993). Afterwards, miRNAs were ubiquitously discovered in all eukaryotic organisms (He and

Hannon 2004). Over 200 and 1000 miRNAs have been discovered in *C. elegans* and Humans, respectively. Initially reported to control the developmental timing in *C. elegans* (Ambros 1989), their roles extended to diverse physiological and pathophysiological processes (Ambros 2003; Aukerman and Sakai 2003; Chen, et al. 2004; Kim 2005; McManus 2003).

Definition and occurrence

MicroRNAs are conserved non-coding regulatory RNAs found in Eukaryotes (Carthew and Sontheimer 2009). They are expressed in a tissue and temporal specific manner. When expressed, they exist in relatively high copy number (Bartel 2004). They are transcribed either from intergenic (more common in plants) or intragenic regions (Shabalina and Koonin 2008). The regulation of miRNA transcription has not yet been clearly described (Sato, et al. 2011). When found intragenically, they are usually transcribed from the promoter of the gene they reside within (Sato, et al. 2011). Other miRNAs can be found within introns and possibly regulated by their own independent promoter (Toyota, et al. 2008). miRNAs can be found within clusters (mostly in animals) (Shabalina and Koonin 2008) leading to the production of a polycistronic transcript (Bartel 2004). However, individual miRNAs within clusters have been documented to be regulated individually as well (Saito, et al. 2006). On the other hand, the biogenesis of the miRNAs has been moderately studied and will be discussed in the following paragraph.

MicroRNA biogenesis

Two biogenesis pathways have been reported. A less common pathway depends on pri-miRNA splicing (O'Carroll and Schaefer 2013; Okamura, et al. 2007) which will give rise to mirtrons. On the other hand, the main biogenesis pathway involves transcription mainly via RNA

polymerase II (III) (Bartel 2004). The transcribed pri-miRNA is capped, possibly polyadenylated (Kim 2005; Ohler, et al. 2004) and has one or more stems, each of about 33 imperfectly paired bases. The stem is bordered by a loop to form a stem-loop structure that is flanked by single stranded regions (Bartel 2004). In the nucleus, the processing is stepwise and initially involves the cleavage of the flanking regions of pri-miRNA by an RNase III called Drosha (Kim 2005) to give rise to double stranded pre-miRNAs. Then, the pre-miRNA will be exported out of the nucleus to the cytoplasm by exportin 5 and Ran-GTP (Bartel 2004) and will be processed by another RNase III known as Dicer (Kim 2005). In plants, Dicer (Dcl-1) mediates both the first and second processing steps in the nucleus after which the miRNA duplex is transported to the cytoplasm (Bartel 2004; Kim 2005). Therefore, Dicer substitutes for both Dicer and Drosha in plants. Cooperatively, Dicer with other regulatory proteins will then cleave pre-miRNA to a miRNA: miRNA* duplex with imperfect complementarity (Carthew and Sontheimer 2009). The duplex will be loaded onto a trimeric complex: Dicer, Ago and TRBP (Hornbeck, et al. 2012). Afterwards, the guide strand will be incorporated to RISC complex while the other passenger strand is discarded. The selection of the guide strand is not restricted to the one with the less stable 5' end (Okamura, et al. 2008; Tomari and Zamore 2005). As its name implies, the guide strand directs the silencing complex to the target sequence. Recognition of the target sequence is generally at the 3' UTR, and is based on a seed sequence (nucleotides: 2-8 in the miRNA) (Carthew and Sontheimer 2009). Reasonably, downstream of the biogenesis pathway, the miRNAs' state and interactions mediate gene regulation (Figure 1.5).

MicroRNA's role in gene regulation

Two major pathways have been hypothesized to describe miRNAs modes of actions. The first is by mRNA cleavage and is more common in plants as a result of the relatively higher degrees of complementarity between miRNA-mRNA target ORF (Bartel 2004; Shabalina and Koonin 2008). In animals, it appears that the default silencing mechanism is translational repression (Shabalina and Koonin 2008). Silencing depends primarily on RISC (i.e. RNA-Induced Silencing Complex) which is formed from Argonaute proteins complexed with several factors, mainly GW182 proteins (Jakymiw, et al. 2005; Liu, et al. 2005).

The Argonaute proteins are a universal and conserved family of proteins with major active roles in the miRNA-mediated gene silencing. They have a bilobal structure with an N-terminal and PAZ (Piwi-Argonaute-Zwilli) domains on one side, and MID (Middle) and PIWI domains on the other end. Some species (e.g. humans) might have more than one type of argonautes, a few of which are characterized by endonucleolytic activity. Also known as slicer, those argonaute proteins interact through their MID domain with the sugar-phosphate backbone of the associated miRNA. Thus, the bases are free to bind to the target mRNAs (Ender and Meister 2010).

Another crucial component of the silencing machinery are the GW182 proteins (i.e. AIN-1 and AIN-2 in *C. elegans*). GW182 binds to AGO through more than one domain (i.e. NED, and silencing domain). In addition, GW182 interacts with the PABC domains found on PABP and EDD (E3 ubiquitin ligase identified by differential display) and acts as a docking site for deadenylase complexes. PABP interacts with a group of players such as PAIP1, PAIP2, and eRF3 to promote translational activation, repression and termination, respectively. Together with

TOP (Transducer of ERBB2) or PAN (poly-A nuclease), PABP also affects mRNA deadenylation and decay. EDD on the other hand associates with other silencing effectors. Thus, GW182 provide a platform for the association of a myriad of proteins with context-dependent functions mainly in target translational regulation (Fabian and Sonenberg 2012). Possibilities of the latter to occur at or post translational initiation have been reported (Ding and Grosshans 2009; Petersen, et al. 2006).

Conceptually, the interplay between translational repression and mRNA destabilization has been discussed (Fabian and Sonenberg 2012), but dissecting the exact pathway is not trivial. Three major models have been reported to explain the phenomenon. The first was described by a possible competition between RISC members with eIF4E to prevent the recruitment of the translational machinery (Mathonnet, et al. 2007). A second model was described as the RISC-dependent recruitment of eIF6, which usually associates with the 60S ribosomal subunit to prevent its premature binding to the translational machinery. Such would disrupt the sequential events occurring at translation initiation (Chendrimada, et al. 2007; Fabian and Sonenberg 2012). Another way could occur through the deadenylation or decapping of the mRNA which prevents circularization and induces the destabilization of the mRNA (Behm-Ansmant, et al. 2006; Fabian and Sonenberg 2012). All would lead to an increase in the susceptibility of exonuclease-dependent degradation of the target mRNAs (Carthew and Sontheimer 2009).

MicroRNA characteristics

An important miRNA feature is evident in its diversity which more likely arises from mutations in the miRNA sequences within their host transcripts than from sequence duplication events. Then, the regulatory sequences (promoters, enhancers) of the host transcript can be

readily used (Lu, et al. 2008) and contribute to their emergence. To add to the enrichment of miRNA-dependent regulations, it has been reported that one miRNA can target many genes, and one gene can be regulated by many miRNAs (Ritchie, et al. 2009; Wu, et al. 2010).

Despite their diversity, miRNAs are known for their precise ends (Carthew and Sontheimer 2009). Though the cleavage is mediated by RNase III family members (Drosha and Dicer), the precision of the cuts is promoted by the cofactors associated with these ribonucleases or dsRNA binding subunits. Dorsha depends on DGCR8. Together, they form the microprocessor as DGCR8 positions Drosha at the intersection of the single and double strands in the pri-miRNA and allows the cleavage 11 bp away from this point (minimal distance required for its action) (Han, et al. 2006). Dicer on the other hand will bind via its PAZ domain more likely to the 3' overhang situating the RNase III domain 22 nucleotides away. This will consequently lead to the cleavage of a ~ 22 nt miRNA duplex (Kim 2005).

Interestingly, RNAi covers only one side of possible miRNA actions. It seems that its regulatory role is context dependent. miRNAs can have activating roles under certain conditions. For example, let-7 becomes a translational activator in G1 arrested cells (Vasudevan, et al. 2007). Another situation is evident in miR-10a which activates translation when interacting with 5' UTRs while it becomes a repressor once interacting with 3' UTR (Orom, et al. 2008). Interestingly, 3' UTR-binding proteins have the potential to antagonize as well as agonize miRNA-mediated silencing by altering the 3' UTR secondary structure. Thus, accessibility of the small RNAs to their targets would be influenced. Such a mechanism has been described to explain miRNA-associated translational activation. In the latter case, a strong transcription repressor is bound in close proximity to the miRNA binding site. RISC competes with the

repressor for mRNA access and leads to an apparent translational activation if the protein is a stronger repressor than RISC (Brodersen and Voinnet 2009).

Hypothesis

We hypothesize that nicotine exposure during the post-embryonic stage in *C. elegans* is associated with transgenerational behavioral effects. Also, we postulate that nicotine causes systematic alterations in the miRNA profiles in L4 *C. elegans* (N2).

Research Objectives

Our main theme is to explore the transgenerational effect of nicotine treated during the early developmental stages in *C. elegans* N2 hermaphrodites. In order to accomplish our aim, our tactic involved dividing our broad hypothesis into three main objectives presented below. Based on previous publications (Sobkowiak, et al. 2011), two nicotine concentrations of a thousand fold difference (20µM and 20mM) were chosen to test for possible dose-dependent effects (Figure 1.4).

Objective One: To study the effect of nicotine on the behavior of *C. elegans* across three generations (Chapter 2).

As detailed in the methods section, video-recordings were performed on worms belonging to three nicotine treatment groups (i.e. control, 20µM, and 20mM) for three generations. The videos were then analyzed using via WormLab software (MBF). Nine endpoints were chosen for analysis: track distance, wavelength, amplitude, maximum amplitude, forward and backward speeds, reversals, omega bends, and bending angles. Output data were exported to excel files for subsequent descriptive and analytic statistics.

Objective Two: To perform a systemic miRNA expression analysis coupled with target prediction analysis after direct nicotine exposure in L4 *C. elegans* belonging to the F0 generation (Chapter 3).

Recently, accumulating evidence suggests the active role of epigenetic factors in gene regulation in response to environmental conditions. The epigenetic phenomena include non-genetic diverse modifications from DNA and histone methylation to non-coding RNA expression patterns. However, to our knowledge, the effect of nicotine on miRNAs involved in addiction pathways has not been previously studied in *C. elegans*. Both objectives two and three were performed starting with RNA extractions, reverse transcription, and gene expression analysis via qRT-PCR. Finally, target prediction and pathway analysis were done using DAVID and GOrilla software.

Objective Three: To determine suitable reference genes to be used in qRT-PCR normalization for transgenerational studies in *C. elegans* L4 exposed to nicotine (Chapter 4).

Our results from the behavioral and molecular assays provided preliminary and potentially novel insights on nicotine's mechanism of action. Based on the behavioral alterations and the complementary miRNA target predictions, future research will be concerned with investigations on protein target genes of interest. The latter will be performed via qRT-PCR which depends on the proper normalization to avoid false positive conclusions. Thus, we investigated the expression levels of sixteen reference gene candidates by qRT-PCR. The gene list was compiled from previous studies and was used to identify the most stable genes based on five approaches (geNorm, NormFinder, BestKeeper, deltaCt method, and RefFinder). Our objective will therefore contribute to the multi-level integrations to dissect nicotine's mechanism of action on post-embryonic development and its inheritance.

References

Altun, Z.F., and D.H. Hall

2009 Introduction. In WormAtlas. doi:10.3908/wormatlas.1.1.

Ambros, V.

1989 A hierarchy of regulatory genes controls a larva-to-adult developmental switch in *C. elegans*. Cell 57(1):49-57.

—

2003 MicroRNA pathways in flies and worms: growth, death, fat, stress, and timing. Cell 113(6):673-6.

Antoshechkin, I., and P. W. Sternberg

2007 The versatile worm: genetic and genomic resources for Caenorhabditis elegans research. Nat Rev Genet 8(7):518-32.

Aukerman, M. J., and H. Sakai

2003 Regulation of flowering time and floral organ identity by a MicroRNA and its APETALA2-like target genes. Plant Cell 15(11):2730-41.

Bartel, D. P.

2004 MicroRNAs: genomics, biogenesis, mechanism, and function. Cell 116(2):281-97.

Behm-Ansmant, I., et al.

2006 mRNA degradation by miRNAs and GW182 requires both CCR4:NOT deadenylase and DCP1:DCP2 decapping complexes. Genes Dev 20(14):1885-98.

Beitel, G. J., S. G. Clark, and H. R. Horvitz

1990 Caenorhabditis elegans ras gene let-60 acts as a switch in the pathway of vulval induction. Nature 348(6301):503-9.

Benowitz, Neal L.

1988 Pharmacologic Aspects of Cigarette Smoking and Nicotine Addiction. New England Journal of Medicine 319(20):1318-1330.

Bird, A.

2007 Perceptions of epigenetics. Nature 447(7143):396-8.

Brenner, S.

1974 The genetics of Caenorhabditis elegans. Genetics 77(1):71-94.

Brodersen, P., and O. Voinnet

2009 Revisiting the principles of microRNA target recognition and mode of action. Nat Rev Mol Cell Biol 10(2):141-8.

Carthew, R. W., and E. J. Sontheimer

2009 Origins and Mechanisms of miRNAs and siRNAs. Cell 136(4):642-55.

CDC

2000–2004 Annual Smoking-Attributable Mortality, Years of Potential Life Lost, and Productivity Losses—United States, 2000–2004. Morbidity and Mortality Weekly Report 2008;57(45):1226–8 [accessed 2012 August 12].

—

2004 The Health Consequences of Smoking: A Report of the Surgeon General. . Atlanta: U.S. Department of Health and Human Services, Centers for Disease Control

and Prevention, National Center for Chronic Disease Prevention and Health Promotion, Office on Smoking and Health.[accessed 2012 August 12].

—

2010 The Biology and Behavioral Basis for Smoking-Attributable Disease: A Report of the Surgeon General. Atlanta (GA): Centers for Disease Control and Prevention (US). Nicotine Addiction: Past and Present. Centers for Disease Control and Prevention (US); National Center for Chronic Disease Prevention and Health Promotion (US); Office on Smoking and Health (US). How Tobacco Smoke Causes Disease 4.

Chalfie, M., et al.

1985 The neural circuit for touch sensitivity in Caenorhabditis elegans. J Neurosci 5(4):956-64.

Changeux, J. P.

1991 Compartmentalized transcription of acetylcholine receptor genes during motor endplate epigenesis. New Biol 3(5):413-29.

Chen, C. Z., et al.

2004 MicroRNAs modulate hematopoietic lineage differentiation. Science 303(5654):83-6.

Chendrimada, T. P., et al.

2007 MicroRNA silencing through RISC recruitment of eIF6. Nature 447(7146):823-8.

Consortium, The *C. elegans* Sequencing

1998 Genome Sequence of the Nematode *C. elegans*: A Platform for Investigating Biology. Science 282(5396):2012-2018.

Dani, J. A., and S. Heinemann

1996 Molecular and cellular aspects of nicotine abuse. Neuron 16(5):905-8.

Ding, X. C., and H. Grosshans

2009 Repression of *C. elegans* microRNA targets at the initiation level of translation requires GW182 proteins. EMBO J 28(3):213-22.

Emmons, S. W.

2005 Male development. WormBook:1-22.

Ender, C., and G. Meister

2010 Argonaute proteins at a glance. J Cell Sci 123(Pt 11):1819-23.

Ewald, C. Y., and C. Li

2009 Understanding the molecular basis of Alzheimer's disease using a Caenorhabditis elegans model system. Brain Struct Funct 214(2-3):263-83.

Fabian, M. R., and N. Sonenberg

2012 The mechanics of miRNA-mediated gene silencing: a look under the hood of miRISC. Nat Struct Mol Biol 19(6):586-93.

Feng, Z., et al.

2006 A *C. elegans* model of nicotine-dependent behavior: regulation by TRP-family channels. Cell 127(3):621-33.

Geary, T. G., and D. P. Thompson

2001 Caenorhabditis elegans: how good a model for veterinary parasites? Vet Parasitol 101(3-4):371-86.

Giacomotto, J., and L. Segalat

2010 High-throughput screening and small animal models, where are we? Br J Pharmacol 160(2):204-16.

Goldberg, A. D., C. D. Allis, and E. Bernstein
2007 Epigenetics: a landscape takes shape. Cell 128(4):635-8.
Greer, E. L., et al.
2011 Transgenerational epigenetic inheritance of longevity in Caenorhabditis elegans. Nature 479(7373):365-71.
Gruber, J., et al.
2009 Deceptively simple but simply deceptive--Caenorhabditis elegans lifespan studies: considerations for aging and antioxidant effects. FEBS Lett 583(21):3377-87.
Hamilton, B., et al.
2005 A systematic RNAi screen for longevity genes in *C. elegans*. Genes Dev 19(13):1544-55.
Han, J., et al.
2006 Molecular basis for the recognition of primary microRNAs by the Drosha-DGCR8 complex. Cell 125(5):887-901.
Hart, A. C., and M. Y. Chao
2010 From Odors to Behaviors in Caenorhabditis elegans. *In* The Neurobiology of Olfaction. A. Menini, ed. Frontiers in Neuroscience. Boca Raton (FL).
He, L., and G. J. Hannon
2004 MicroRNAs: small RNAs with a big role in gene regulation. Nat Rev Genet 5(7):522-31.
Hornbeck, P. V., et al.
2012 PhosphoSitePlus: a comprehensive resource for investigating the structure and function of experimentally determined post-translational modifications in man and mouse. Nucleic Acids Res 40(Database issue):D261-70.
Hulme, S. E., and G. M. Whitesides
2011 Chemistry and the worm: *Caenorhabditis elegans* as a platform for integrating chemical and biological research. Angew Chem Int Ed Engl 50(21):4774-807.
Jakymiw, A., et al.
2005 Disruption of GW bodies impairs mammalian RNA interference. Nat Cell Biol 7(12):1267-74.
Jones, A. K., et al.
2007 The nicotinic acetylcholine receptor gene family of the nematode Caenorhabditis elegans: an update on nomenclature. Invert Neurosci 7(2):129-31.
Kaletta, T., and M. O. Hengartner
2006 Finding function in novel targets: *C. elegans* as a model organism. Nat Rev Drug Discov 5(5):387-98.
Kazazian, H. H., Jr.
2004 Mobile elements: drivers of genome evolution. Science 303(5664):1626-32.
Kim, V. N.
2005 MicroRNA biogenesis: coordinated cropping and dicing. Nat Rev Mol Cell Biol 6(5):376-85.
Kirienko, N. V., K. Mani, and D. S. Fay
2010 Cancer models in *Caenorhabditis elegans*. Dev Dyn 239(5):1413-48.
Kokel, D., et al.
2006 The nongenotoxic carcinogens naphthalene and para-dichlorobenzene suppress apoptosis in Caenorhabditis elegans. Nat Chem Biol 2(6):338-45.

Lai, C. H., et al.
2000 Identification of novel human genes evolutionarily conserved in Caenorhabditis elegans by comparative proteomics. Genome Res 10(5):703-13.
Lee, R. C., R. L. Feinbaum, and V. Ambros
1993 The *C. elegans* heterochronic gene lin-4 encodes small RNAs with antisense complementarity to lin-14. Cell 75(5):843-54.
Leung, M. C., et al.
2008 Caenorhabditis elegans: an emerging model in biomedical and environmental toxicology. Toxicol Sci 106(1):5-28.
Liu, J., et al.
2005 A role for the P-body component GW182 in microRNA function. Nat Cell Biol 7(12):1261-6.
Loer, C.
2010 Neurotransmitters in Caenorhabditis elegans. WormAtlas.
Lu, J., et al.
2008 The birth and death of microRNA genes in Drosophila. Nat Genet 40(3):351-5.
Markaki, Maria, and Nektarios Tavernarakis
2010 Modeling human diseases in *Caenorhabditis elegans*. Biotechnology Journal 5(12):1261-1276.
Mathonnet, G., et al.
2007 MicroRNA inhibition of translation initiation in vitro by targeting the cap-binding complex eIF4F. Science 317(5845):1764-7.
Matta, S. G., et al.
2007 Guidelines on nicotine dose selection for in vivo research. Psychopharmacology (Berl) 190(3):269-319.
Maupus, E.
1990 Modes et formes de reproduction des nematodes Exp. Gen. 8:463-624.
McGraw-Hill-Higher-Education
2011 Caenorhabditis elegans: Genetic Portrait of a Simple Multicellular Animal. [WWW document] URL: http://highered.mcgraw-hill.com/sites/dl/free/007352526x/387004/Reference_C.pdf.
McManus, M. T.
2003 MicroRNAs and cancer. Semin Cancer Biol 13(4):253-8.
Mitchell, P., et al.
2010 A differential role for neuropeptides in acute and chronic adaptive responses to alcohol: behavioural and genetic analysis in Caenorhabditis elegans. PLoS One 5(5):e10422.
O'Carroll, D., and A. Schaefer
2013 General principals of miRNA biogenesis and regulation in the brain. Neuropsychopharmacology 38(1):39-54.
Ohler, U., et al.
2004 Patterns of flanking sequence conservation and a characteristic upstream motif for microRNA gene identification. RNA 10(9):1309-22.
Okamura, K., et al.
2007 The mirtron pathway generates microRNA-class regulatory RNAs in Drosophila. Cell 130(1):89-100.

Okamura, K., et al.
2008 The regulatory activity of microRNA* species has substantial influence on microRNA and 3' UTR evolution. Nat Struct Mol Biol 15(4):354-63.
Orom, U. A., F. C. Nielsen, and A. H. Lund
2008 MicroRNA-10a binds the 5'UTR of ribosomal protein mRNAs and enhances their translation. Mol Cell 30(4):460-71.
Peng, X., et al.
1994 Nicotine-induced increase in neuronal nicotinic receptors results from a decrease in the rate of receptor turnover. Mol Pharmacol 46(3):523-30.
Petersen, C. P., et al.
2006 Short RNAs repress translation after initiation in mammalian cells. Mol Cell 21(4):533-42.
Pinkston, J. M., et al.
2006 Mutations that increase the life span of *C. elegans* inhibit tumor growth. Science 313(5789):971-5.
Rea, S. L., N. Ventura, and T. E. Johnson
2007 Relationship between mitochondrial electron transport chain dysfunction, development, and life extension in Caenorhabditis elegans. PLoS Biol 5(10):e259.
Riddle, DL, T Blumenthal, and BJ Meyer
1997 *C. elegans* II. 2nd edition. . Cold Spring Harbor (NY): Cold Spring Harbor Laboratory Press Section I(The Biological Model).
Ritchie, William, Stephane Flamant, and John E. J. Rasko
2009 Predicting microRNA targets and functions: traps for the unwary. Nat Meth 6(6):397-398.
Saito, Y., et al.
2006 Specific activation of microRNA-127 with downregulation of the proto-oncogene BCL6 by chromatin-modifying drugs in human cancer cells. Cancer Cell 9(6):435-43.
Sartor, G. C., G. St Laurent, 3rd, and C. Wahlestedt
2012 The Emerging Role of Non-Coding RNAs in Drug Addiction. Front Genet 3:106.
Sato, F., et al.
2011 MicroRNAs and epigenetics. FEBS J 278(10):1598-609.
Schulz, T. J., et al.
2007 Glucose restriction extends Caenorhabditis elegans life span by inducing mitochondrial respiration and increasing oxidative stress. Cell Metab 6(4):280-93.
Shabalina, S. A., and E. V. Koonin
2008 Origins and evolution of eukaryotic RNA interference. Trends Ecol Evol 23(10):578-87.
Shiffman, S.
1989 Tobacco "chippers"--individual differences in tobacco dependence. Psychopharmacology (Berl) 97(4):539-47.
Siddiqui, S. S., et al.
2008 *C. elegans* as a model organism for in vivo screening in cancer: effects of human c-Met in lung cancer affect *C. elegans* vulva phenotypes. Cancer Biol Ther 7(6):856-63.
Sobkowiak, R., M. Kowalski, and A. Lesicki
2011 Concentration- and time-dependent behavioral changes in Caenorhabditis elegans after exposure to nicotine. Pharmacol Biochem Behav 99(3):365-70.

Sonnhammer, E. L., and R. Durbin
1997 Analysis of protein domain families in Caenorhabditis elegans. Genomics 46(2):200-16.
Sulston, J. E.
1983 Neuronal cell lineages in the nematode Caenorhabditis elegans. Cold Spring Harb Symp Quant Biol 48 Pt 2:443-52.
Sulston, J. E., et al.
1983 The embryonic cell lineage of the nematode Caenorhabditis elegans. Dev Biol 100(1):64-119.
Tomari, Y., and P. D. Zamore
2005 Perspective: machines for RNAi. Genes Dev 19(5):517-29.
Toyota, M., et al.
2008 Epigenetic silencing of microRNA-34b/c and B-cell translocation gene 4 is associated with CpG island methylation in colorectal cancer. Cancer Res 68(11):4123-32.
Vasudevan, S., Y. Tong, and J. A. Steitz
2007 Switching from repression to activation: microRNAs can up-regulate translation. Science 318(5858):1931-4.
Voisine, C., et al.
2007 Identification of potential therapeutic drugs for huntington's disease using Caenorhabditis elegans. PLoS One 2(6):e504.
Von Stetina, S. E., M. Treinin, and D. M. Miller, 3rd
2006 The motor circuit. Int Rev Neurobiol 69:125-67.
Wada, E., et al.
1989 Distribution of alpha 2, alpha 3, alpha 4, and beta 2 neuronal nicotinic receptor subunit mRNAs in the central nervous system: a hybridization histochemical study in the rat. J Comp Neurol 284(2):314-35.
Waggoner, L. E., et al.
2000 Long-term nicotine adaptation in Caenorhabditis elegans involves PKC-dependent changes in nicotinic receptor abundance. J Neurosci 20(23):8802-11.
Wang, D., and X. Xing
2008 Assessment of locomotion behavioral defects induced by acute toxicity from heavy metal exposure in nematode Caenorhabditis elegans. J Environ Sci (China) 20(9):1132-7.
Ward, Samuel, and John S. Carrel
1979 Fertilization and sperm competition in the nematodeCaenorhabditis elegans. Developmental Biology 73(2):304-321.
White, J. G., et al.
1986 The structure of the nervous system of the nematode Caenorhabditis elegans. Philos Trans R Soc Lond B Biol Sci 314(1165):1-340.
Wilson , A. M., R. P. Hunt , and A. C. Wolkow
2010 Using *Caenorhabditis elegans* To Study Bioactivities of Natural Products from Small Fruits. *In* Flavor and Health Benefits of Small Fruits. Pp. 227-238. ACS Symposium Series: American Chemical Society.
Wu, S., et al.
2010 Multiple microRNAs modulate p21Cip1/Waf1 expression by directly targeting its 3' untranslated region. Oncogene 29(15):2302-8.

Zhang, X., and S. M. Ho
2011 Epigenetics meets endocrinology. J Mol Endocrinol 46(1):R11-32.
Zheng, Y., et al.
1999 Neuronal control of locomotion in *C. elegans* is modified by a dominant mutation in the GLR-1 ionotropic glutamate receptor. Neuron 24(2):347-61.

Table 1.1: A summary of the documented nicotine-dependent alterations in human physiologies and metabolisms (NIC 1992).

Actions of nicotine in human body physiologies and systems
CNS Arousal or relaxation
Enhanced concentration, vigilance
Appetite suppression
Electroencephalographic changes
Cardiovascular Increased heart rate, cardiac contractility, blood pressure
Cutaneous vasoconstriction
Systemic venoconstriction
Increased muscle blood flow
Catecholamine release
Metabolic lipolysis with fatty acid release
Increased energy expenditure
Endocrine Increased growth hormone
Adrenocorticotrophic hormone/cortisol
Vasopressin
Beta endorphins
Inhibition of prostacyclin synthesis

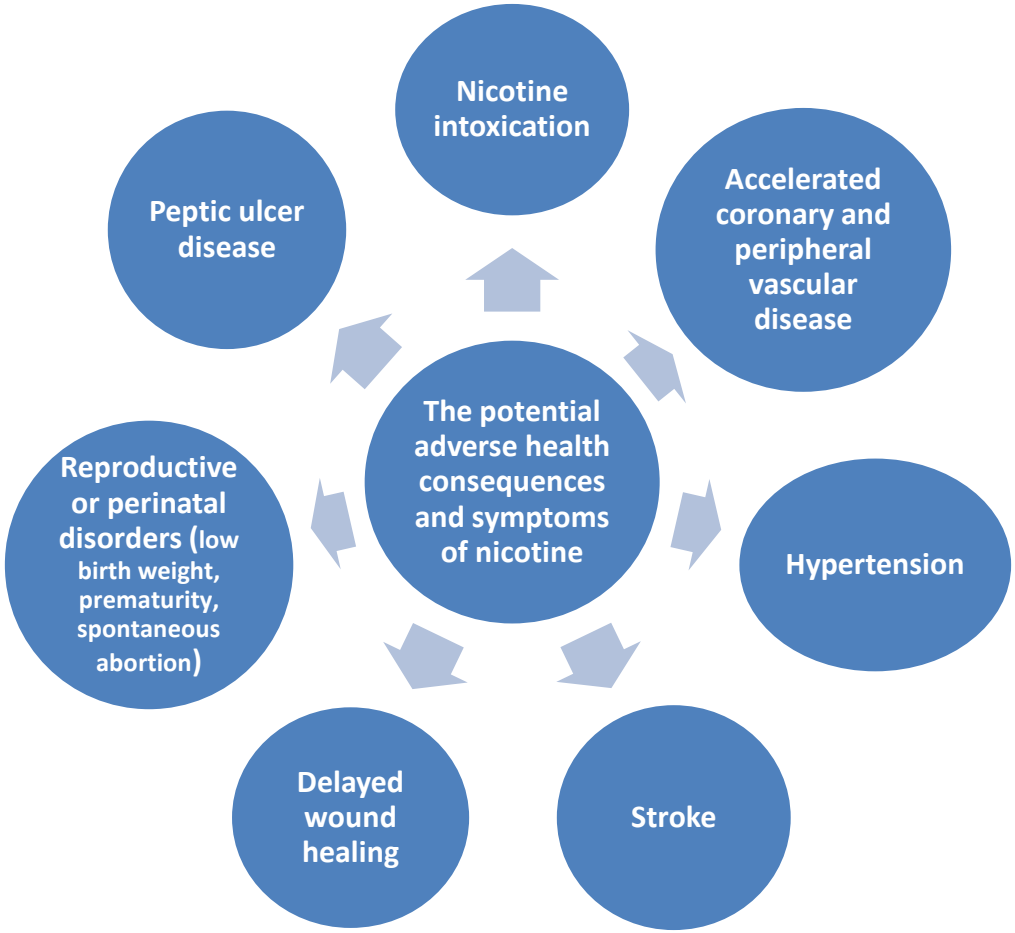

Figure 1.1: A summary of nicotine-associated symptoms in humans (NIC 1992).

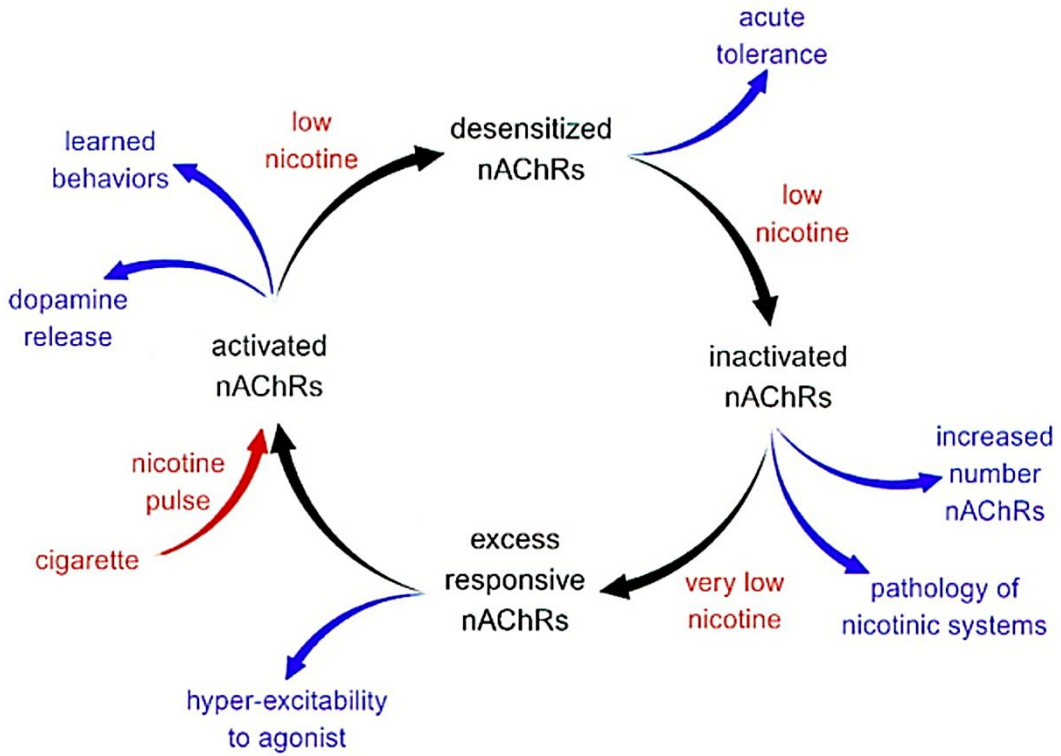

Figure 1.2: A hypothetical model for time and concentration-dependent, differential, nicotine-induced AchR sensitization (Dani and Heinemann 1996).

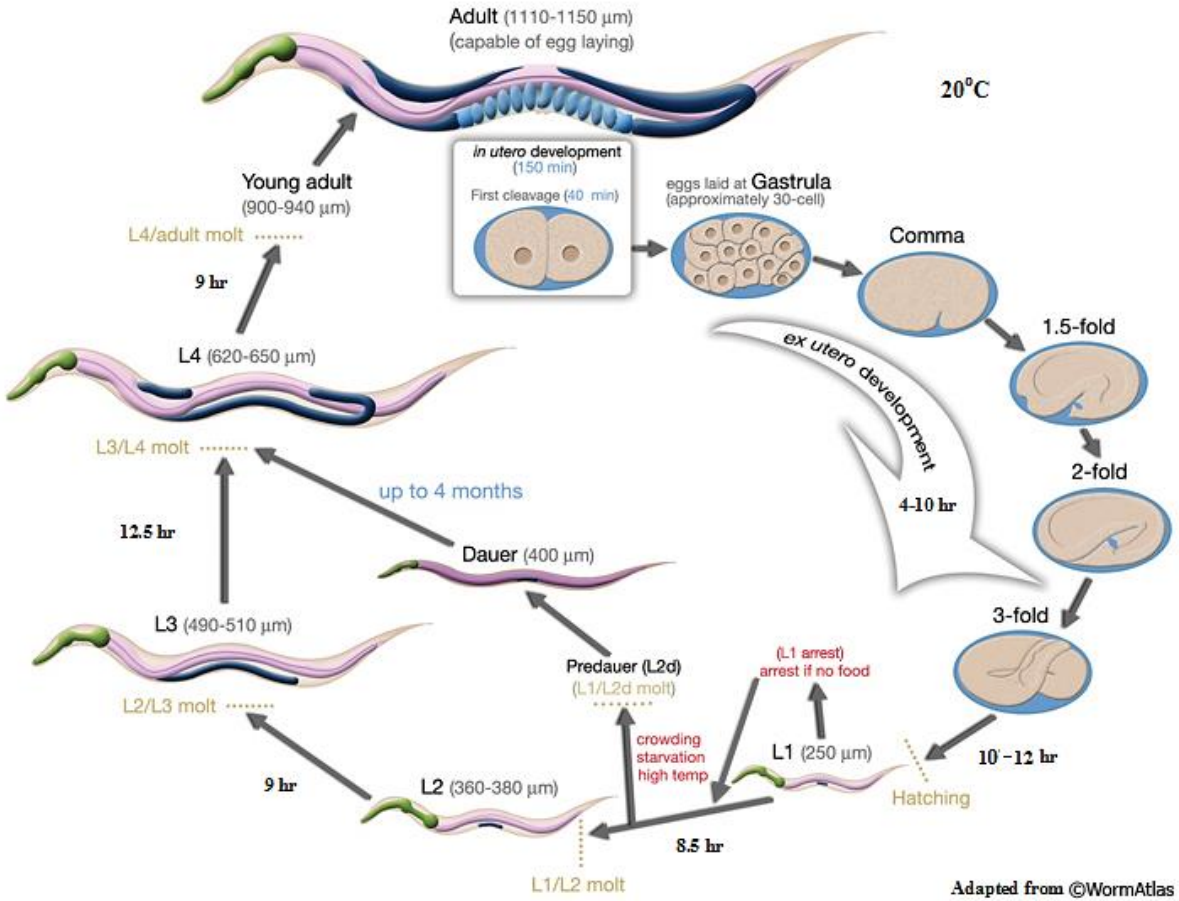

Figure 1.3: The lifecycle of *C. elegans* at 20°C. 0 min is fertilization. 40 minutes afterwards marks the first cleavage, while 150 minutes after fertilization is when eggs are laid at the gastrula stage. Numbers along the arrows indicate the length of time for each stage. The length of the animal at each stage is marked next to the stage name in micrometers (µm) (Adapted from (Altun and Hall 2009)).

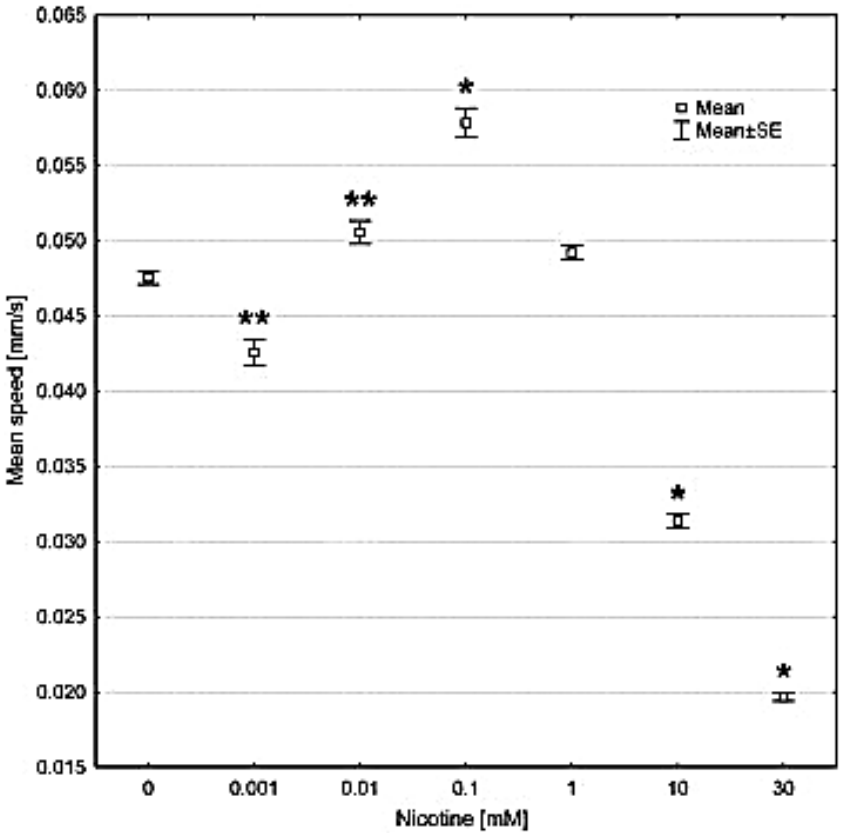

Figure 1.4: Selection of nicotine concentrations based on dose-dependent nicotine effect on *C. elegans* speed as reported by Sobkowiak et al. (Sobkowiak, et al. 2011). ”Worms were tracked on plates with 0, 0.001, 0.01, 0.1, 1, 10, and 30 mM nicotine. In each experiment, worms were tracked for 30 s every 10 min. The treatment lasted 300 min. The mean speed was calculated from all collected data. Significance of differences from the control: *P < 0.01 and **P < 0.05 (Kruskal–Wallis test) n ≥ 1461”.

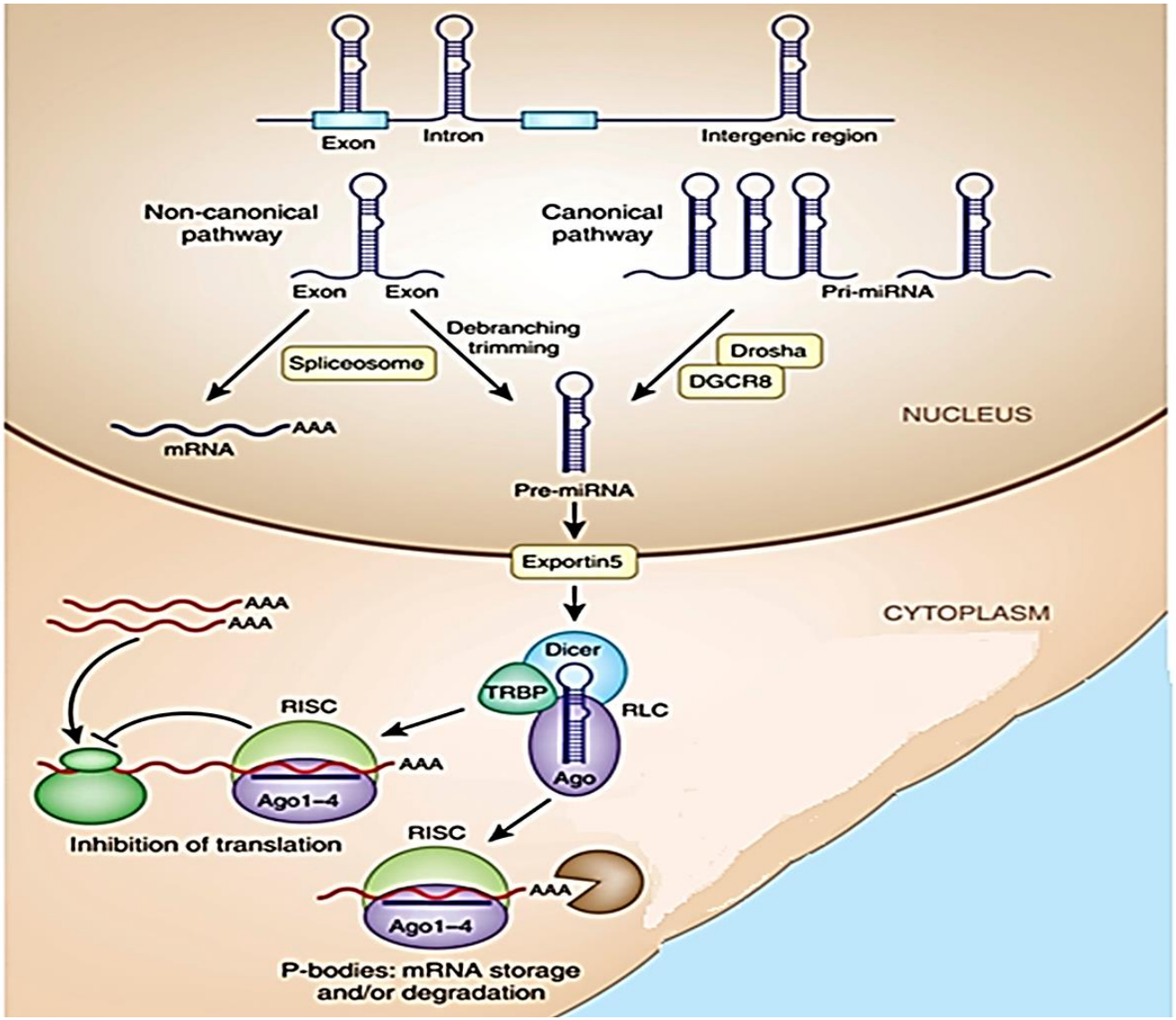

Figure 1.5: Schematic representation depicting miRNA biogenesis pathway. Adapted from (O'Carroll and Schaefer 2013).

Chapter Two: Nicotine exposure caused significant transgenerational behavior changes in *C. elegans*

Abstract

Passive and active exposure to tobacco smoking among youth is directly associated with immediate as well as long term health deterioration. Despite all pubic heath policies and efforts, the percentage of teenage smokers is still relatively high, especially in developing countries. Very few, if any, studies have been done on the trans-generational effect of nicotine exposed during the more sensitive, early developmental stages. We employed *C. elegans* as a biological model to study the multigenerational impact of chronic nicotine exposure. Nicotine treatment was limited to the N2 hermaphrodites of the F0 generation. It was strictly treated to L1-L4 (~31 hours) period after which worms were transferred to a fresh NGM plate. L4 developmental stage was used for behavioral analysis across three generations: F0, F1, and F2. Our results show that nicotine was associated with changes in sinusoidal locomotion, speed, and body bends in L4 larvae in all three tested generations. Despite having different patterns, those behavioral alterations were not restricted to F0, but were observed in F1 and F2 generations which were never exposed to nicotine. Our study is the first to reveal that nicotine addiction is heritable using *C. elegans* as a model organism. These results underscore the sensitivity of early development stages, with hope to spread more awareness to encourage the avoidance of nicotine exposure, especially at a young age.

Key words: *Nicotine, C. elegans, L4, post-embryonic stage, sensitivity to stress, trans-generational effect, addiction, behavior*

Introduction

Nicotine is a tertiary amine composed of a pyridine and a pyrrolidine ring. In its non-ionized form, nicotine can readily penetrate membranes (e.g. BBB). The major role of nicotinic receptors in nicotine's mechanism of action has been established. Nicotine aversively affects several organs and systems (Table 1.1) (NIC 1992). Its impact on the central and peripheral nervous systems contributes to the behavioral phenotypes in organisms (Benowitz 1988). This is primarily manifested in drug addiction symptoms such as compulsive drug seeking and taking behaviors (Le Foll and Goldberg 2009). Generally, nicotine-associated phenotypes are complex and depend of several factors such as dose, duration of exposure, and developmental stage (Hatsukami 2008). As a psychoactive component of tobacco, nicotine abusers experience vomiting, tremors, convulsions, as well as depressant effects after initial exposure and even death at extreme doses (Dani and Heinemann 1996; Herberg, et al. 1993). Later, continuous use leads to tolerance as they adapt to nicotine-effects (Hatsukami 2008). The dependence becomes more evident in the drug seeking behavior and positive reinforcement (e.g. enhance the sense of well-being, produce arousal or relaxation, help maintain vigilance, and reduce anxiety (Benowitz 1988)) after drug taking. Individuals become addicted to nicotine and experience strong withdrawal side effects (e.g., teeth chattering, chewing, gasping, writhing, head shakes, body shakes, tremors, headache, nausea, constipation or diarrhea, falling heart rate and blood pressure, fatigue, drowsiness and insomnia, irritability, difficulty concentrating, anxiety, depression, increased hunger and caloric intake, increased pleasantness of the taste of sweets, and tobacco cravings) (Le Foll and Goldberg 2009) that promote being entrapped in a cycle of continuous nicotine use and relapses.

Early developmental stages as well as adolescence are highly sensitive and vulnerable to nicotine (Ajarem and Ahmad 1998; Duncan, et al. 2009; Dwyer, et al. 2009; Hatsukami 2008; Leslie 2013; Wickstrom 2007). More so, children who are exposed to smoking are more likely to become addicted smokers as they progress to adulthood. Unfortunately about 40% of children are exposed to smoking in their environments (WHO 2012). Despite the increasing research on the effects of nicotine upon direct exposure and use, some studies have investigated a possible heritable effect of nicotine addiction (Heath, et al. 1995; True, et al. 1997) , but the latter only studied the relationship between genes and the environment in smoking susceptibility. Other studies on nicotine transgenerational effects were concerned with nicotine exposure during embryonic and perinatal stages (Ajarem and Ahmad 1998; Holloway, et al. 2007). Due to the high incidence of tobacco smoking among teenagers and exposure among children (Kim, et al. 2009; WHO 2012), we were interested in investigating possible long term consequences of early smoking habits. To our knowledge, no studies have been done on the transgenerational effect of nicotine exposed strictly during the post-embryonic and adolescent stages.

Our choice of a model system was based on advantages detailed in Chapter 1 and can be summarized by the ease of maintenance, and ethical, behavioral and biotechnological investigations. In *C. elegans*, nicotine altered some behaviors such as egg laying, pharyngeal pumping, muscle contraction, and male spicule ejection (Matta, et al. 2007). The invertebrate was able to recapitulate complex behavior associated with nicotine treatment in higher organisms such as acute response, tolerance, withdrawal, and sensitization (Feng, et al. 2006). Recently, motivation and drug seeking behaviors were reported in experiments that measured the approach of pretreated worms based on a gradient chemotaxis experimental design (Sellings, et al. 2013). The vulnerability of the post-embryonic stages was also highlightes in a *C. elegans* study that

showed nicotine-dependent motivation in pretreated young worms in comparison to the older adult counterparts (Sellings, et al. 2013). Thus, we took advantage of the wealth of previous research on nicotine and *C. elegans* in our experimental design. The choice of nicotine concentrations was based on dose and time-response investigations by Sobkowiak et al. (Sobkowiak, et al. 2011) (Figure 1.4) which were complimented with addiction-related behavior assays done by Feng et al. and Sellings et al. (Feng, et al. 2006; Sellings, et al. 2013).

Briefly, worms were exposed to nicotine strictly in the postembryonic stage (L1-L4) for about 30 hours. Subsequently, the behaviors of L4 larvae belonging to three generations: F0, F1 and F2 were analyzed. Our study is the first to report the heritability of nicotine addiction starting from the post-embryonic stage.

Methods and Material

Nicotine exposure and sampling

Nicotine was purchased from Acros Organics (New Jersey, USA). Nicotine was dissolved in phosphate buffer as 1 M and 0.001 M stocks. NaCl, peptone, agar and water mixture were first autoclaved and kept at 70 °C covered under the hood. Equal amounts were transferred to individual small autoclaved flasks cooled and kept at 55 °C. After the addition of cholesterol, $CaCl_2$, $MgSO_4$ and KH_2PO_4, nicotine solution was added to give the corresponding final concentrations 20µM and 20mM in the medium.

C. elegans hermaphrodite N2 Bristol wild type was used. Maintenance and worm transfer were done after NGM plates were seeded with OP50, and then kept at 20^{o}C. Egg synchronization was done via bleaching method described by Sulston and Hodgkin, with slight modifications (Sulston and Hodgkin 1988a). Briefly adult gravid worms were washed off the plate with M9

buffer into a 15 ml Falcon tube (for a medium sized pellet). Then the Falcon tube was centrifuged at 2000 rpm for 2 minutes to collect worm pellet and was followed by another wash. Then, 5 ml of synchronization solution was added for 5 minute-shake until the eggs were dispersed in solution. The eggs were pelleted after centrifugation at 2000 rpm for 2 minutes. The supernatant was removed and followed by four time wash using 5-ml M9 washes. The eggs were finally suspended in the last wash and were placed on a shaker in the 20^{o}C incubator for about 14 hours. After hatching, all progeny were stuck at L1. The latter were seeded onto corresponding treatment plates.

Figure 1.2 shows the general protocol for worm treatment and sampling. F0- L1 larvae were transferred to the three treatment groups which included the control group along with the low and high nicotine concentrations. F0 exposure lasted around 31 hours until end of L3-beginning of L4. Later, around 20 worms were then picked from each of 4 replicates into 4-treatment matched 3.5cm petri-plates. The plates were previously seeded with OP50 and left to dry for subsequent behavioral studies. Worms were washed off the plates and transferred to an eppendorf tube. Then, the pellet was washed twice with M9 interrupted by centrifugation and supernatant removal. The worms were then transferred into OP50-seeded NGM plates, left to dry, and were sealed and placed back in the 20^{o}C incubator to grow until second day of adulthood-associated with egg laying peak. Plates were washed for synchronization. The whole procedure was repeated twice until collecting the F2 generation.

Two hours after the transfer, a 5-8 minute video was taken per replicate for every treatment group. The video was set at (15 frames/sec) with the same magnification for all treatment groups. The videos were then analyzed via Wormlab software (MBF bioscience). Output data included endpoints for every tracked worm (i.e. mean track length, mean

wavelength, mean amplitude, mean maximum amplitude, mean smoothed forward speed, mean smoothed backward speed, mean bending angle, omega bends, and reversals ratios). Video image noise was taken into consideration when choosing among the calculated speed indices. Image noise represent a signal detected during tracking and is generally not originating from the target (as in the case of uneven illumination). With the assumption that the target is associated with medium-sized features in comparison to noise, a smoothing approach reduces the small features while preserving the larger shapes. Smoothing is applied to remove the unwanted variation (Kan 2012). So, as done by Faumont, et al (Faumont, et al. 2011), the speed was calculated as the average instantaneous velocity over a specific time frame. With such rationale in mind, we chose smoothed speed to study the effect of nicotine on the locomotion velocity.

Data Analysis

Data provided by Wormlab software was exported to an Excel spreadsheet. Mean track length, wavelength, amplitude and maximum amplitude variable for each tracked worm were used from the track summary output. Each of the smoothed speed, bending angle, omega bend, and reversals ratios was calculated as the average/frame for each tracked worm. The smoothed speed was divided into positive (forward) and negative (backward) speeds. Both speeds were binned into intervals, and the number of worms with speeds falling in the right range was counted to get a frequency table. Contingency tables were used for speed statistical analysis. The Chi-square test was used for overall statistical significance, and the speed pairwise comparison among treatment groups was based on z-tests. As for the other endpoints, data from each individual worm was pooled from the four replicates per treatment group for statistical analysis via omnibus hypothesis testing one-way ANOVA. Statistical significance was reported when

P<0.05. Data analysis was done via SPSS (19). Each endpoint is defined based on Wormlab software as described in (Figure 2.2) (Bioscience 2012).

Results

The transgenerational impact of nicotine on locomotion

In the F0 generation, the mean track length, amplitude, maximum amplitude, and wavelength, were significantly affected by direct nicotine exposure with $F(2,460)=29.655$; $F(2,460)=52.635$; $F(2,460)=150.104$; and $F(2,460)=705.101$ at $P<0.001$. A peak was observed for the low concentration treatment groups for the track length and maximum amplitude values ($P=0.027$). As the concentration increased, the values for all of the four endpoints significantly decreased ($P<0.001$) when comparing the high concentration (20mM) treatment groups to both control (0µM) and low concentration (20µM) treatment groups (Figure 2.3). In the following generations, for the most part, an increase was observed more noticeably in F1 after which it was diluted in F2. The F1 generation had statistically significant changes in track length [$F(2,315)=3.619$, $P=0.028$], maximum amplitude [$F(2,315)=3.715$, $P=0.025$], amplitude [$F(2,315)=4.974$, $P=0.007$] and wavelength [$F(2,315)=7.206$, $P=0.001$]. Post-Hoc pairwise comparison testing showed that the mean wavelength increased in both 20µM ($P=0.001$) and 20mM ($P=0.002$) treatment groups when compared to control. A dose-dependent increase in the amplitude and the maximum amplitude was observed to summit in the 20mM treatment group ($P\leq0.007$). Also, the track length and the amplitude were even noticeably greater than the 20µM treatment group ($P=0.008$ and $P=0.022$, respectively). From F1 to F2, statistical significance was observed only in the wavelength [$F(2,198)=4.913$, $P=0.016$] where elevation was observed in both the low and high concentration treatment groups ($P=0.012$ and $P=0.014$, respectively).

Interestingly, though not statistically significant, all of the locomotion endpoints were higher in the nicotine treatment groups than control (Figure 2.3).

Mutigenerational effects of nicotine on the dynamic body movements on C. elegans

There was an opposing pattern between F0, and F1 and F2. In F0, the reversals decreased in a dose-dependent but not a statistically significant manner. However, both F1 and F2 reversed more. The stronger increase was seen in F1 [$F(2,236)=3.939$; $P=0.021$]. The 20mM treatment groups out-reversed the control ($P=0.008$) and 20µM treatment groups ($P=0.021$). In F2, the 20mM treatment group continued to have more reversals than that of the lower nicotine concentration even at F2 ($P=0.045$) (Figure 2.4).

A dose dependent decrease in the average bending angle was observed in F0 and F2. With an impact factor of $F=39.336$ at $P<0.001$, F0 worms exposed to high nicotine concentration bent with a smaller angle than control and 20µM treatment groups ($P<0.001$). From F0 to F1, worms exposed to 20mM nicotine continued to have a narrower bending angle than the 20µM-exposed worms ($P=0.034$) (Figure 2.4).

As for the omega bend, major differences were not observed in the 20µM treatment group. On the contrary, an increase was evident in the 20mM treatment group in all the generations. The increase was the strongest in F0 [$F(2,460)=10.039$], particularly in the 20mM treatment group when compared to both control and 20µM treatment groups ($P\leq0.001$). The omega impact factor decreased in a generation-dependent manner to become $F(2,315)=4.375$; $P=0.013$ in F1. The increase was statistically significant with $P=0.023$ and $P=0.004$ when compared with control and 20µM -F1 groups, respectively. Despite the transgenerational depression in the effect, a dose-dependent increase was also observed in F2 with the 20mM treatment compared to control with $P=0.027$ (Figure 2.4).

The trans-generational effect of nicotine on speed in C. elegans

Forward speed

Nicotine exposure had the strongest impact on the F0 generation worm population on the overall forward speed among the treatment groups ($\chi 2=68.707$; $P<0.001$). Contrary to the distribution of the worm proportion for the 20µM treatment group which didn't deviate with statistical significance from the control at any speed range, the 20mM worm proportion statistically differed from the control in 4 of the 5 speed ranges. Most of the 20mM-treated worms moved with forward speed falling in 0-20µm/s range. In the latter, our data reveal a ([52.3:47.7:84.5] %) relative worm distribution among each of the control, 20µM, and 20mM treatment groups, respectively. Consequently, both the control and 20µM treatment groups had a higher worm frequency in the speed ranges: 20-40µm/s, 40-80µm/s, 80-160µm/s, >160µm/s. 14.3% of the worms in the control, and 10.2% of the worms in the 20µM treatment group moved with speed range of 40-80µm/s. Only 1.7% of worms treated with the high nicotine concentration moved with that speed range. A similar pattern was observed at the >160µm/s speed range. An average of 3.5% of the worms belonging to both control and the 20µM treatment groups moved with forward speed >160µm/s, while only 0.4% of worms belonging to the 20mM nicotine treatment group moved at that speed range (Figure 2.5).

The impact on forward speed was robust as it was observed in the F1 generation ($\chi 2=43.421$; $P<0.001$). The frequency of worms, exposed to 20mM nicotine, continued to have a statistically significant peak ([19.8:12.4:53.6] %) in the 0-20µm/s range. The relative worm peaks for those exposed to 20µM nicotine showed a new set of proportions with statistically significant elevations ([19.8:24.7:8.9] %) and ([5.8:16.5:3.6] %) at speed ranges of 40-80µm/s and 80-160µm/s when compared to both control and 20mM groups (Figure 2.5).

The worm proportions versus speed range distribution became more similar among the treatment groups in the F2 generation. However, the proportion of worms treated with 20µM nicotine ([42.6:60.3:54.0] %) was statistically higher with respect to control at the 20-40µm/s while both the control and the high concentration treatment groups had more worms with higher speed ranges e.g. ([16.4:9.5:22.0] %) at the 40-80µm/s (Figure 2.5).

Backward speed

Nicotine exposure significantly affected the worm's backward speed on F0 generation ($P<0.001$). To state the statistically significant pairwise comparisons, around 76.6% of the 20mM-treated worms belonged to the slowest speed range (0-20µm/s) when only 23.8% and 35.2% of the control and 20µM-treated worms were in this range. Meanwhile, the difference in the peaks between control and treatment groups was statistically significant in the 20-40µm/s speed range ([45.2:26.1:20.0] %). Also, though not significant, another high proportion of worms was observed for the 20µM treatment group at the 40-80µm/s ([23.8:30.6:25.5] %). The proportion of the 20mM-treated worms decreased from 20.0 % to about 0.0-2.5 % in the faster speed ranges, three of which were statistically significant (Figure 2.5).

Statistically significant differences in the worm proportions were also detected in the F1 generation and that was limited to the high concentration treatment group. 34.5% of the 20mM treated worms had a 0-20µm/s speed range in comparison to the 18.6% 20µM treated worms. Another statistically significant difference was observed for the high-concentration treatment group (1.8%) at the 80-160µm/s speed range while the control and low concentration treatment groups had worm proportions of 10.7 and 14.4%, respectively, at that range (Figure 2.5).

As for the F2 generation, though the worm proportion peaks became more alike and in the 20-40µm/s range ([38.3:40.7:34.7] %), the 20mM-nicotine-treated worms peaked with

statistical significance at a faster range with 42.8% of its worms at the 40-80µm/s speed range while the 0µM and 20µM treatment groups had 25.0% and 32.2% of their worms in this speed range (Figure 2.5).

Discussion

Nicotine is a potent stimulant and a cholinergic agonist. There is no uniform standard molecular phenotype associated with nicotine as alterations in cholinergic receptors in the brain ranged from states like stimulation, inactivation, and increase or decrease in the turnover rate of nicotinic receptors on the cell membranes. Its action is therefore not only context-dependent, but it is also based on the dose and duration of its exposure (Schafer 2002). *In C. elegans,* it has been documented that nicotine treatment is associated with hyper-contraction of body wall-muscles, stimulation of egg laying, increased pharyngeal pumping as well as a decrease in the efficiency of male spicule in mating (Matta, et al. 2007; Schafer 2002).

We were interested in studying the addictive nature of nicotine. With smoking being so prevalent in regions like the Middle East (e.g. Lebanon), the chances of persistent nicotine exposure among the younger groups remain high. Early developmental stages have been proven to be more sensitive to any sort of stresses such as nicotine exposure. Of notice, the highest male to female-teenage smokers was reported in Lebanon, a 66:54% in 2005-2010 (WHO 2012). It was reported that even a limited nicotine exposure during adolescence may lead to symptoms of dependence and that this sensitivity might be due to the neurochemical changes in the brain that is different from those of adults (CDC 2010; Slotkin 2002). We were interested in assessing the extent of the nicotine-induced alterations. We wanted to explore if effects caused by early development nicotine exposure would be passed on to the offspring. Thus, nicotine exposure was

limited to the L1-late L3/early L4 period. Hence, adult hermaphrodite worms and the subsequent F1 and F2 generations were never in direct contact with nicotine.

Understanding the patterns and relationships in our data

Speed can be calculated as wavelength x oscillation frequency. Therefore, the wavelength and the speed are directly proportional. That is consistent with our data for the F0 generation where a decrease in speed in the 20mM group was associated with a decrease in wavelength. Also, in F1 and F2 generations, both the forward speed and the wavelengths increased.

The omega bend is summarized in 3 steps: With reference to the body centroid point, the worm has a bending angle $<90^{o}$. Then, the worm bends to less than 45^{o}. The omega bend ends with the worm opening its body with a bending angle $>90^{o}$. Hence, one would expect that there is an inverse relationship between omega bend and bending angle (Figure 2.4).

F0 generation models direct nicotine toxicity, and addiction (tolerance)

The high concentration treatment group modeled nicotine-induced toxicity as it was negatively affected in all the locomotive indices. Their movement remained confined to a small area as evident in the lower track length, and had lower wavelengths and amplitudes. Also most of the worms had minimal forward and reverse speeds (0-20µm/s). Thus the 20mM treated worms seemed paralyzed, and that is in agreement with previously reported results (Sobkowiak, et al. 2011). Having said that, the increase in bends might not specifically reflect the omega bends. It seemed as if the worms were unable to free themselves and appeared to be in coiled structures (data not shown). The latter could have been mistakenly detected as omega bends by the software. The decrease in amplitudes in the 20mM may support this conclusion as it is reasonable to expect a directly proportional relationship between omega bend and amplitudes.

Nicotine is involved in locomotion stimulation when applied acutely. The stimulating effect is evident when applied in a specific concentration range. The 20µM treatment group falls within this range (Sobkowiak, et al. 2011). However, no increase in forward speed was detected. One difference in the experimental settings was the duration of nicotine application. Therefore, the "apparently" normal speed may represent chronic nicotine tolerance and adaptation which has been previously documented (Feng, et al. 2006). However, the worms did show a faster negative speed. Such indicated a faster reversal movement and is logical with the AVA command neurons, which regulate reversals, being a nicotine target (Chalfie, et al. 1985; Feng, et al. 2006; Von Stetina, et al. 2006; Zheng, et al. 1999). In normal food-replete conditions, worms tend to be "dwelling"-a behavior with frequent reversals and increased turn angles and lower forward speed. This was not totally observed in our case since the forward speed for the 20µM group was not lowered. Instead, the worms performed fewer reversals and more omega bends.

The F1 and F2 generations modeled inherited toxicity and addiction (withdrawal)

The effect of nicotine on the forward speed

Overlaying the speed curves allowed us to see two major peaks in the F1 generation worm population. The control (0µM) and 20µM treatment groups had most of their worms moving in the 20-40µm/s range. Overall, 45.3% of the 20µM treated worms were faster than those in the control (31.4%). As for the 20mM treatment group, the peak was in the 0-20µm/s speed range. However, unlike the case in the F0 generation, we can notice the absence of any statistically significant difference in comparison to the 0µM treatment group. Hence, in the F1 generation, more 20mM-nicotine-treated worms moved with higher forward speed. Thus, their behavior is becoming closer to the wild type untreated worms.

Reaching the F2 generation, all of the treatment groups peaked at the same speed range (20-40µm/s) with the 20µM group having the largest worm proportion. On the other hand, taking into consideration the highest four speed ranges, it seemed that the highest worm proportion belonged to the 20mM-treatment group (80%), which is close to that of the 20µM (79.4%), and the least was that of the control (68.8%) treatment groups.

The effect of nicotine on backward speed

We previously described a three-peak-speed-pattern in the F0 generation worm population occurring in the 20µM treatment group which reversed faster than 0µM and the 20mM treatment groups, respectively. 77% of worms treated with the 20mM nicotine concentration moved at the 0-20µm/s speed range, while only 34% of their offspring in the F1 generation worm population moved at that speed. This proportion remained almost the same in the two successive faster speed ranges (33%, 29%, respectively). From a bird's eye view, it seems that two peaks appeared for F1. Most of the worms in the low and high nicotine treatment groups reversed with 40-80µm/s speed, while those of the control group reversed with a slower speed (20-40µm/s). Thus, the 20mM treated worms became far from paralyzed, as was observed in the F0 generation, and seemed to be catching up with by increasing their reversing speed.

The pattern seems to get exacerbated in the F2 generation, as the proportion of worms treated with nicotine high concentration peaked at the faster speed 40-80µm/s in comparison to both the control and the low concentration treated worms. The latter two had similar patterns across the speed ranges.

Withdrawal serves as a better index than tolerance (CDC 2010). Both nicotine-dependent and nicotine non-dependent smokers did not differ in tolerance after being exposed to it.

However, they differed significantly with their behavior during nicotine abstinence (CDC 2010).Interestingly, the phenotypes observed in the F1 and F2 generations may be models of withdrawal since worms were grown on fresh NGM all along, but still exhibited altered speed (Schafer 2002). The hyperactive behavior can be reflective of craving or uneasiness in worms as they are no longer getting their addicting and satisfying nicotine dose. Looking at our data, we suspect that this addicting dose (that is not associated with direct toxicity) is around that of the low concentration (20µM range) as evident in the F1 individuals. It is expected that an effect might be diluted across generations. Progressing from the F1 to the F2, there was a dilution/amelioration in the 20mM nicotine toxic paralyzing effect, until it became comparable to that induced in the 20µM range. Eventually, the progeny of the 20mM treated parents had the highest speed (most anxious) in the F2 generation. We can deduce that the higher the parental exposed concentration, the further down the effect is tracked and inherited.

Omega and reversals and overall locomotion indices in response to nicotine treatment

Three behavioral patterns are defined for *C. elegans* as a function of food supply. When food is present, short reversals and infrequent omega bends occur. When transferred to a food-free- medium, long reversals, frequent omega bends, and an increase in forward speed are observed. The third pattern is seen after longer periods of food abstinence, when both reversals and omega bends decrease to allow the worm to seek food. In short, the omega bends are generally proportional "coupled" to reversals-though the opposite is not a prerequisite (Gray, et al. 2005; Wakabayashi, et al. 2004). However, our data does not fully support this. In the F0 generation, the relationship between reversals and omega bend is opposite and this pattern was dose dependent to become statistically significant at 20mM treatment group. It is noteworthy to mention that this behavior was specific to the F0 individuals which were in direct nicotine

exposure. The pattern was different in the F1 and F2 generations, both of which were not exposed to nicotine and modeled withdrawal. It is important to exclude any biased interpretations to nicotine specific, addiction independent, symptoms.

In the F1 and F2 generations, both the omega bends and reversals only differed in the high concentration treatment group. Though they were "coupled", it still didn't model the normal situation where omega bends should have been infrequent due to the availability of food as seen in the control. Though the omega bends did increase in the three generations, the omega bends occurring in the F0 individuals had less amplitude than control and may therefore not be true omega bends, while those in the F1 and F2 individuals were more vigorous with increasing amplitude in comparison with control. It is documented that when the environment is declining, the frequency of reversals and sharp turns increases, and vice versa (Gray, et al. 2005). Such may pinpoint that the worms were not comfortable in the normal settings, and perhaps they were in a "craving" status. The latter point can be complimented by the conclusion provided by Zhoa et al. (Zhao, et al. 2003). They considered reversals as a way that allows the worm to constantly reassess its priorities (i.e. as reversals were initially a way of avoidance from harsh contact and later became a way of foraging). Hence, this shift in behavior is reflective of withdrawal symptoms and might insinuate the inheritance of nicotine addiction.

Logically, the alterations in reversals and body bends point to the effect of nicotine on particular neurons. It has been documented that the AVA neuron is involved in reversals, while the SMD, RIV, and SMB are involved in omega bends and regulation of its amplitude (Gray, et al. 2005). It would be interesting to dissect the cellular pathways involved in the response to nicotine. Whether it majorly involves acetylcholine receptors as upstream effectors or its acts

directly on different effectors (e.g. serotonergic system) in a cell-type specific manner is worth further studying.

References

Ajarem, J. S., and M. Ahmad

1998 Prenatal nicotine exposure modifies behavior of mice through early development. Pharmacol Biochem Behav 59(2):313-8.

Benowitz, Neal L.

1988 Pharmacologic Aspects of Cigarette Smoking and Nicotine Addiction. New England Journal of Medicine 319(20):1318-1330.

Bioscience, MBF

2012 Wormlab Help; How do I view and interpret my data? *In* [WWW document] URL: http://www.biolucida.net/wormlab/help/Content/HOW/howinterpret.htm.

CDC

2010 The Biology and Behavioral Basis for Smoking-Attributable Disease: A Report of the Surgeon General.

Chalfie, M., et al.

1985 The neural circuit for touch sensitivity in Caenorhabditis elegans. J Neurosci 5(4):956-64.

Dani, J. A., and S. Heinemann

1996 Molecular and cellular aspects of nicotine abuse. Neuron 16(5):905-8.

Duncan, J. R., et al.

2009 Prenatal nicotine-exposure alters fetal autonomic activity and medullary neurotransmitter receptors: implications for sudden infant death syndrome. J Appl Physiol 107(5):1579-90.

Dwyer, J. B., S. C. McQuown, and F. M. Leslie

2009 The dynamic effects of nicotine on the developing brain. Pharmacol Ther 122(2):125-39.

Faumont, S., et al.

2011 An image-free opto-mechanical system for creating virtual environments and imaging neuronal activity in freely moving Caenorhabditis elegans. PLoS One 6(9):e24666.

Feng, Z., et al.

2006 A *C. elegans* model of nicotine-dependent behavior: regulation by TRP-family channels. Cell 127(3):621-33.

Gray, J. M., J. J. Hill, and C. I. Bargmann

2005 A circuit for navigation in Caenorhabditis elegans. Proc Natl Acad Sci U S A 102(9):3184-91.

Hatsukami, D. K.

2008 Nicotine addiction: past, present and future. Marian Fischman lecture given at the 2007 meeting of CPDD. Drug Alcohol Depend 92(1-3):312-6.

Heath, A. C., et al.

1995 Personality and the inheritance of smoking behavior: a genetic perspective. Behav Genet 25(2):103-17.

Herberg, L. J., A. M. Montgomery, and I. C. Rose

1993 Tolerance and sensitization to stimulant and depressant effects of nicotine in intracranial self-stimulation in the rat. Behav Pharmacol 4(4):419-427.

Holloway, A. C., et al.

2007 Transgenerational effects of fetal and neonatal exposure to nicotine. Endocrine 31(3):254-9.

Kan, Andrey

2012 Automated Analysis of Time Lapse Microscopy Images. PHD thesis. Department of Computing and Information Systems, The University of Melbourne.

Kim, S. , et al.

2009 Determinants of Hair Nicotine Concentrations in Nonsmoking Women and Children: A Multicountry Study of Secondhand Smoke Exposure in Homes. Cancer Epidemiology Biomarkers & Prevention 18(12):3407-3414.

Le Foll, B., and S. R. Goldberg

2009 Effects of nicotine in experimental animals and humans: an update on addictive properties. Handb Exp Pharmacol (192):335-67.

Leslie, F. M.

2013 Multigenerational epigenetic effects of nicotine on lung function. BMC Med 11(1):27.

Matta, S. G., et al.

2007 Guidelines on nicotine dose selection for in vivo research. Psychopharmacology (Berl) 190(3):269-319.

NIC

1992 National Cancer Institute. Monograph 2: Smokeless Tobacco or Health: An International Perspective available at http://www.cancercontrol.cancer.gov/brp/tcrb/monographs/2/index.html. Accessed on 3/25/2013.

Schafer, William R.

2002 Neuropsychopharmacology: The Fifth Generation of Progress. Lippincott, Williams, & Wilkins, Philadelphia, Pennsylvania section 2(Chapter 21).

Sellings, L., et al.

2013 Nicotine-motivated behavior in Caenorhabditis elegans requires the nicotinic acetylcholine receptor subunits acr-5 and acr-15. Eur J Neurosci 37(5):743-56.

Slotkin, T. A.

2002 Nicotine and the adolescent brain: insights from an animal model. Neurotoxicol Teratol 24(3):369-84.

Sobkowiak, R., M. Kowalski, and A. Lesicki

2011 Concentration- and time-dependent behavioral changes in Caenorhabditis elegans after exposure to nicotine. Pharmacol Biochem Behav 99(3):365-70.

Sulston, J, and J Hodgkin

1988 The Nematode Caenorhabditis elegans, W.B. Wood, ed. New York: Cold Spring Harbor Laboratory Press:p. 587.

True, W. R., et al.

1997 Genetic and environmental contributions to smoking. Addiction 92(10):1277-87.

Von Stetina, S. E., M. Treinin, and D. M. Miller, 3rd

2006 The motor circuit. Int Rev Neurobiol 69:125-67.

Wakabayashi, T., I. Kitagawa, and R. Shingai

2004 Neurons regulating the duration of forward locomotion in Caenorhabditis elegans. Neurosci Res 50(1):103-11.

WHO

2012 World Health Statistics.Global Health Observatory. World Health Organization. Retrieved from http://www.who.int/gho/publications/world_health_statistics/EN_WHS2012_Full.pdf.

Wickstrom, R.

2007 Effects of nicotine during pregnancy: human and experimental evidence. Curr Neuropharmacol 5(3):213-22.

Zhao, B., et al.

2003 Reversal frequency in Caenorhabditis elegans represents an integrated response to the state of the animal and its environment. J Neurosci 23(12):5319-28.

Zheng, Y., et al.

1999 Neuronal control of locomotion in *C. elegans* is modified by a dominant mutation in the GLR-1 ionotropic glutamate receptor. Neuron 24(2):347-61.

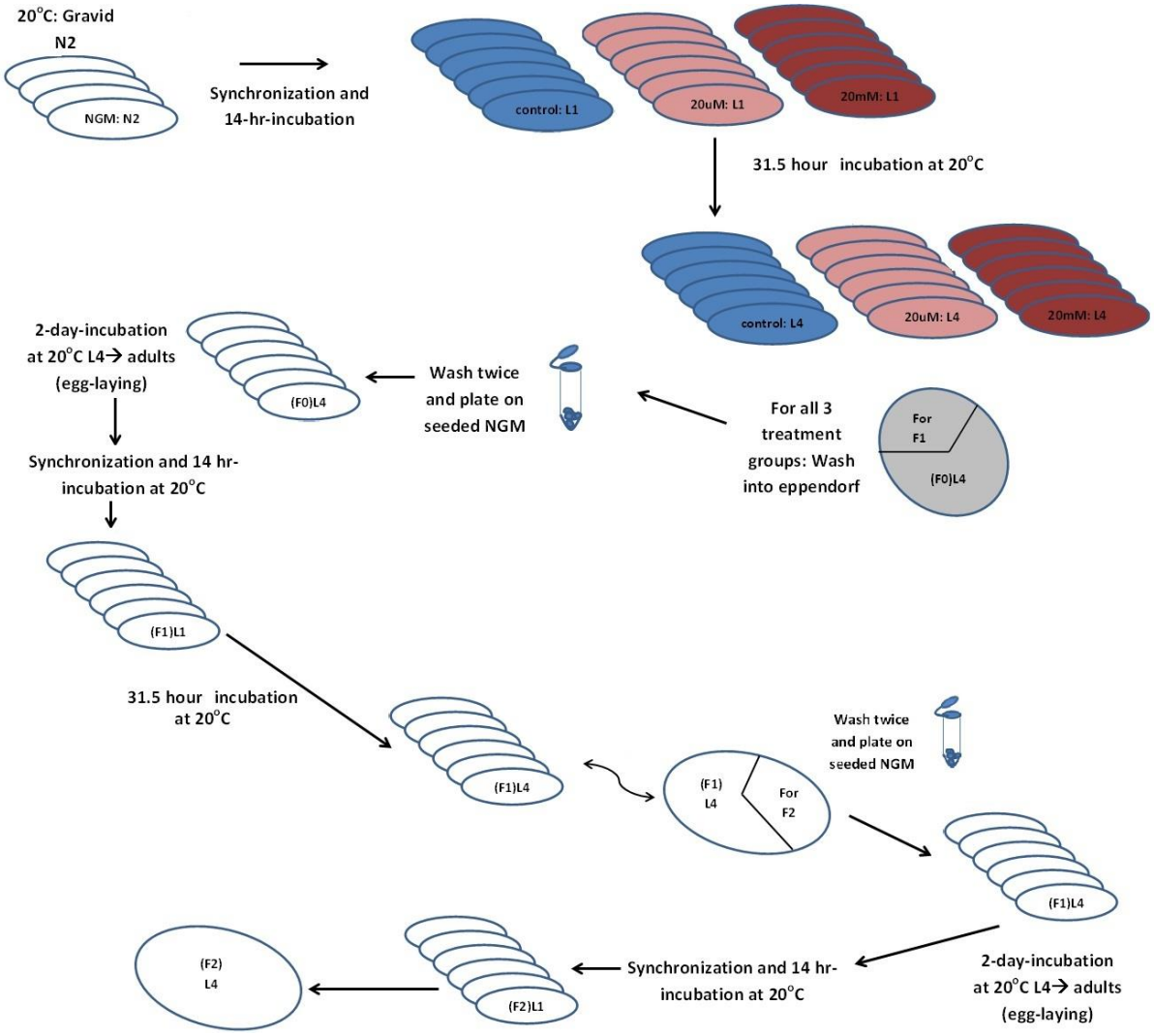

Figure 2.1: Description of nicotine exposure on *C. elegans* hermaphrodites and sampling for assays of interest.

Track length	The additive distance travelled from one frame to another.
Wavelength	Distance between negative and positive inflection points
Amplitude	The average centroid displacement over the entire track. The blue dot is the default average median axis. The green dot is the center location of the median axis
Maximum amplitude	The maximum centroid displacement over the entire track.
Smoothed Speed	A three-frame moving average speed smoothed over a 20 second span. The moving average speed is the instantaneous velocity along the worm's central line averaged over a number of frames.
Bending angle	The angle between the centroids of both the head and the tail.
Omega bend	Occurs when the worm makes an omega-shaped movement.

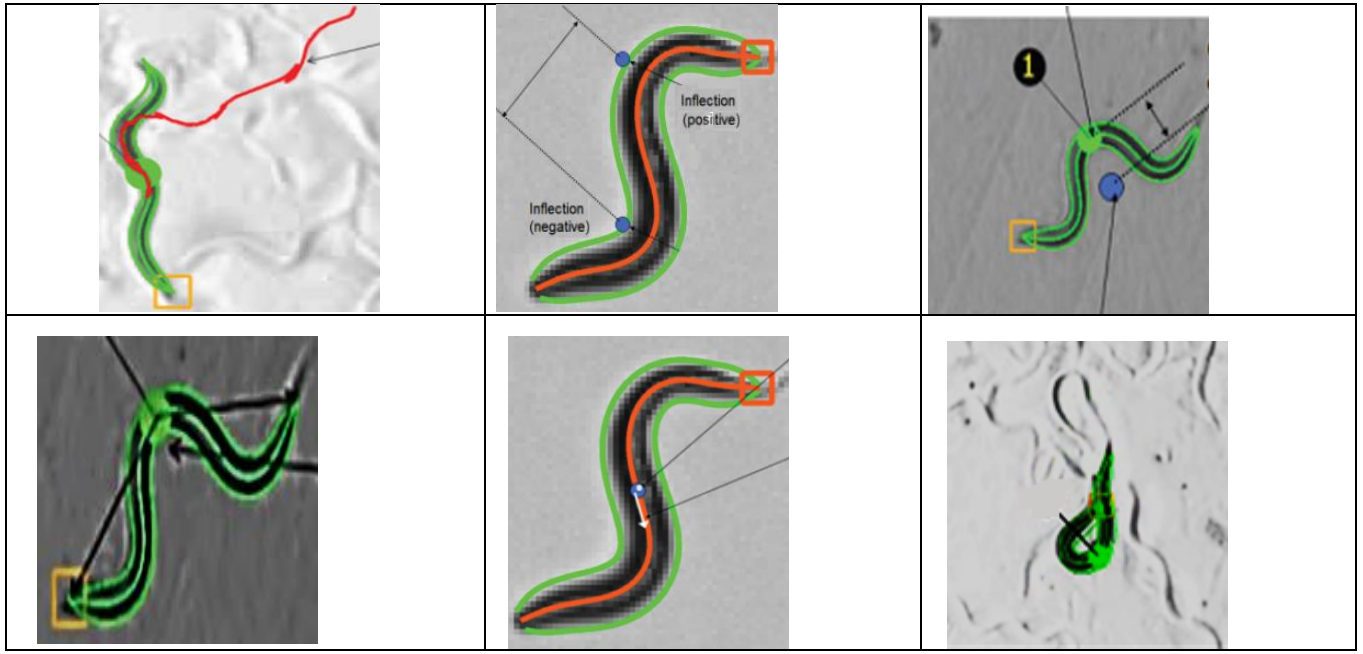

Figure 2.2: Summary of endpoints definitions as analyzed by the Wormlab MBF software.

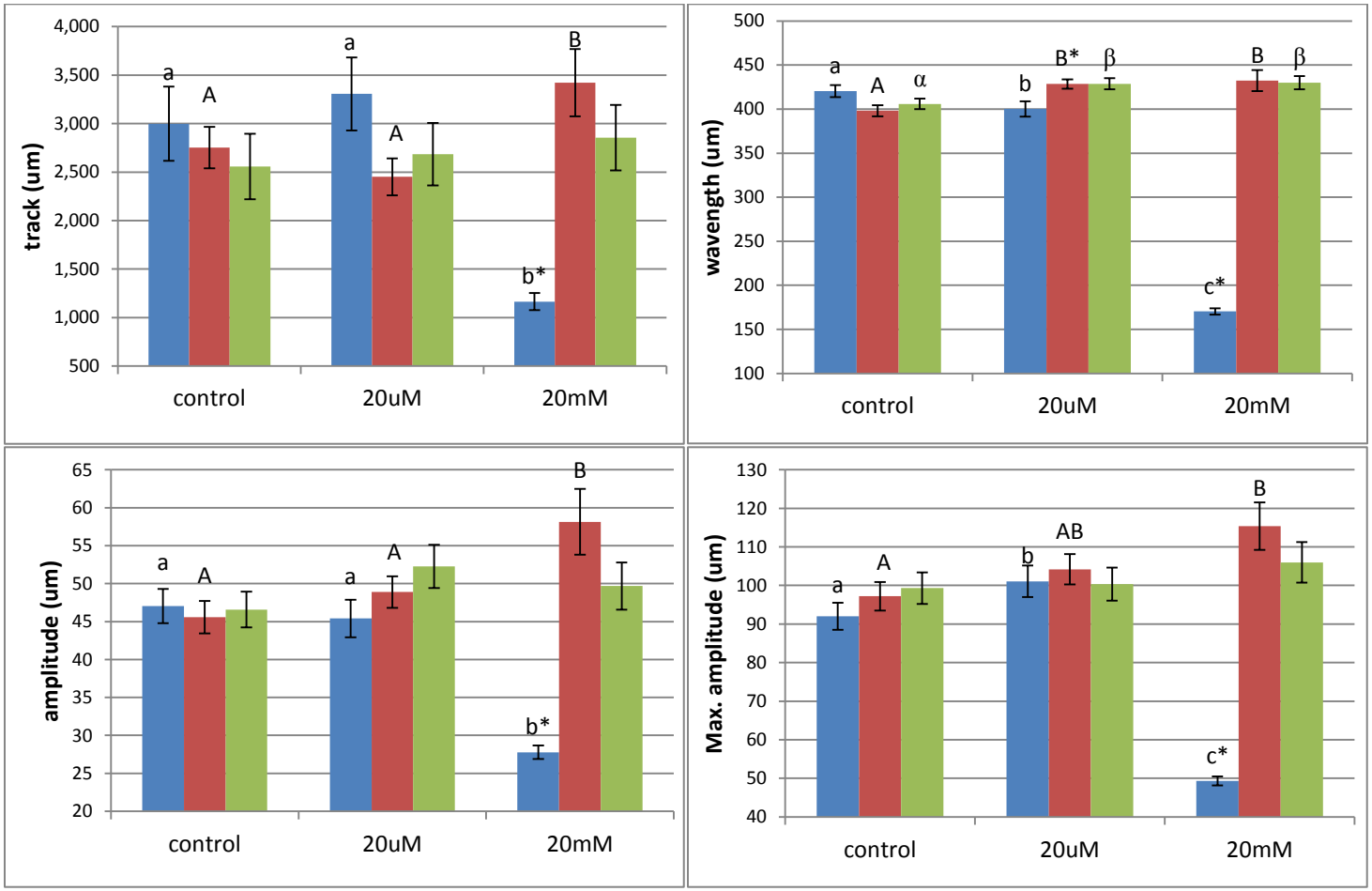

Figure 2.3: An overview of the variation in the different endpoints' pattern as a function of nicotine dose on L4 hermaphrodite *C. elegans* across the three generations. From left to right, bars represent F0, F1, and F2, respectively. The x-axis represents nicotine concentrations used. Control is the group without nicotine. (P*)≤0.001.

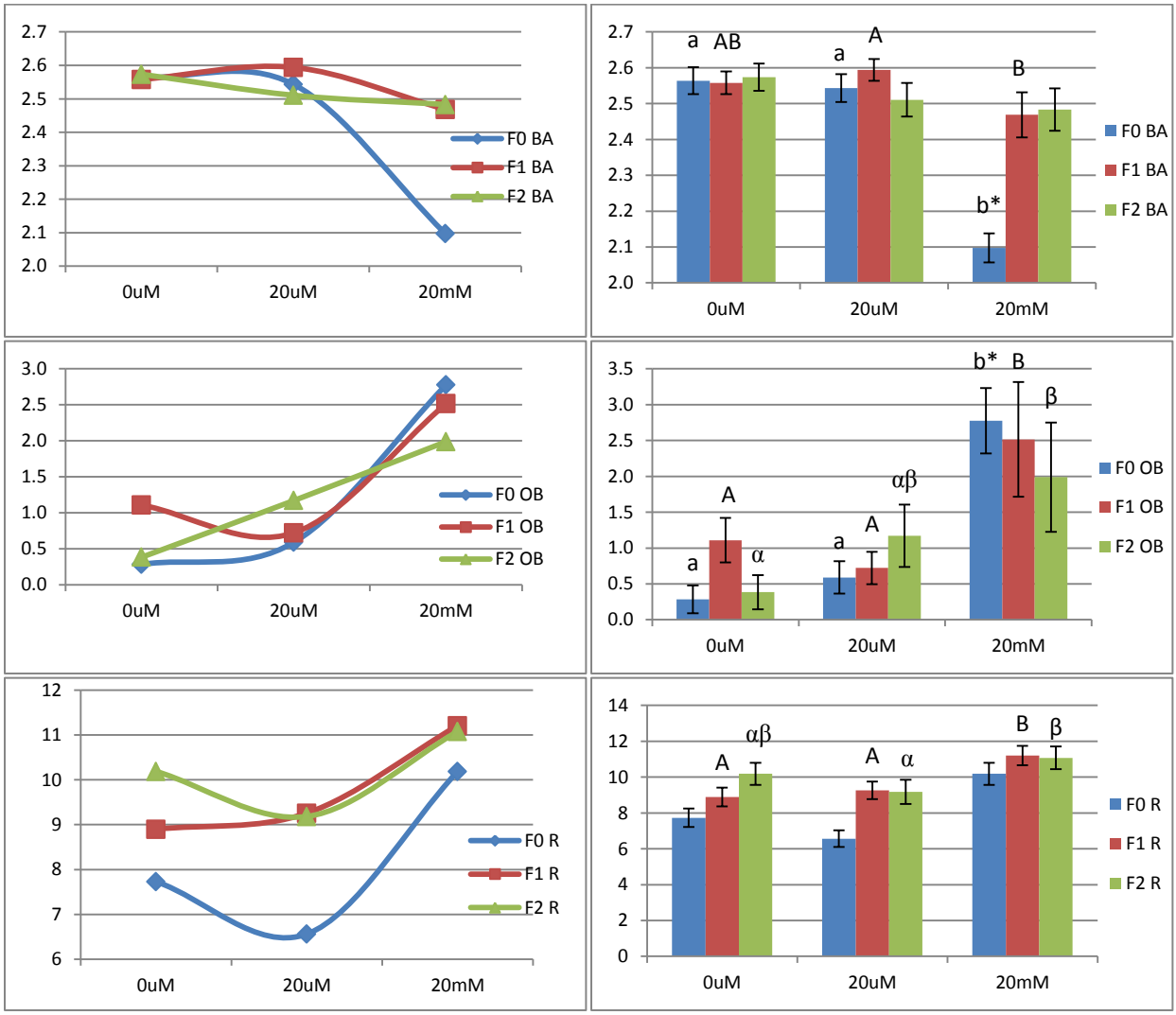

Figure 2.4: An overview of the variation in the patterns of body bends and reversal behavior in L4 hermaphrodite *C. elegans* as a function of nicotine dose across the three generations. BA: Bending angle; OB: Omega bend; R: Reversals. In the bar graphs, bars from left to right represent F0, F1, and F2 generations, respectively. Pairwise comparisons were performed among treatment groups within same generation. (ab), (AB), (αβ) are for F0, F1, and F2, respectively. Different letters correspond to statistically significant differences. (P*)≤0.001.

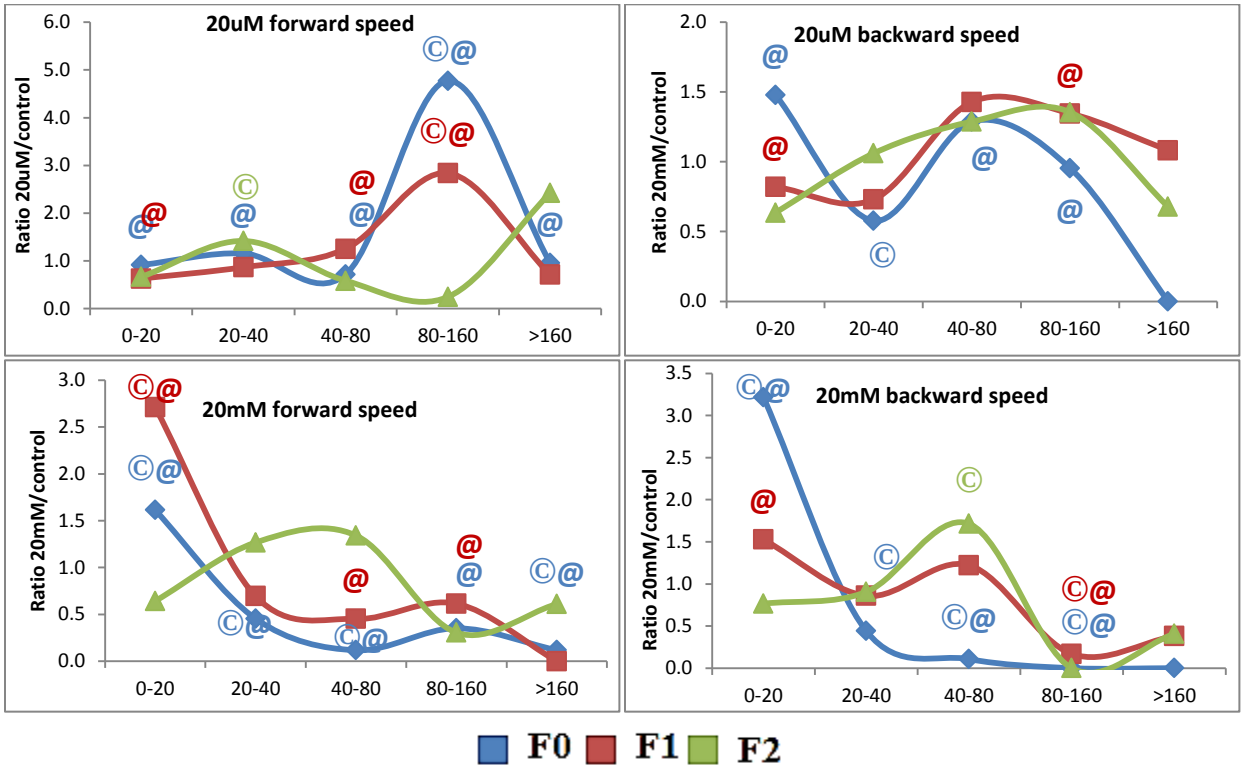

Figure 2.5: The impact of nicotine on the forward and backward speed (um/s) in L4 *C. elegans* hermaphrodites. The y-axis represents a ratio calculated from the proportion of worms in each treatment group normalized to control. (©) represents P<0.05 with respect to control. (@) represents P<0.05 with respect to the other nicotine treatment group. It represents a ratio calculated from the proportion of worms in each treatment group normalized to control. The x-axis represents speed (um/s) divided into 5 ranges.

Chapter Three: Chronic Nicotine Exposure Systemically Alters MicroRNA Expression Profiles during Post-embryonic Stages in *C. elegans*

Abstract

Tobacco smoking is associated with many diseases including addiction, which is of the most notorious. The tobacco dependence is mostly attributed to nicotine, which is considered one of the most addictive chemicals. In our study, we chose *C. elegans* as a biological model to systemically investigate the effect of chronic nicotine exposure and their regulated biochemical pathway. Nicotine treatment (20μM and 20mM) was limited to the post-embryonic stage from L1-L4 (~31 hours) period after which worms were collected for genome-wide miRNA profiling. Our results show that nicotine significantly altered the expression patterns of 40 miRNAs. The effect was proportional to the nicotine dose and was expected to have an additive, more robust response. Based on pathway enrichment analysis coupled with nicotine-induced miRNA patterns, we inferred that miRNAs as a system mediates "regulatory hormesis", manifested in biphasic behavioral and physiological phenotypes. We proposed a model where nicotine addiction is mediated by miRNAs' regulation of fos-1 and is maintained by epigenetic factors. Thus, our study offers new insights for a better understanding of the sensitivity of early developmental stages to nicotine.

Key words: nicotine, miRNA, *C. elegans*, dose-dependent, redundancy, addiction, regulatory hormesis, biphasic response, post-embryonic exposure

Introduction

Serious research has been devoted to dissect the factors involved in gene regulation and has provided clues concerned with the environmental contribution in shaping physiological phenotypes. MicroRNAs are an extensive class of newly discovered small regulatory RNAs. Over 200 and 1000 miRNAs have been sequenced in *C. elegans* and Humans, respectively. Due to their conserved and pleiotropic roles in gene regulation processes ((Ambros 2003; Aukerman and Sakai 2003; Chen, et al. 2004; Kim 2005; McManus 2003), miRNAs are considered biomarkers of an innate response to environmental fluctuations. Several studies have reported nicotine-induced alterations of miRNAs in different biological systems (e.g. PDLSC (Ng, et al. 2013), mouse fetal neuroepithelial precursors (Balaraman, et al. 2012), rodents and PC12 cell model (Huang and Li 2009), canines (Shan, et al. 2009), humans (Kassie, et al. 2010; Shin, et al. 2011)) (Table3.1) . Nicotine-induced miRNA alterations were associated with its negative effect on stem cell regeneration (Ng, et al. 2013). It was a tumorigenic agent as it upregulated oncogenic miRNAs (e.g. miR-16nd miR-21) in AGS cells (Shin, et al. 2011). Nicotine also antagonized and upregulated ethanol-induced miRNAs (Balaraman, et al. 2012). Interestingly, a study done by Huang and Li demonstrated the role of miR-140* in nicotine addiction using rodents and PC12 cells. The researchers showed that miR-140* targeted dynamin, the latter of which is crucial for neuronal plasticity and hence addiction-related processes (Huang and Li 2009). Taken collectively, these studies show a role or miRNAs in nicotine-dependent mechanisms. We were interested in investigating molecular mediators of nicotine-addiction in the larval stage in *C. elegans*. MicroRNA research is still in the juvenile stages, thus preliminary studies would follow a top-to-bottom approach to study the effect of nicotine on the global miRNA profile. Broad approaches like the latter provide more specific information about

miRNAs that were more highly altered in response to nicotine. To our knowledge, no previous study has been done on the impact of nicotine on the systemic miRNA expression in L4 *C. elegans* (N2). Our study offers new molecular insights related to the vulnerability of post-embryonic stages to chronic nicotine exposure. The systemic miRNA profiling was coupled to target enrichment analysis funneled down our interpretation to specific pathways that might be relevant to nicotine's mechanism of action. Our aim is to identify possible miRNA patterns that are linked to nicotine-induced behavioral (e.g. addiction) and protein disorders (e.g. receptor desensitization).

Material and Methods

Chemicals and Strains

Purified nicotine was purchased from Acros Organics (New Jersey, USA). 1 M and 0.001 M stocks were prepared by diluting nicotine in phosphate buffer. Nicotine solution was introduced to molten NGM agar (Stiernagle 2006) before being poured onto plates. NaCl, peptone, agar and water mixture were first autoclaved and kept at 70 °C covered under the hood. Equal amounts were transferred to individual small autoclaved flasks cooled and kept at 55 °C. After the addition of cholesterol, $CaCl_2$, $MgSO_4$ and KH_2PO_4, nicotine solution was added to give the corresponding final concentrations 20µM and 20mM in the medium.

C. elegans hermaphrodite N2 Bristol wild type was used. Maintenance and worm transfer were done after NGM plates were seeded with OP50 and left to dry (around 10-15 minutes), and then kept at 20^{o}C. *E. coli* stocks were stored as an LB pellet at -20^{o} C.

Egg synchronization was done via bleaching according to a standard method with slight modification (Sulston and Hodgkin 1988b). Briefly, adult gravid worms were washed off the plate with M9 buffer into a 15 ml Falcon tube (for a medium sized pellet). Then the Falcon tube

was centrifuged at 2000 rpm for 2 minutes, respectively. The supernatant was then removed leaving the pellet. The wash was then repeated with 5 ml M9 followed by centrifugation and supernatant removal. Then, 5 ml of synchronization solution was added. The tube was shaken for 4 minutes until the adult worms burst leaving the eggs dispersed in solution (a maximum of 4-5 minutes in bleach solution). The tubes were then spun at 2000 for 2 minutes. The supernatant was removed and three to four 5-ml M9 washes followed leaving the last wash without centrifugation. The tubes with the suspended eggs were placed on a shaker in the 20^{o}C incubator for 14-18 hours maximum (to avoid starvation). After hatching, the progeny were all stuck at L1. The latter were seeded plated onto treatment plates accordingly supplied with fresh OP50. Exposure lasted around 31 hours until end of L3-beginning of L4.

miRNA expression profile

Total RNA extraction was performed for all treatment groups according to protocol using mirVana™ miRNA Isolation Kit. Briefly, the sample was denatured using a lysis buffer. RNA was then separated from DNA and other proteins via acid-phenol extraction. Then, ethanol was added to the sample followed by centrifugation to allow it to pass through a glass-filter. Several washes preceded the elution of the RNA with DNase/RNase-free water. RNA quantification and evaluation was done using the NanoDrop ND-1000 Micro-Volume UVVis Spectrophotometer (NanoDrop Technologies, Wilmington, DE).

Reverse transcription was performed using TaqMan microRNA Reverse Transcription kit (Applied Biosystems, Foster City, CA) to reverse transcribe extracted RNA to cDNA for all 231 miRNAs . A total of 200ng of RNA was used for each RT reaction. The reactions were then run using thermal cycler for 16^{o}C for 30 min followed by 42^{o}C for 30 min, 85^{o}C for 5 min and was

finally held at 4^{o}C. The samples were then diluted in 80µL DNase/RNase-free water for qRT-PCR.

The expression levels of miRNAs were analyzed after performing qRT-PCR on 384-well-plate using the ViiA^{TM} Real-Time PCR System (Applied Biosystem). Briefly, each well carried a 15µL reaction of 5.5µL DNase/RNase free water, 7.5µL SYBR Green master mix, 1µL diluted cDNA, 1µL primer mix. A minimum of 3 biological replicates were used. The reaction was carried out for 10 min at 95^{o}C for enzyme activation followed by denaturation for 15 sec at 95^{o}C and an annealing/extension step for 60 sec at 60^{o}C. The latter 2 steps were repeated for 40 cycles.

The Ct values from the qRT-PCR were exported to an excel file. The average of the total miRNA (231) Ct-values was used for normalization. The delta Ct (ΔCt) values were calculated as $Ct_{(miRNA)}$-$Ct_{(avg\ miRNAs)}$. The delta delta Ct (ΔΔCt) was calculated as the difference in the ΔCt values between control and treatment. Then the fold change was calculated as $2^{(\Delta\Delta CT)}$. Statistical analysis was based on *t*-test for independent samples via SPSS(20). The results were further narrowed based on two criteria. Only the genes whose expression changed with a $P<0.05$ and a fold change$\geq$0.5, when compared to control, were considered as differentially expressed and were subjected to further analysis.

Fold change values ($2^{(\Delta\Delta CT)}$-1) were used to construct heat maps coupled with non-supervised hierarchical clustering using Euclidean distance and single linkage analysis and included all genes and samples. The latter approach was done for both total miRNAs as well as miRNAs that underwent statistically significant expression alterations using MeV (MultiExperiment Viewer) (AI, et al. 2006; Schmittgen, et al. 2008).

Target prediction and pathway analysis

miRNAs that showed fold changes higher than ±1 were used to perform target prediction using mirSOM software (Heikkinen, et al. 2011). To prepare the input for analysis, duplicates were removed and thus only unique values of targets with perfect seed match were used. The predicted targets were ranked according to the frequency of occurrence in the originally compiled gene list. Such a frequency reflects the number of miRNAs predicted to target a gene. The list was used as input for DAVID (Huang, et al. 2009a; Huang, et al. 2009b) for analysis. Gene ranking was based on functional annotation clustering (highest stringency) provided by DAVID. Target genes belonging to clusters with enrichment values ≥2 were used based on the order of the clusters to prepare a ranked list. The latter included 321 genes and was used as an input for GOrilla (process ontology) (Eden, et al. 2009). GOrilla provided DAG (directed acyclic graph) showing relationships among enriched processes. miRNA-target networks were constructed using cytoscape (Smoot, et al. 2011).

Results

Genome-wide miRNA expression profiling

We studied the effect of nicotine on the expression levels of 231 miRNAs in L4 *C. elegans* (N2). The average of the total miRNA expression remained constant between control and each treatment group (Figure 3.1A). Thus, it was considered for normalization of the Ct values for the 231 miRNAs. Fold change values were calculated in comparison to control and were used to construct a heat map. After performing unsupervised hierarchical clustering, the high concentration treatment groups clustered together (Figure 3.1C). On the other hand, the low concentration treatment groups were ordered next to each other without being clustered.

Complimentarily, the expression graphs of all miRNAs across treatment groups showed less variation in worms treated with the higher nicotine concentration in comparison to those treated with the lower one (Figure 3.1B).

We investigated if nicotine was associated with a statistically significant alteration in the miRNA patterns. As explained above, miRNAs whose expression changed by more than 0.5 folds with ($P<0.05$) were considered. In total, nicotine affected the expression of 40 miRNAs (17.3%) whose expression changed significantly and was consistent within and between control and treatment groups (Figure 3.1B). Then, the same unsupervised hierarchical clustering was performed coupled with leaf optimization for both miRNAs and samples (Figure 3.1D). We noticed that the upper-limit distance for sample clustering decreased by about 31% due to the decrease in inter-sample variations. Similarly, groups exposed to the high nicotine concentration clustered together, while those exposed to the lower concentration still showed more variation and were therefore only closely ordered. In addition, taking the 1.39 distance as a cutoff, the miRNAs were binned into two major clusters. The smaller one included 8 miRNAs (mir-1820, mir-358St, mir-55, mir-259, mir-235, mir-58, mir-1821, and lin-4). The remaining miRNAs belonged to the second bin except for mir-2220 that clustered separately. Opposite patterns were characteristic of the two clusters. MicroRNAs belonging to the larger cluster were mostly upregulated (red color) in the worm groups exposed to the higher nicotine concentration (20mM), while they were variable in the lower nicotine treatment groups. Also, miRNAs belonging to the smaller cluster were more downregulated in response to higher nicotine treatment than they were in response to the lower nicotine concentration.

Quantitative assessment of differentially regulated miRNAs

Three miRNAs were altered in response to the lower nicotine concentration (20µM). MiR-80 and miR-79 were upregulated by 1 (P=0.045) and 0.9 (P=0.022) fold, respectively. Conversely, the expression of miR-230* decreased by 0.5 fold (P=0.019). On the other hand, the expression of thirty eight miRNAs changed with statistical significance in worms treated with high nicotine concentration (20mM). The fold changes and p-values are shown in (Table 3.2). About 78% of the altered miRNAs were upregulated with fold changes ranging from 0.5 to 3 folds. The most upregulated miRNAs were miR-2220 with 3.4 fold change (P=0.034) followed by mir-90 (P=0.045) and mir-2210 (P=0.03) with >1.5 fold change. Other miRNAs, such as mir-47* (P=0.027), mir-2216* (P=0.034), mir-49 (P=0.019), mir-38 (P=0.004), mir-255(P=0.003), mir-1829b (P=0.037), mir-785(P=0.003), mir-241 (P=0.017) and mir-242 (P=0.035) were up-regulated by at least 100%.The remaining 22% miRNAs that were affected by the 20mM nicotine treatment were downregulated by 30% to 50%. The most downregulated miRNAs were mir-58 (P=0.014) followed by mir-1821 (P=0.03) and lin-4 (P=0.002) (Table 3.2). In addition, miR-80 was the only miRNA upregulated in both low and high nicotine concentrations (Figure 3.2).

Functional analysis of differentially expressed miRNAs through target prediction and biochemical pathways analysis

Systematic miRNA→gene prediction→pathways

To investigate the potential function of these differentially expressed miRNAs in response to nicotine, we performed miRNA target prediction coupled with enrichment analyses based on two online software, DAVID and GOrilla. 13 miRNAs, with $\geq \pm 1$ fold changes, were

used for target prediction. The number of gene targets varied among those miRNAs from tens to hundreds. In decreasing order, mir-47* was predicted to target 549 genes followed by mir-785 (521), mir-80 (501), mir-255 (265), mir-241 (224), mir-90 (167), mir-2220 (148), mir-2210 (140), mir-49 (127), mir-1829b (89), mir-38 (72), mir-242 (55), and mir-2216* (19) (Figure 3.4B). A unique list of 2395 genes was used as input for DAVID analysis. After functional annotation clustering, a ranked list of 321 genes was prepared based on the decreasing order of clusters with enrichment values ≥2.

DAG computed by GOrilla showed the enrichment of 5 major hubs (Figure 3.3). The "biological regulation" (1.6, $P<10^{-5}$), was generally divided into a molecular level summarized by metabolic and biosynthetic processes (e.g. RNA) and gene regulation (e.g. transcription). The second sub- level covered cellular and behavioral phenotypes such as neurogenesis and locomotion and location, respectively. Another major hub involved "response to stimulus" (2.3, $P<10^{-5}$) which was linked to neuro-related pathways through taxis. The highest enrichment was reported for immunity (56.8, $P<10^{-5}$) and was mainly reflected by response to other organisms (i.e. fungus). Also, one of the upstream nodes was "cellular process" (1.11, $P<10^{-5}$) and it branched to include growth, development, projection and organization, and recognition (e.g. axon guidance). The highest statistical significance was observed for "metabolic process" (1.17, $P<10^{-7}$) which comprised protein and phosphate-related modifications, single organism processes, and primary metabolism.

Enriched processes→genes→miRNAs

A bottom-top approach was then used to check the involvements of each of the 13 miRNAs in the enriched processes. Hence, we extracted the genes involved in 94 pathways outputted in GOrilla with p-values < 10^{-3} (Figures 3.3 and 3.4). Then, we overlapped them with the predicted

targets for each of the 13 miRNAs. miR-47* was the only miRNA predicted to target genes belonging to all of the 94 pathways. In decreasing order, mir-80, mir-255 and mir-241 covered 93%, 85%, and 82% of the processes and had a similar involvement pattern that did not include some cellular processes (e.g. recognition, migration, development, growth). A slightly different pattern was observed for mir-785 and mir-2220 which covered 75% and 62% of the pathways, respectively, but were not involved in immunity and development. The situation was the same for mir-38 (62%) and mir-90 (57%), but both were also less involved in response to stimulus. Four of the remaining miRNAs [mir-49 (37%), mir-2210 (32%), mir-1829b (18%), and mir-242 9%)] were not predicted to target genes involved in the nucleotide metabolism and biosynthesis or gene regulation. Instead, the target genes were more concentrated around protein metabolism and modifications as well as response to stimulus. Finally, mir-2216* did not show any match with any of the functions.

Commonly targeted genes

Network construction for all the 13 highly altered miRNAs with the total target list revealed a very complex network as seen in (Figure 3.5A). A simpler network was obtained after considering only the 13 commonly targeted genes (Figure 3.5B). Based on the originally compiled unique target list, only F40F11.2 (0.04%) was predicted to be targeted by 5 miRNAs. 0.5% of the genes were commonly targeted by 4 miRNAs, while 2% and 14% were common targets for only 3 and 2 miRNAs, respectively. Only the genes targeted by at least 4 miRNAs were used in network construction. From the most to least involved, mir-47* was predicted to target all 13 genes. Mir-785 targeted all except for B0336.3. All of the 8 genes targeted by mir-241 (B0336.3, C48A7.2, ceh-44, fos-1, let-75, ptc-1, sem-4, and tag-97) were common to mir-255. The latter also targeted F10D2.10 for a total of 9 genes. Also, ain-2, F40F11.2, sax-3, and

tsp-14 matched with mir-2210, whereas 1829b had only 3 and did not include F40F11.2. Finally, mir-80 matched with only one gene (B0336.3), while mir-49 and mir-242 targeted F40F11.2 and F10D2.10, respectively. Together, they comprised an intricate network as shown in Figure 3.5B. Complimentarily, we ran functional annotation via DAVID which summarized all functions associated with the genes of interest. The 13 genes were concerned with four major ontologies: development and growth, reproduction, metabolism and transcriptional regulation (Table 3.3).

Five major enriched functional hubs

GOrilla enriched for five major hubs that can be summarized as: biological regulation, response to stimulus, immune processes, cellular and metabolic processes. After overlapping miRNA-target genes with the corresponding functional hub, we constructed a network that depicted the relationship between most of the highly regulated miRNAs with enriched nicotine-induced biological pathways. The network reflected a "nicotine-butterfly effect", where most miRNAs were involved in the metabolic processes, while more specific miRNAs were involved in regulation of immune response (Figure 3.5C).

Discussion

Nicotine is a potent stimulant and a cholinergic agonist. There is no uniform standard molecular phenotype associated with nicotine. Its action is therefore not only context-dependent, but is also based on the dose and duration of its exposure (Schafer 2002).With smoking being so prevalent in countries in the Middle East (e.g. Lebanon), the chances of persistent nicotine exposure among the younger groups remain high. Of notice, the highest ratio for male: female teenage smokers reached 66:54% in 2010 (WHO 2012). Early developmental stages are more sensitive to any sort of stresses. When considering nicotine, the case is not different. It is

reported that even a limited nicotine exposure during adolescence may lead to symptoms of dependence and that this sensitivity might be due to the neurochemical changes in the brain that is different from those of adults (CDC 2010; Slotkin 2002). Consequently, children exposed to nicotine are more prone to become smokers when they grow up, therefore initiating a vicious cycle of nicotine usage. We were interested in assessing the extent of the nicotine-induced alterations on simpler organisms such as *C. elegans* that enables extrapolations to higher organisms. In *C. elegans,* it has been documented that nicotine treatment is associated with hyper-contraction of body wall-muscles, stimulation of egg laying, increased pharyngeal pumping as well as a decrease in the efficiency of male spicule in mating (Matta, et al. 2007; Schafer 2002). However, no previous studies have investigated the impact of nicotine on the genome-wide miRNA profile. In our study, we limited nicotine exposure to the post-embryonic stage and investigated miRNA patterns as well as target predictions and networks occurring in the L4 stage in response to nicotine. Here we report that nicotine altered the expression of 17% of total miRNAs, most of which (78%) were dramatically upregulated in response to high nicotine concentration. Also, the degree of statistically significant upregulation ranged between 0.5 and 3.4, while that of the downregulation was less than 1 fold in both treatment groups.

Comparison between nicotine-induced behavioral versus miRNA responses

From the behavioral perspective, it has been reported that different nicotine concentrations and exposure durations correlated with a "biphasic" response in the treated organisms. The mean speed increased in worms exposed to lower nicotine concentrations (10-100µM). On the contrary, the mean speed decreased when exposed to higher nicotine concentrations (10-30mM) (Sobkowiak, et al. 2011). Nicotine psychopharmacologic effects can stimulate or depress a variety of processes (e.g. central and peripheral nervous, cardiovascular,

endocrine systems) (USDHHS 1988). All together were summarized as dose-dependent psychoactive effects (Shadel, et al. 2000) ranging from skeletal muscle relaxation, increases in brain serotonin and pituitary hormone, etc. (USDHHS 1988) to symptoms like tremor, nausea, and weakness (Benowitz 1988). How does that overlap with molecular level alterations?

Unlike the behavior, the increasing nicotine doses did not cause an inverse miRNA expression pattern. However, the degree of fold change (1 versus 3.4 fold) as well was the number of altered miRNAs (1.3% versus 16.4%) increased with increasing nicotine concentrations. Such a dose-dependent response was also manifested in the heat map after hierarchical clustering by distinct color gradients for mir-2220 and the two other multi-miRNA clusters (Figure 3.1CD). Thus, the molecular miRNA response was proportional and can generally be approximated as hyperbolic as a function of nicotine dose.

Understanding the molecular basis of nicotine-induced behavior

The relation between molecular and behavioral levels can be described as "regulatory hormesis". In normal conditions, homeostasis prevails in an organism. After lower exposure of a stressor, it responds with moderation. Such an intermediate level of regulation (e.g. regulatory miRNAs) can be associated with a stimulatory or a beneficial phenotype. However, as the stressor increases, the regulative response is inflated and could become aberrant and depressive. An established example is the response to vaccination (e.g. positive reinforcing immunity) versus the response to primary exposure to high toxicant levels (e.g. overwhelmed immunity and shock) (Figure 3.6A).

Figures 3.4 and 3.5 reveal similar as well as distinct functional patterns associated with each of the most highly altered miRNAs. mir-2216* was not predicted to regulate any of the enriched processes, while mir-47St was the most pleiotropic miRNA. The remaining miRNAs

were involved in one or more of the enriched pathways. Also, mir-80 was the only miRNA whose expression was differentially altered in response to the lower nicotine dose. However, twelve other miRNAs were dramatically affected in response to the higher nicotine concentration. Eight of them, namely mir-90, mir-38, mir-2220, mir-785, mir-241, mir-255, mir-80, and mir-47St co-regulate common processes (e.g. transcription). Presumably, the additive effect of eight miRNAs is associated with a more robust phenotype. For example, nicotine alters the expression levels of acetylcholine receptors. A small increase or decrease in the cell surface receptors might be associated with increased receptivity or saturation and therefore a resulting excitation of the downstream pathways such as muscle contraction. Conversely, a dramatic upregulation or depression in the transcription of the receptors might lead to a permanent transduction or an inhibition of the signal. Such is consistent with previously reported studies where nicotine increased muscle contraction, egg laying and hindered male reproduction behavior at lower levels, finally leading to muscle paralysis at high concentrations (Feng, et al. 2006; Sobkowiak, et al. 2011; Waggoner, et al. 2000).

Interestingly, mir-80 belongs to the mir-58 family that includes mir-58, mir-80, mir-81, mir-82, and mir-1834 (Alvarez-Saavedra and Horvitz 2010). The deletion of mir-80 was associated with healthy ageing, decrease in body and brood size (Vora 2011). Therefore, one can anticipate a generally reversed phenotype in L4 worms exposed to nicotine during their larval stages. Nicotine can therefore have a negative effect on lifespan, while it alters the body size and reproduction and such can be partially mediated by nicotine-induced mir-80 upregulation.

Nicotine induces addiction

A more holistic approach takes into consideration all miRNAs as a system. A slight trigger can be inductive to certain pathways, while strong stimuli can render the system

hyperactive and eventually problematic. However, induction is not necessarily positive as it may initiate or promote the activation of pathological pathways (e.g. drug dependence). Thus, it is intriguing to understand nicotine-linked phenotypes, particularly at the lower doses. Indeed, nicotine did cause an increase in locomotion and egg laying in *C. elegans* at 20µM. However, nicotine is also very addictive. Addiction is defined as a maladaptive form of neuroplasticity. The latter refers to the ability to adapt and respond to fluctuations in the environment. It promotes seeking and recognizing effectors important for survival while avoiding dangerous signals. However, long periods of stress (e.g. drugs of abuse) cause structural (e.g. alterations in receptors) as well as molecular changes (Nestler 2001; Robinson and Kolb 2004).

Gene expression is regulated by a variety of players such as transcriptional factors. The Fos family of transcription factors is important for the induction and maintenance of long-term plasticity and is induced and stabilized in response to wide range of acute stimuli, while it is desensitized after chronic treatment (e.g. drugs of abuse). Histone modifications have been reported to have a role in promoting the transient versus permanent transcriptional states for fos-1(Maze and Nestler 2011).

Fos-1 has a role in dendrite development. In drosophila single neuron model, fos-1 related alterations was restricted to only a small time window during development and was not recapitulated when introduced during adulthood (Vonhoff, et al. 2013). Interestingly, in our study, fos-1 was one of the genes predicted to be highly targeted (≥4 miRNAs) and might thus mediate an "addiction-like" behavior in *C. elegans* larvae. As a conclusion, we hypothesized a model that might explain nicotine addiction phenotype (Figure 3.6B). Chronic nicotine treatment limited to the post-embryonic stages alters miRNA expression levels (e.g. mir-47*, mir-241, mir-255, and mir-785) which negatively regulate fos-1 expression. The downstream effects would be

remodeling of dendrite branching and disruption in axon guidance and other neurotransmitters and receptors. As conclusion, the effect of miRNAs on fos-1, complemented by epigenetic modifications, may mediate nicotine addiction initiated during post-embryonic stages.

Finally, the highest shift in nicotine-induced fold changes was observed for mir-2220. However, mir-2220 was not predicted to regulate any of the 13, highly targeted genes. Perhaps, when miRNAs act redundantly, the additive increase in their expression levels fulfills the finetuning of their targets in response to the environment. On the contrary, when a miRNA targets more specific genes, a more dramatic shift in its expression is observed to accomodomate and respond to the new condition.

We limited our analysis based on criteria described above in an attempt to buffer possible signal from noise. Our data showed that nicotine altered the profiles of several miRNAs predicted to have pleiotropic roles. Therefore, its impact would be expected to be extensive and involves major pathways. miRNAs are known to co-target many genes. Researchers interpreted such a phenomenon as a mean to fine tune gene expression and provide robustness against environmental perturbations. Rather than completely switching gene expression, miRNAs' impact is cumulative. Together they fine tune and stabilize regulatory networks to establish relatively normal physiologies in response to fluctuating environments (Li, et al. 2009).

References

Saeed, AI, et al.
2006 TM4 microarray software suite. Methods in Enzymology 411:134-93.

Alvarez-Saavedra, E., and H. R. Horvitz
2010 Many families of C. elegans microRNAs are not essential for development or viability. Curr Biol 20(4):367-73.

Ambros, V.
2003 MicroRNA pathways in flies and worms: growth, death, fat, stress, and timing. Cell 113(6):673-6.

Aukerman, M. J., and H. Sakai
2003 Regulation of flowering time and floral organ identity by a MicroRNA and its APETALA2-like target genes. Plant Cell 15(11):2730-41.

Balaraman, S., U. H. Winzer-Serhan, and R. C. Miranda
2012 Opposing actions of ethanol and nicotine on microRNAs are mediated by nicotinic acetylcholine receptors in fetal cerebral cortical-derived neural progenitor cells. Alcohol Clin Exp Res 36(10):1669-77.

Benowitz, Neal L.
1988 Pharmacologic Aspects of Cigarette Smoking and Nicotine Addiction. New England Journal of Medicine 319(20):1318-1330.

CDC
2010 The Biology and Behavioral Basis for Smoking-Attributable Disease: A Report of the Surgeon General.

Chen, C. Z., et al.
2004 MicroRNAs modulate hematopoietic lineage differentiation. Science 303(5654):83-6.

Eden, E., et al.
2009 GOrilla: a tool for discovery and visualization of enriched GO terms in ranked gene lists. BMC Bioinformatics 10:48.

Feng, Z., et al.
2006 A C. elegans model of nicotine-dependent behavior: regulation by TRP-family channels. Cell 127(3):621-33.

Heikkinen, L., M. Kolehmainen, and G. Wong
2011 Prediction of microRNA targets in Caenorhabditis elegans using a self-organizing map. Bioinformatics 27(9):1247-54.

Huang, da W, BT Sherman, and RA Lempicki
2009a Bioinformatics enrichment tools: paths toward the comprehensive functional analysis of large gene lists. Nucleic Acids Res 37(1):1-13.

—
2009b Systematic and integrative analysis of large gene lists using DAVID Bioinformatics Resources. Nature Protoc 4(1):44-57.

Huang, W., and M. D. Li
2009 Nicotine modulates expression of miR-140*, which targets the 3'-untranslated region of dynamin 1 gene (Dnm1). Int J Neuropsychopharmacol 12(4):537-46.

Kassie, F., M. Jarcho, and A. Endalew
2010 Abstract PR-06: Upregulation of microRNA-21 (miR-21) in human bronchial epithelial cells chronically exposed to 4-(methylnitrosamino)-1-(3-pyridyl)-1-butanone

(NNK) plus nicotine and modulation of these effects by diindolylmethane. Cancer Prev Res; ;3(1 Suppl):PR-06.doi: 10.1158/1940-6207.PREV-09-PR-06

Kim, V. N.
2005 MicroRNA biogenesis: coordinated cropping and dicing. Nat Rev Mol Cell Biol 6(5):376-85.

Li, X., et al.
2009 A microRNA imparts robustness against environmental fluctuation during development. Cell 137(2):273-82.

Matta, S. G., et al.
2007 Guidelines on nicotine dose selection for in vivo research. Psychopharmacology (Berl) 190(3):269-319.

Maze, I., and E. J. Nestler
2011 The epigenetic landscape of addiction. Ann N Y Acad Sci 1216:99-113.

McManus, M. T.
2003 MicroRNAs and cancer. Semin Cancer Biol 13(4):253-8.

Nestler, E. J.
2001 Molecular basis of long-term plasticity underlying addiction. Nat Rev Neurosci 2(2):119-28.

Ng, T. K., et al.
2013 Nicotine Alters MicroRNA Expression and Hinders Human Adult Stem Cell Regenerative Potential. Stem Cells Dev 22(5):781-90.

Robinson, T. E., and B. Kolb
2004 Structural plasticity associated with exposure to drugs of abuse. Neuropharmacology 47 Suppl 1:33-46.

Schafer, William R.
2002 Neuropsychopharmacology: The Fifth Generation of Progress. Lippincott, Williams, & Wilkins, Philadelphia, Pennsylvania section 2(Chapter 21).

Schmittgen, T. D., E. J. Lee, and J. Jiang
2008 High-throughput real-time PCR. Methods Mol Biol 429:89-98.

Shadel, W. G., et al.
2000 Current models of nicotine dependence: what is known and what is needed to advance understanding of tobacco etiology among youth. Drug Alcohol Depend 59 Suppl 1:S9-22.

Shan, H., et al.
2009 Downregulation of miR-133 and miR-590 contributes to nicotine-induced atrial remodelling in canines. Cardiovasc Res 83(3):465-72.

Shin, V. Y., et al.
2011 NF-kappaB targets miR-16 and miR-21 in gastric cancer: involvement of prostaglandin E receptors. Carcinogenesis 32(2):240-5.

Slotkin, T. A.
2002 Nicotine and the adolescent brain: insights from an animal model. Neurotoxicol Teratol 24(3):369-84.

Smoot, M. E., et al.
2011 Cytoscape 2.8: new features for data integration and network visualization. Bioinformatics 27(3):431-2.

Sobkowiak, R., M. Kowalski, and A. Lesicki

2011 Concentration- and time-dependent behavioral changes in Caenorhabditis elegans after exposure to nicotine. Pharmacol Biochem Behav 99(3):365-70.

Stiernagle, T.

2006 Maintenance of C. elegans. WormBook, ed. The C. elegans Research Community.

Sulston, J. , and J. Hodgkin

1988 Methods In: The Nematode Caenorhabditis elegans. (Ed.): W.B. Wood. Cold Spring Harbor Laboratory Press: New York 587-606.

USDHHS

1988 The Health Consequences of Smoking: Nicotine Addiction. US Government Printing Office, Washington, DC DHHS Publication No.CDC-88-8406.

Vonhoff, F., et al.

2013 Temporal coherency between receptor expression, neural activity and AP-1-dependent transcription regulates Drosophila motoneuron dendrite development. Development 140(3):606-16.

Vora, M.M.

2011 MicroRNA modulation of Caenorhadbitis elegans dietary restriction and longevity (PhD Dissertation). Retrieved from ProQuest Dissertations and Theses:301 pages; 3494602.

Waggoner, L. E., et al.

2000 Long-term nicotine adaptation in Caenorhabditis elegans involves PKC-dependent changes in nicotinic receptor abundance. J Neurosci 20(23):8802-11.

WHO

2012 World Health Statistics.Global Health Observatory. World Health Organization. Retrieved from http://www.who.int/gho/publications/world_health_statistics/EN_WHS2012_Full.pdf.

Yook, Karen, et al.

2012 WormBase 2012: more genomes, more data, new website. Nucleic Acids Research 40(D1):D735-D741.

Table 3.2: A summary of differential miRNA-fold change (±SE) in response to low (20µM) and high (20mM) nicotine treatments in L4 *C. elegans* (N2). (* and β) denote P<0.05 in response to high and low nicotine doses, respectively.

	Low			High		
	P value	Fold change ± SE		P value	Fold change ± SE	
***Lin4**	0.761	0.12 ±	0.34	0.002	-0.56 ±	0.08
***miR1018**	0.375	0.33 ±	0.29	0.013	0.54 ±	0.13
***miR1022**	0.491	0.67 ±	0.80	0.040	0.58 ±	0.12
***miR1817**	0.627	0.10 ±	0.18	0.038	0.70 ±	0.23
***miR1820**	0.861	-0.07 ±	0.36	0.000	-0.49 ±	0.03
***miR1821**	0.669	-0.15 ±	0.31	0.030	-0.58 ±	0.10
***miR1829b**	0.839	-0.13 ±	0.57	0.037	1.10 ±	0.36
***miR1833**	0.723	0.11 ±	0.26	0.018	0.82 ±	0.21
***miR2209a**	0.796	-0.08 ±	0.26	0.000	0.47 ±	0.02
***miR2210**	0.207	0.57 ±	0.31	0.030	1.55 ±	0.28
***miR2215**	0.772	0.09 ±	0.28	0.035	0.79 ±	0.15
***miR2216St**	0.235	1.05 ±	0.62	0.034	1.32 ±	0.25
***miR2218aSt**	0.814	0.07 ±	0.28	0.024	0.74 ±	0.12
***miR2218bSt**	0.405	0.52 ±	0.56	0.036	0.91 ±	0.29
***miR2220**	0.465	0.52 ±	0.58	0.034	3.44 ±	0.65
βmiR230St	0.019	-0.49 ±	0.07	0.600	0.27 ±	0.44
***miR235**	0.935	0.03 ±	0.28	0.043	-0.52 ±	0.11
***miR241**	0.753	0.16 ±	0.45	0.017	1.02 ±	0.14
***miR242**	0.469	0.47 ±	0.59	0.035	0.99 ±	0.19
***miR243**	0.371	-0.09 ±	0.08	0.025	0.64 ±	0.10
***miR255**	0.981	-0.01 ±	0.59	0.003	1.19 ±	0.14
***miR258**	0.351	-0.23 ±	0.19	0.021	0.47 ±	0.07
***miR259**	0.492	-0.14 ±	0.18	0.002	-0.49 ±	0.07
***miR358St**	0.316	-0.26 ±	0.23	0.023	-0.49 ±	0.08
***miR38**	0.359	0.23 ±	0.22	0.004	1.20 ±	0.08
***miR47St**	0.164	0.74 ±	0.34	0.027	1.34 ±	0.22
***miR49**	0.984	-0.01 ±	0.45	0.019	1.30 ±	0.18
***miR54**	0.712	0.07 ±	0.16	0.023	0.89 ±	0.14
***miR55**	0.081	-0.36 ±	0.11	0.003	-0.52 ±	0.03
***miR58**	0.623	0.19 ±	0.35	0.014	-0.67 ±	0.08
***miR76**	0.885	-0.06 ±	0.36	0.029	0.59 ±	0.10
***miR785**	0.220	0.47 ±	0.30	0.003	1.08 ±	0.16
***miR789**	0.076	0.64 ±	0.19	0.014	0.49 ±	0.12
βmiR79	0.022	0.86 ±	0.20	0.392	-0.11 ±	0.10
***miR794**	0.617	0.19 ±	0.33	0.000	0.56 ±	0.02
***miR798**	0.970	-0.01 ±	0.26	0.032	0.89 ±	0.16
***miR799**	0.512	-0.15 ±	0.19	0.014	0.46 ±	0.05
β*miR80	0.045	1.01 ±	0.30	0.011	0.86 ±	0.09
***miR800**	0.755	0.11 ±	0.31	0.016	0.60 ±	0.15
***miR90**	0.251	0.33 ±	0.23	0.045	1.69 ±	0.37

Table 3.3: A list of proposed genes that are targeted by ≥4 miRNAs. Gene descriptions were summarized from DAVID and WormBase (Yook, et al. 2012) .

Gene symbol	Description	Function
ain-2	ain-1 paralogue	no obvious function in mass RNAi assays. Belongs to GW182 protein family.
B0336.3		body morphogenesis, regulation of growth, regulation of growth rate, positive regulation of growth rate, positive regulation of growth
C48A7.2		reproductive developmental process, ion transport, phosphate transport, anion transport, intracellular protein transport, sex differentiation, protein localization, embryonic development ending in birth or egg hatching, protein transport, inorganic anion transport, vesicle-mediated transport, cellular protein localization, negative regulation of vulval development, regulation of vulval development, hermaphrodite genitalia development, establishment of protein localization, intracellular transport, regulation of post-embryonic development, negative regulation of post-embryonic development, genitalia development, cellular macromolecule localization
ceh-44	Homeobox	transcription, regulation of transcription, DNA-dependent, intra-Golgi vesicle-mediated transport, vesicle-mediated transport,regulation of transcription, intracellular transport, Golgi vesicle transport, regulation of RNA metabolic process
F10D2.10		Unknown function, lipase putative
F40F11.2		embryonic development ending in birth or egg hatching, oxidation reduction
fos-1	FOS (B-Zip transcription factor) homolog	cell fate specification, morphogenesis of an epithelium, reproductive developmental process, regulation of transcription, DNA-dependent, regulation of transcription from RNA polymerase II promoter, sex differentiation, positive regulation of biosynthetic process, positive regulation of macromolecule biosynthetic process, positive regulation of macromolecule metabolic process, positive regulation of gene expression, positive regulation of cellular biosynthetic process, regulation of gene-specific transcription, hermaphrodite genitalia development, positive regulation of gene-specific transcription, cell fate commitment, regulation of transcription, positive regulation of transcription, DNA-dependent, positive regulation of nucleobase, nucleoside, nucleotide and nucleic acid metabolic process, positive regulation of transcription, positive regulation of transcription from RNA polymerase II promoter, tissue morphogenesis, genitalia development, positive regulation of nitrogen compound metabolic process, regulation of RNA metabolic process, positive regulation of RNA metabolic process, regulation of syncytium formation by plasma membrane

		fusion, epithelium development
let-75	LEThal	nematode larval development, larval development, muscle system process, muscle contraction, post-embryonic development, embryonic development ending in birth or egg hatching, growth
ptc-1	PaTChed family	M phase of mitotic cell cycle, mitotic cell cycle, M phase, nuclear division, nematode larval development, larval development, cell cycle, mitosis, behavior, post-embryonic development, embryonic development ending in birth or egg hatching, molting cycle, protein-based cuticle, oviposition, molting cycle, collagen and cuticulin-based cuticle, reproductive behavior, cell cycle process, cell cycle phase, multicellular organism reproduction, reproductive behavior in a multicellular organism, growth, molting cycle, organelle fission, reproductive process in a multicellular organism, cell division
sax-3	Sensory AXon guidance	regulation of growth, regulation of growth rate, positive regulation of growth rate, positive regulation of growth
sem-4	SEx Muscle abnormal	behavior, oviposition, reproductive behavior, multicellular organism reproduction, reproductive behavior in a multicellular organism, regulation of growth, regulation of growth rate, positive regulation of growth rate, positive regulation of growth, reproductive process in a multicellular organism
tag-97	Temporarily Assigned Gene name	regulation of transcription, DNA-dependent, regulation of transcription, regulation of RNA metabolic process
tsp-14	TetraSPanin family	defense mechanisms

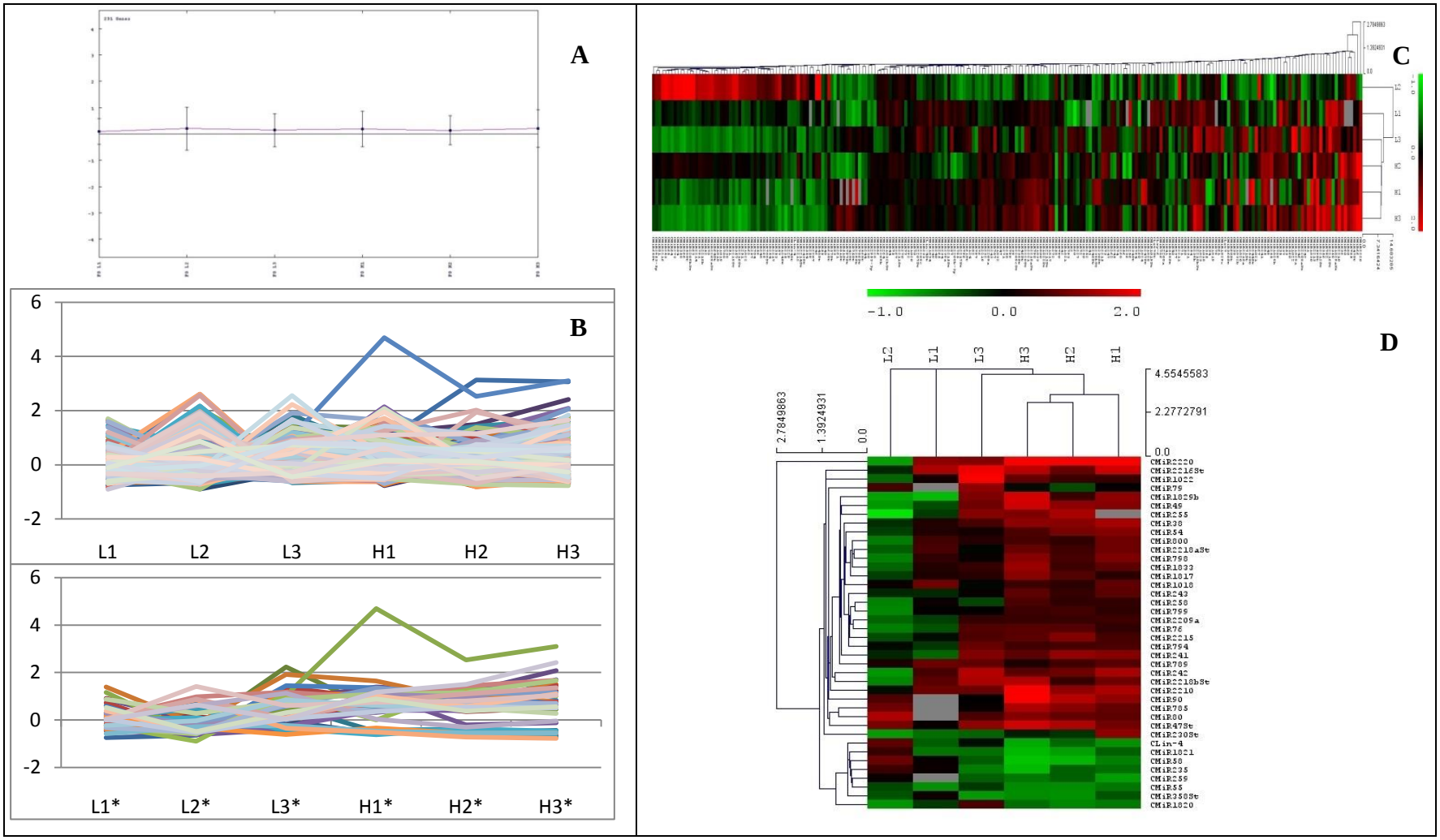

Figure 3.1 Analyzing nicotine-induced alterations in miRNA expression levels through heat map and hierarchical clustering. (A) Centroid graph showing the stability of the total mean fold change of the 231 miRNAs.(B) Expression graphs for 231 miRNAs (top) and 40 miRNAs that showed differential expression in response to nicotine (bottom). Each line represents one the expression of one miRNA across the treatment groups. (C) Heat map showing expression profiles of 231 miRNAs. (D) Heat map of 40 miRNAs considered to be differentially regulated. Hierarchical clustering was performed with Euclidean distance based on single linkage for each of the miRNAs among all the treatment groups. Note: from left to right, three biological replicates of each: 20µM (L), and 20mM (H) treatment groups. Each cell represents a MFC compared to control (Mean Fold Change: $2^{(\Delta\Delta CT)}$ -1). In the figures, color red, green, and black represnet up-regualtion, down-regulation and no change, respectively. Heat maps and clustering were done using Mev software.

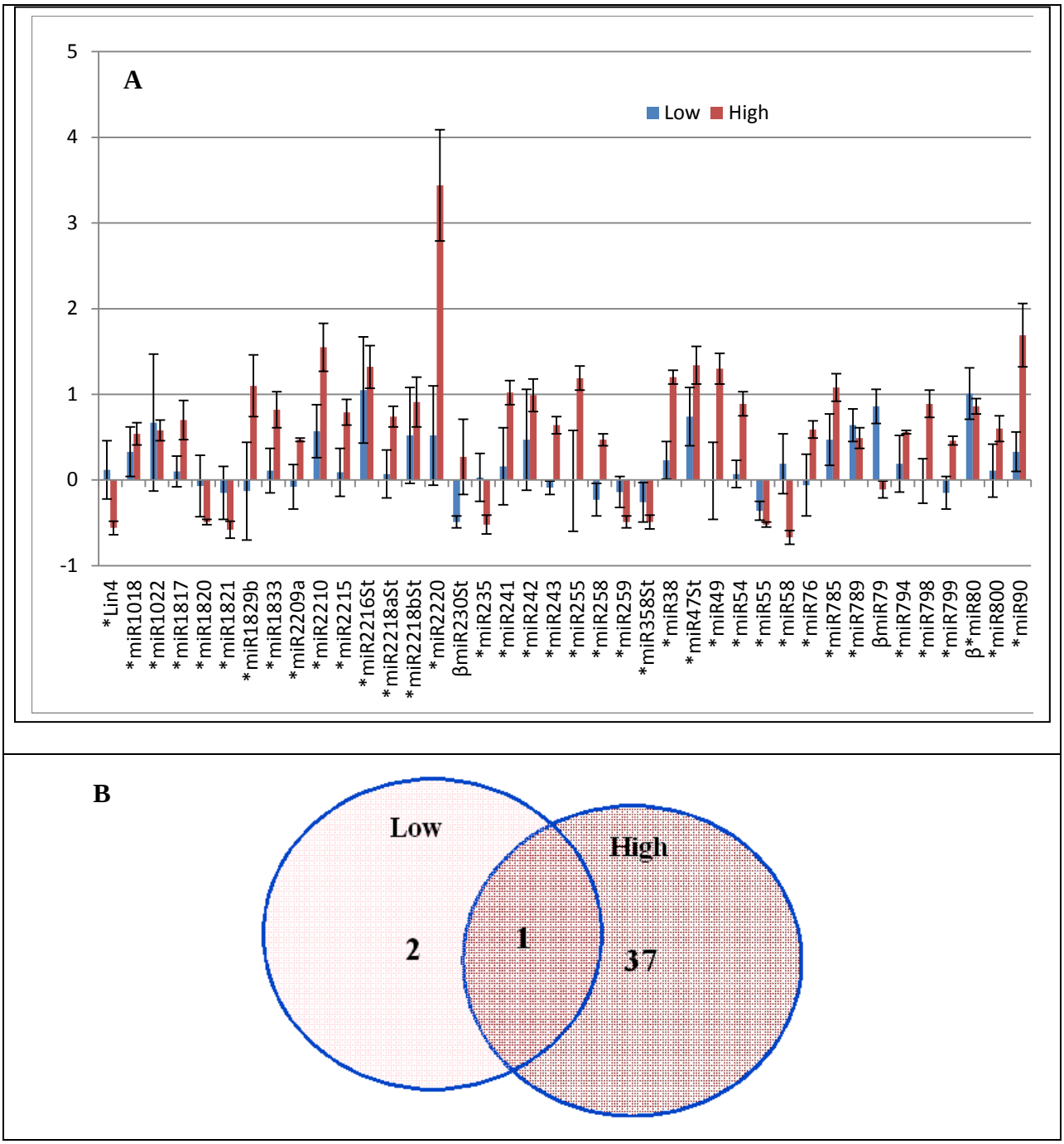

Figure 3.2: Nicotine treatment was associated with altered expression of 40 miRNAs in L4 *C. elegans* (N2). (A) miRNA expression is represented as fold change $2^{\Delta\Delta Ct}$. ($\Delta\Delta Ct=\Delta Ct_{control}-\Delta Ct_{treatment}$). miRNAs whose expression changes with a $P<0.05$ and fold change ≥ 0.5 and ≤ -0.5, respectively. (*) and (β) denote $P<0.05$ for the high and low treatment groups, respectively in comparison to control. B) Venn diagram showing the number of miRNAs whose expression was altered in response to low, high, or both nicotine concentrations.

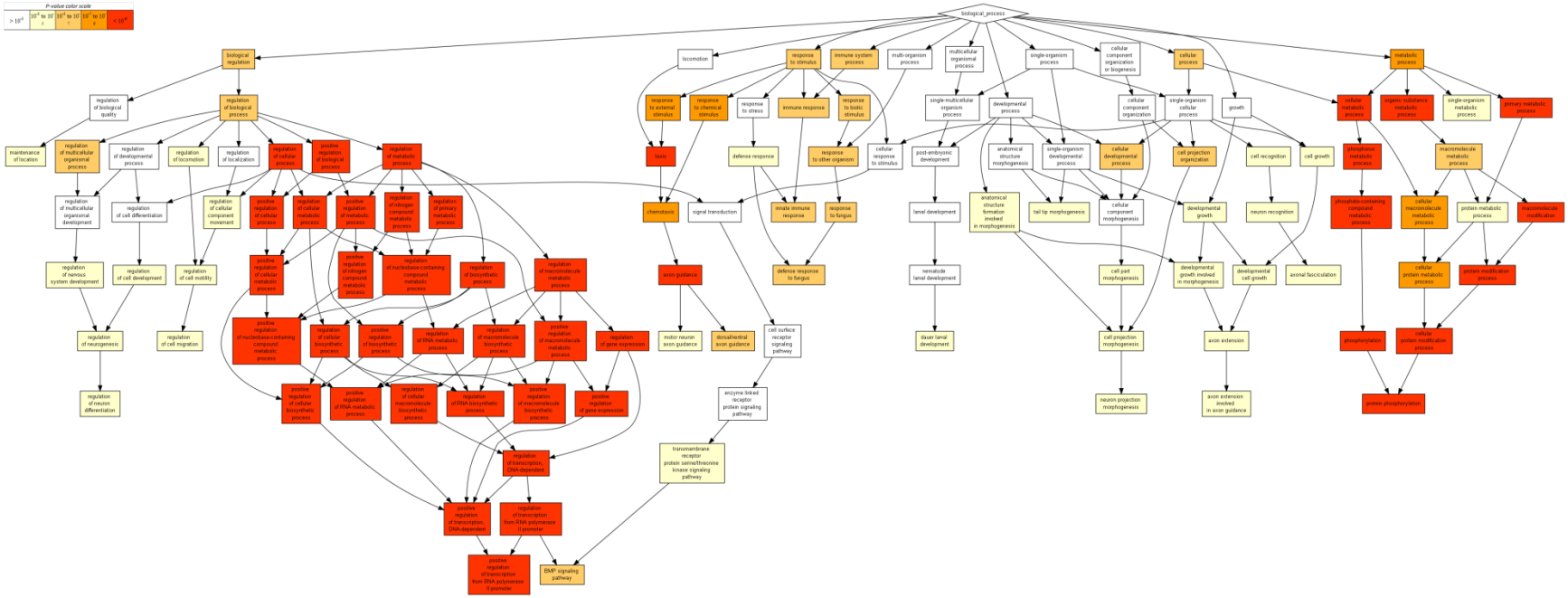

Figure 3.3: Directed acyclic graph (DAG) performed by GOrilla. It shows the relationships among the enriched pathways targeted by miRNAs altered in response to nicotine treatment. Colors represent P-values. From white to dark orange, P-values range from >10^-3 to <10^-9.

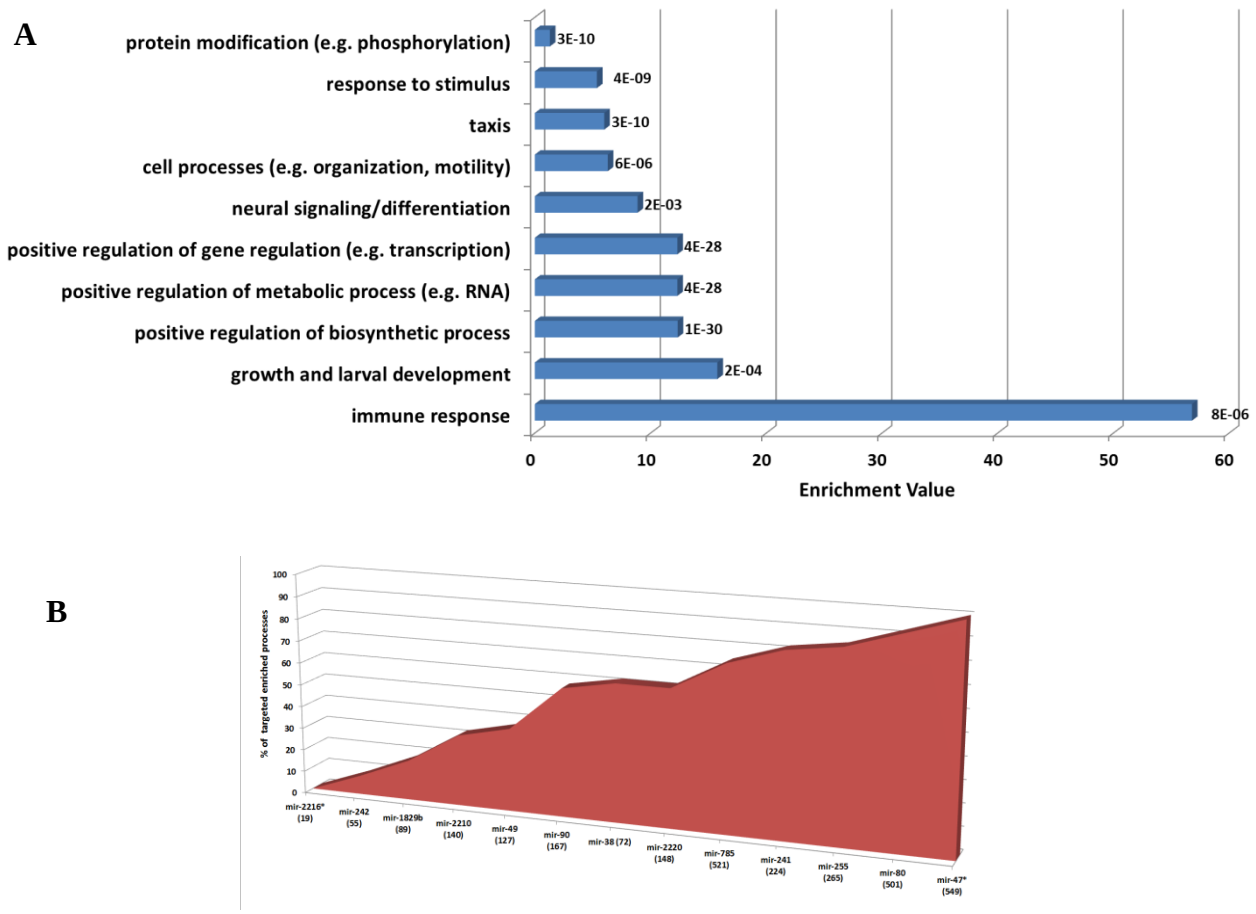

Figure 3.4: Nicotine-induced miRNAs differentially regulate five major biological pathways. (A) summary of pathways enriched by GOrilla based on the predicted target genes for the 13 most highly altered miRNAs (MCF>1). The data labels at the edge of each bar represent the p-values calculated for each enrichment value. (B) Functional distribution of the 13 most highly altered miRNAs in response to nicotine. Each miRNA was associated with none, one or more, or all of the enriched pathways. Next to each miRNA name ( ) is the number of targets predicted for each miRNA by mirSOM.

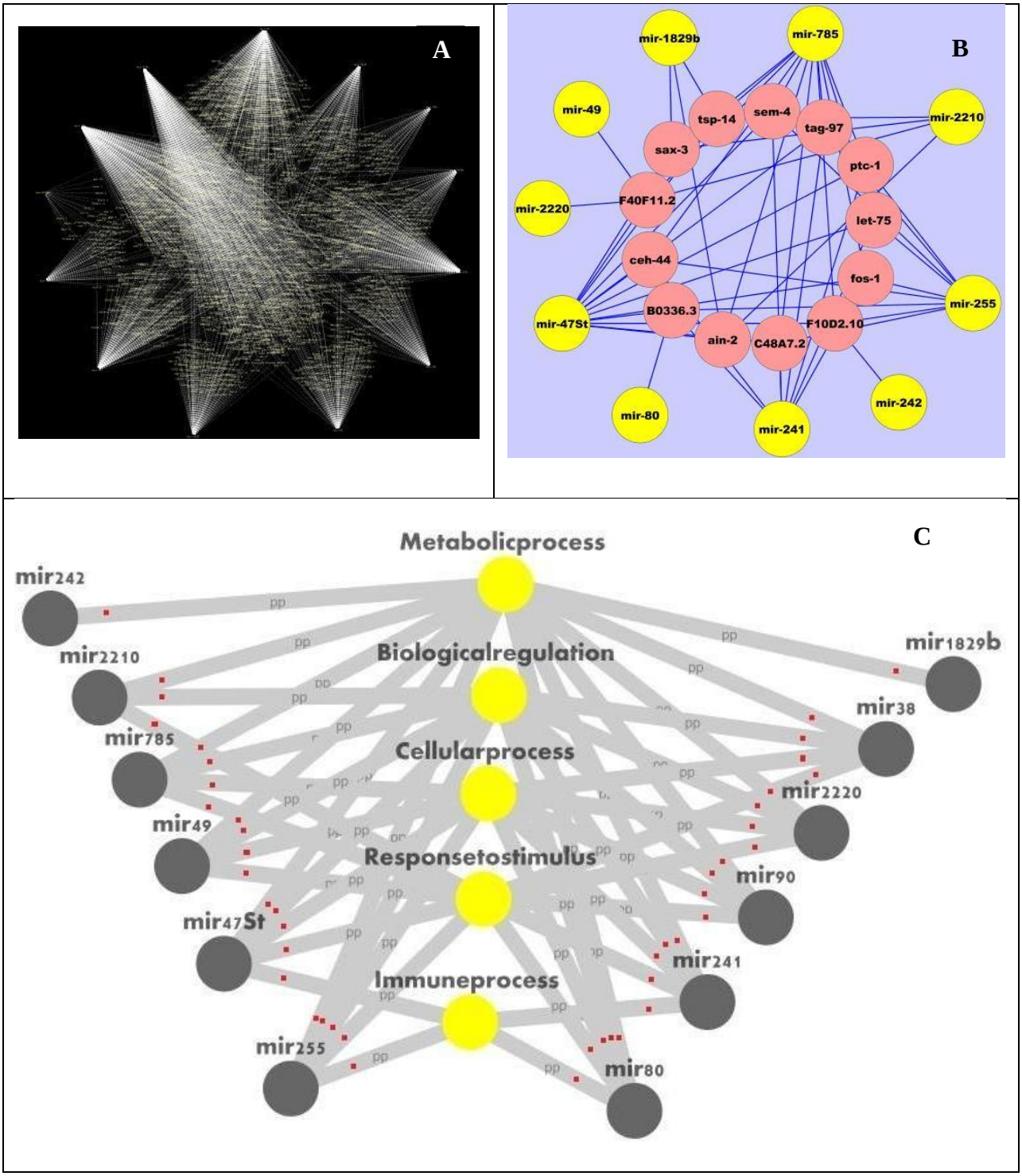

Figure 3.5: A miRNA-target network showing the pleiotropic and redundant nature of all of the highly altered miRNAs in response to nicotine treatment in L4 *C. elegans* (N2). (A) The network included 13 miRNAs and 2877 predicted targets. (B) Only genes commonly targeted by at least 4 of the differentially altered miRNAs were used. Thus 13 miRNAs and 13 gene targets were used to construct this network. (C) Nicotine-butterfly effect shows possible matches among each of the highly altered miRNAs with the five enriched functional hubs (GOrilla). Networks were constructed by Cytoscape. Each red dot represents a match between one miRNA and one hub.

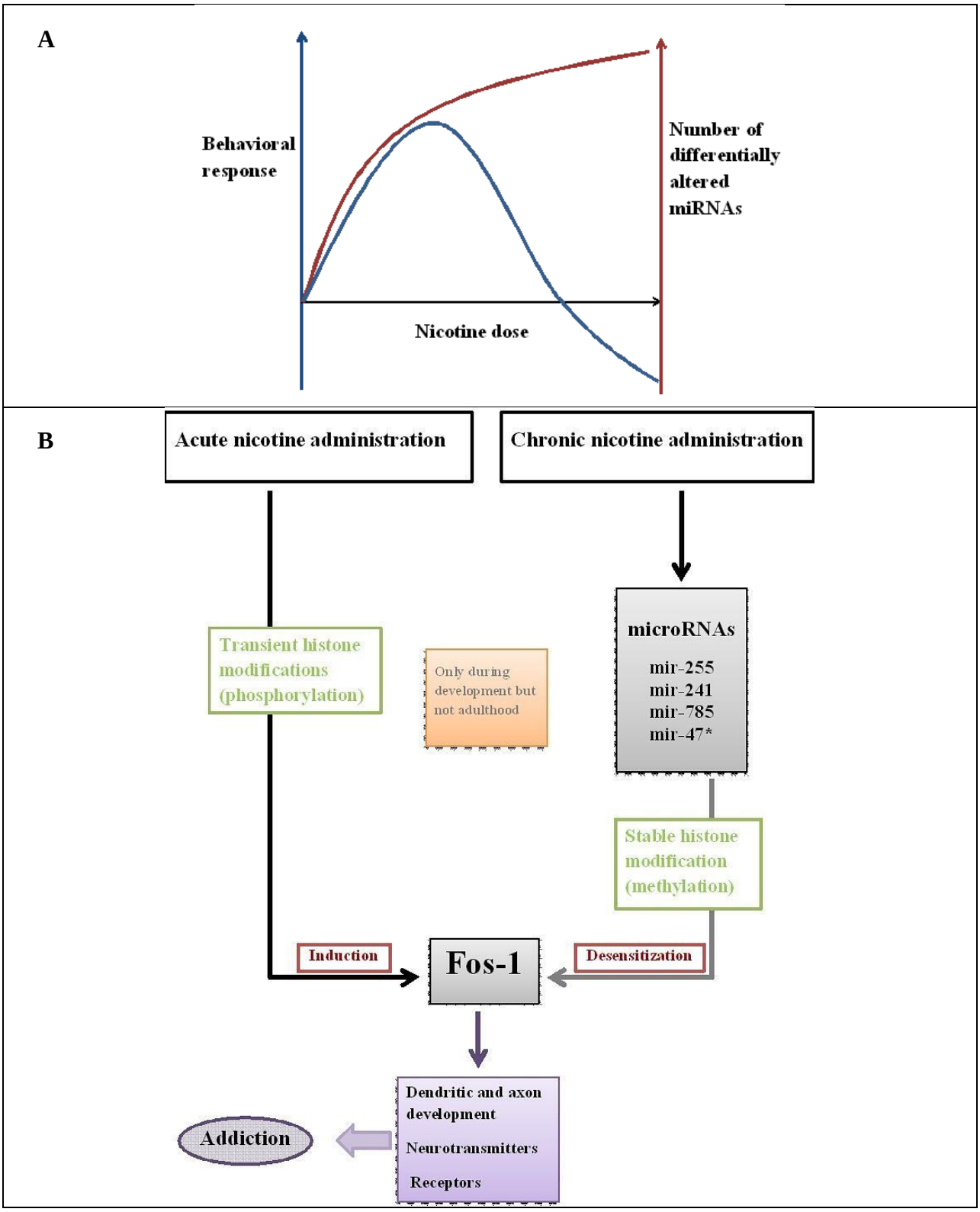

Figure 3.6: A miRNA system mediates "regulatory hormesis" and addiction. (A) As nicotine concentration increases, the number of affected miRNAs increases. The latter is associated with a biphasic behavioral and physiological phenotype. (B) A proposed model that explains nicotine addiction as a function of miRNAs's regulation of fos-1 and maintenance of effect by epigenetic factors.

Chapter Four: Determination of reliable reference genes for multi-generational qRT-PCR gene expression analysis on *C. elegans* exposed to nicotine drug of abuse.

Abstract

Recently, an increasing number of studies have been focused on multi-generational toxicogenomics impacts. Such studies rely on behavioral as well as genetic and epigenetic analyses using a range of biotechniques. Of these technologies, qRT-PCR is considered to be a mature "discovery and validation tool". Nevertheless, the interpretation of the resulting gene expression necessitates the establishment of reliable internal controls for normalization. No study has been performed to identify reliable reference genes in multi-generational settings. In this study, we exposed the model organism *C. elegans* to nicotine in the F0 generation, and investigated the relative stabilities of 16 housekeeping genes in L4 larvae across three generations (F0, F1, and F2). Based on results from five statistical approaches (geNorm, ΔCt method, NormFinder, BestKeeper, and ReFinder), TBA-1 and CDC-42 were the two most stable reference genes for performing reliable gene expression normalization and interpretation of the multigenerational impact of nicotine exposure.

***Key words*:** qRT-PCR, reference genes, multi-generational, *C. elegans*, nicotine, drugs of abuse

Introduction

Transcriptome studies have revolutionized molecular biology. Despite the increasing popularity of some advanced "discovery" technologies such as next generation sequencing (NGS) (e.g. RNA-seq), those high-throughput, sensitive technologies are still at a juvenile stage. Major drawbacks are attributed to the absence of standardized data analyses approaches and inability to distinguish between signal and noise (Pertea 2012). Inconsistencies in the data are further corrected and validated via more established technologies such as qRT-PCR that has been serving as a valuable mature tool for the validation of various transcriptome-related micro-arrays and NGS (Git, et al. 2010).

qRT-PCR is a mature biotechnique with both advantages and limitations. Efforts to correct for biases and variations caused by experimental errors and data handling have long been investigated and reported (Lefever, et al. 2009). In qRT-PCR, such can be accounted for by many factors, including the total RNA quantity and integrity, enzymatic efficiencies, total transcriptional status of cells or organisms as a whole, as well as pipetting errors (Ginzinger 2002). To correct some of these false positive results, genes of interest are normalized to genes (i.e. reference genes) that ideally have almost constant expression levels in the tested environmental conditions. The choice of a reference gene is not trivial. It has been concluded that there is no "universally suitable" reference gene. With this in mind, control genes should be selected based on the nature of the investigation and are expected to be resistant to the induced perturbations and modifications (Hruz, et al. 2011).

Many studies have been done to investigate the mechanism of action of nicotine in different organisms (e.g. cell culture, rats, mice, *drosophila*, *zebrafish*, *C. elegans*) (Matta, et al. 2007). Of the 4000 chemicals in tobacco smoking, nicotine has received a lot of attention due to

its addictive and toxic properties (CDC 1988; CDC 2010). Unfortunately, addiction is a universally notorious disease that affects millions worldwide. Despite concentrated efforts to limit nicotine exposure, the rate of tobacco smoking remains high in many developing countries and particularly among youth and children (WHO 2012). The obscurity of the molecular mechanisms of maladaptive neuroplasticity like addiction, especially on children, necessitates further in depth research to understand the extent of physiological disruptions. Our ongoing study implies the extension of addictive behavioral and molecular biomarkers across generations. Such an association is expected to trigger further replications and more in depth experiments involving protein coding as well as non-coding genes. For reasons described below, we employed *C. elegans* as our model organism to investigate the systemic mechanism of action of nicotine.

C. elegans is one of the major model organisms (Brenner 1974) which can be easily and economically maintained. Research on *C. elegans* is free of ethical concern and has contributed to advances in the biomedical fields. Up to 80% of its genome is homologous to that of humans (Beitel, et al. 1990) and is characterized by fewer genetic redundancies in coding and non-coding sequences (Kazazian 2004; Kirienko, et al. 2010). So far, extensive toxicogenomics research has been conducted on *C. elegans* in specific developmental stages and in response to different treatments (Karp, et al. 2011; Lant and Storey 2010; Pincus, et al. 2011; Viñuela, et al. 2010). However, correct interpretations and extrapolations on the genetic level necessitate reliable and sensitive control reference genes. With transgenerational nicotine addiction being the main focus of our research, our objective was concerned with finding suitable gene candidates to correct for any false-positive results and conclusions.

In this study, we compiled a list of reference gene candidates from previous publications that included both protein coding and RNA genes. We were interested in investigating the relative stabilities of the selected genes in response to nicotine across three generations. In our experiment, wild type L1 worms (N2) were distributed into three treatment groups: 0μM (control), 20μM and 20mM nicotine NGM plates. Worms were exposed to nicotine until early L4 stage (~30 hours). Exposure was restricted to the F0 generation, but we continued sampling L4 worms in both F1 and F2 generations. Among the sixteen selected genes, we aimed to determine the most reliable gene candidate(s) that can be used in nicotine related transgenerational molecular studies. To accomplish our objective, we used four of the most popular reference gene analysis software tools: geNorm, NormFinder, comparative ΔCt method, and BestKeeper. Taking all into consideration, the most stable gene(s) candidate was (were) determined by an overall comprehensive ranking approach (Xie, et al. 2012).

As a summary, recent evidence shows that environmental exposure can cause multigenerational impacts on animal growth and development and even some diseases (Contreras, et al. 2012; Tominaga, et al. 2003; Yu, et al. 2012). On the other hand, several other reports have demonstrated that chemicals may induce transgenerational alterations in gene expression (Ashe, et al. 2012; Braunschweig, et al. 2012; Manikkam, et al. 2012). However, no study has been performed to examine the effect of any chemical on housekeeping genes and thus no reliable reference genes exist for mutigenerational investigations. In this study, we employed *C. elegans* as an animal model system to evaluate and identify the most reliable reference genes for future mutigenerational toxico-genomics approaches and gene expression analyses related to nicotine addiction.

Material and methods

Chemicals and C. elegans strains

Nicotine was purchased from Acros Organics (New Jersey, USA). 1 M and 0.001 M stocks were prepared by diluting nicotine in phosphate buffer. From the two stock solutions, nicotine was then added into the NGM medium, after the addition of cholesterol, $CaCl_2$, $MgSO_4$, and KH_2PO_4, to give final concentrations of 20 µM and 20 mM, respectively.

C. elegans hermaphrodite N2 Bristol wild type was used. Worms were constantly transferred via chunking method to a new NGM plate freshly seeded with OP50.

Egg synchronization was done via bleaching (Sulston and Hodgkin 1988a). Briefly, M9 buffer was used to wash adult gravid worms off the plate into 15 ml Falcon tubes. Then the Falcon tube was centrifuged at 2000 rpm for 2 minutes, respectively. After discarding the supernatant, the wash was repeated. Then, 5 ml of synchronization solution (70% dH_2O, 10% NaOH, and 20% bleach) was added. The tubes were vigorously shaken (or vortexed) for a maximum of 5 minutes until the adult worms burst leaving the eggs dispersed in solution. The tubes were then spun at 2000 for 2 minutes. The supernatant was removed and three to four 5-ml M9 washes followed leaving the last wash without centrifugation. The tubes with the suspended eggs were placed on a shaker in the 20^oC incubator for 14-18 hours maximum (to avoid starvation). After hatching, the L1 larvae were pooled and randomly transferred to the different treatment groups.

The three treatment groups included the control group, the 20µM and 20mM nicotine treatment groups. L1 larvae of the F0 generation were incubated at 20^oC on seeded control and treatment plates for about 31 hours until end of L3-beginning of L4. From each plate, worms were unequally harvested off the plates into two eppendorf tubes. The one with the larger pellet

was intermittently centrifuged two times at 2000 rpm then 3000 rpm to separate the worms from bacteria and debris. Consequentially, the pellet was flash frozen in liquid nitrogen, and then stored at -80^{o}C until molecular analysis. As for the tube with the smaller pellet, the L4 worms were then transferred into OP50-seeded NGM plates, left to dry, then sealed and placed back in the 20^{o}C incubator to grow until egg-laying peaked (around second day of adulthood). Adults were then collected for synchronization to gather the eggs for the subsequent generation. The whole procedure was repeated until L4 of the F2 generation was reached.

RNA extraction and qRT-PCR

Total RNA extraction was performed according to protocol using mirVana™ miRNA Isolation Kit (Ambion, Austin, TX). Briefly, the sample was denatured using a lysis buffer. RNA was then separated from DNA and other proteins via acid-phenol extraction. Then, ethanol was added to the sample followed by passing through a glass-filter. Several washes preceded the elution of the RNA with low ionic strength solution.

RNA quantification and evaluation were done using the NanoDrop ND-1000 Micro-Volume UV/Vis Spectrophotometer (NanoDrop Technologies, Wilmington, DE) and were based on the concentration (ng/µL) and absorbance ratios of 260/280 and 260/230.

Reverse transcription was performed using TaqMan microRNA Reverse Transcription kit from Applied Biosystems (Foster City, CA) to reverse-transcribe RNA to cDNA for both protein coding genes and small RNAs . The poly-T was used for protein-coding genes and specific primers were used for small RNAs. For each reaction, the final reaction volume was 15 µL and included 1000ng of total RNAs, 0.19µL RNase inhibitor (20U/µL), 0.15µL of 100mM dNTPs, 1.5µL of reverse transcription buffer (10X), 2µL of primer mix, and 1µL of reverse transcriptase (50U/µL). The samples were then run via thermal cycler using the program: 16^{o}C for 30 min

followed by 42^{o}C for 30 min, 85^{o}C for 5 min and were finally held at 4^{o}C. The samples were diluted in 80µL DNase/RNase-free water for subsequent qRT-PCR.

The expression levels of selected genes were analyzed after performing qRT-PCR on 96-well-plate using the 7300 Real-Time PCR System (Applied Biosystem) using the SYBR Green PCR master mix from SuperArray Bioscience Corp. (Frederick, MD). Specific reverse and forward primers were used for each tested gene (Table 4.1). Briefly, each well carried a 20µL reaction resulting from the combination of 7µL DNase/RNase free water, 10µL SYBR Green master mix, 1µL cDNA, 2µL primer mix. A minimum of three biological replicates with two technical replicates were run. The qRT-PCR program was started at 95^{o}C for 10 min for enzyme activation followed by denaturation for 15 sec at 95^{o}C and an annealing/extension step for 60 sec at 60^{o}C. The latter 2 steps were repeated for 40 cycles.

Primer specificity and efficiency have been previously calculated. Moreover, descriptive statistics (i.e. mean, SD) were calculated via SPSS for the raw Ct values of each gene candidate. Boxplot graphs were done via SPSS20 (Figure 4.1; Table 4.2).

Determination of gene stability

Five different statistical approaches (geNorm, ΔCt method, NormFinder, BestKeeper, and ReFinder) were employed to determine the stability of each tested reference gene candidate.

The geNorm (Vandesompele, et al. 2002) applet allows the determination of the most stable reference gene(s) based on pairwise comparisons between each gene with all other candidates. The variation in expression levels of each gene is calculated as the geometric mean of the standard deviation relative to all other genes. Such a stability index is described as the 'M-value'. Ranking is achieved after sequential elimination of most variable gene, followed by recalculation of the 'M-value'. Finally, genes with the lowest 'M-value' will be ranked with

highest stability in comparison with the other tested genes. Conceptually, geNorm assumes that an ideal-gene pair will have the least variation in expression in all samples regardless of experimental conditions. GeNorm goes beyond that to estimate the minimal *n* (e.g. number of genes) needed to perform reliable normalization. This is based on pairwise variation [V_n/V_{n+1}] calculated for each gene pair normalization factors [NF_n, NF_{n+1}]. Through this approach, the need for the inclusion of an additional reference gene would be reflected by a high variation (i.e. >0.15 established cutoff value), and vice versa.

To prepare the input for geNorm, relative quantification from raw Ct values among all samples was done for each gene. Briefly, the smallest Ct value was determined for each gene among all samples. Then, this value was subtracted from all the other Ct values related to this gene. Therefore, the minimal value would be zero. Then, each value is transformed using the formula: $2^{\wedge(Ctoriginical-Ctmin)}$. The resulting converted data were used as input for geNorm with the names of the genes and samples in the first row and column, respectively. Together, they were saved in the provided input directory. After loading the input file into geNorm, the analysis was run and two charts were automatically generated as shown in Figure 4.2.

The comparative delta Ct method (Silver, et al. 2006) is a relatively similar approach that depends on pairwise comparisons between genes. This method can be easily done on an excel spreadsheet without the help of a designed program. In addition, its development facilitated gene expression normalization for experiments with non-ideal sample sizes and purity. Simply, a set of comparisons is performed where each gene is compared against all other gene candidates. The ΔCt was calculated for every gene pair in each sample across all treatment groups. For every gene pair, the mean ΔCt and SD were calculated. A high SD reflects that one or both genes are not stable. Then, an overall average SD was calculated for every gene being compared against all

others (i.e. gene pair set). Including more genes into the comparison will allow for the selection of the one with the least variability. Thus, the gene with the least SD will be the top-ranked candidate for normalization. Calculations for the comparative ΔCt method were done using excel spreadsheet as described above. Boxplots were generated via SPSS20. For each gene set, different colors represent different 'gene pairs' as shown in Figure 4.3 and Table 4.4.

Whereas pairwise comparison approaches focus on intra-group variation with less, if any, consideration on the inter-group variation, NormFinder (Andersen, et al. 2004) ranks gene stability based on minimal variation of samples not only among all treatment groups, but also within each group. NormFinder prevents the exclusion of stable genes with different expression levels that would otherwise be ranked as one of the least stable through pairwise comparison. In addition false positive results caused by co-regulated genes with similar expression patterns would be avoided. Through NormFinder, a top-ranked gene would introduce the least systemic error when used for normalization.

Another excel-based applet is BestKeeper (Pfaffl, et al. 2004) that allows the analysis of 10 reference gene candidates as well as target genes for many samples. For that, we excluded the 6 least stable genes (AMA-1, RBD-1, PMP-3, ACT-2, Ce234.1, and U18) based on geNorm, NormFinder, and delta Ct method. Its ranking is a result of a stepwise process that starts with the exclusion of genes with expressions having an SD>1. To analyze the relationships of candidate genes with one another, a series of pairwise comparisons between each pair is calculated as Pearson's correlation coefficient [r]. Then, based on the most highly correlated genes, the geometric mean of the Ct values is used to calculate an index. After a pairwise-correlation analysis of each candidate gene with BestKeeper index, genes with the highest statistically significant correlation coefficient represent the most stable genes, and vice versa.

Results

Descriptive statistics for expression levels of candidate reference genes

Figure 4.1 demonstrates the expression levels of each reference gene candidate. The expression levels were calculated from the original Ct values for all samples belonging to three nicotine treatment groups (control, 20µM, and 20mM) across three generations (F0, F1 and F2). Taking the median Ct values into consideration, the three genes that had the least median Ct values were 18s rRNA, ACT-2, and TBA-1 with Ct_{median} of 14.16, 20.39, and 20.65, respectively. On the other hand, the ones with the highest Ct values were RBD-1, ARP-6, and U18 with Ct_{median} values of 23.79, 24.77, and 25.00, respectively. However, looking at the variations in the Ct values among treatment groups and generations, it appears that the least variable genes were 18s RNA, U6 and PMP-3 with SD values of 0.49, 0.61, and 0.63, respectively. Conversely, the three most variable genes were CSQ-1, ACT-2, and U18 with SD values of 1.28, 1.29, and 1.48, respectively. Of the 16 tested genes, U18 would not be a reliable reference gene as it had the lowest and the most variable expression levels among all the samples. Also, ACT-2 would not be a reliable reference gene because its expression level varied greatly among different treatments and across different generations.

Generally speaking, a good reference gene should have an expression level that is in the similar range relative to the targeted genes (Cappelli, et al. 2008). Although 18S rRNA had a relatively stable expression level, it might not be considered as a suitable reference gene because its expression is too high. Thus, simple statistical criteria based solely on numerical values may mask genomic context. More measures should be taken into account when selecting the top reference gene(s) from the candidate list for particular experimental settings. With this in mind, we took advantage of five previously established statistical approaches (geNorm, NormFinder,

BestKeeper, comparative ΔCt method, and comprehensive ranking) to evaluate each individual reference gene candidate. This facilitated the final determination of more reliable reference genes for qRT-PCR normalization in *C. elegans* across three generations after parental nicotine exposure.

Reference gene ranking based on geNorm

GeNorm ranks the reference genes based on the stability value (M value). The lower the M-value, the more stable the gene. Figure 4.2 clearly shows that CDC-42 and Y45F10D.4 were the most stable genes among the gene candidates with the least M-value of 0.198. ARP-6 (0.223), EIF3.C (0.271), and TBA-1 (0.292) had close M-values. The least stable genes were RBD-1 (0.542), U18 (0.603), AMA-1(0.679), Ce234.1 (0.741) and PMP-3 (0.794). The rank of Y45F10D.4 was consistent with previous studies using IIS-mutants, dauers and L3 worms (Hoogewijs, et al. 2008) as well as L4 worms treated with copper oxide (Zhang, et al. 2012). However, a drastic change in PMP-3 stability index was evident as it was ranked as the least stable gene in our experimental settings. The rank of CDC-42 was consistent with one study (Hoogewijs, et al. 2008), but not the other (Zhang, et al. 2012).

In order to examine the minimal number of genes required for reliable normalization, the V-value for all the gene pairs was calculated and was less than 0.15 (the default cutoff) (Figure 4.2). This suggests that the introduction of a new gene was not associated with high variation in the relative expression levels. Thus, taking both indices (M and V-values) together, it can be inferred that CDC-42 and Y45F10D.4 are enough for a reliable normalization (Figure 4.2).

Reference gene ranking based on NormFinder

Based on NormFinder, TBA-1(0.18), EIF3.C (0.22), ARP-6 (0.27), CDC-42 (0.29), and MDH-2 (0.31) show the lowest stability values (Table 4.5) and may serve as the top five reliable reference genes. This rank was similar to that of geNorm, although the exact order was not identical. The inclusion of TBA-1, EIF3.C, ARP-6, and CDC-42 among the top-ranked genes was common to both analyses. Previous reports using the same methods placed TBA-1 and EIF3.C among the top five stable genes (Zhang, et al. 2012). As for the least stable genes, our results show that ACT-2 (0.71), U18 (0.93), AMA-1 (0.95), Ce234.1 (1.00), and PMP-3(1.04) were ranked last. Interestingly, the lowest four genes were ordered exactly like geNorm as mentioned above. AMA-1 was also found among the least stable with other experimental conditions, but this was not the case for PMP-3 (Zhang, et al. 2012).

Reference gene ranking based on comparative ΔCt method

Comparative ΔCt method ranked TBA-1(0.595), CDC-42 (0.606), EIF3.C (0.607), ARP-6 (0.614), and Y45F10D.4 (0.631) as the most stable reference genes among the 16 candidate genes (Table 4.5). Although the order was slightly different, it was similar to the top five genes ranked in geNorm and top four genes ranked in NormFinder. On the other hand, the least stable genes were ACT-2 (0.852), U18 (1.064), AMA-1(1.098), Ce-234.1(1.131), PMP-3(1.162) (Figure 4.3; Table 4.4). Most were consistent with results from NormFinder and geNorm. Despite the fact that this method depends on a simpler statistical methodology, it agreed with other sophisticated approaches. Comparing our results with studies that used the ΔCt method, TBA-1, EIF-3 and Y45F10D.4 were also among the more stable genes (Zhang, et al. 2012).

Also, AMA-1 was of the least reliable genes for normalization, while ARP-6, and CDC-42 were among the least stable in their study (Zhang, et al. 2012).

Reference gene ranking based on BestKeeper

BestKeeper calculations depend on two criteria to deduce suitable reference genes. The initial analysis was based on the SD values and ranked 18s rRNA (0.40), U6 (0.49), EIF3.C (0.69), TBA-1(0.70), ARP-6 (0.79) with the least variable expression levels (Table 4.3). The results obtained from BestKeeper did not completely agree with those obtained from geNorm, NormFinder, and ΔCt method. Despite its relatively stable expression, 18s rRNA had a much higher expression level compared to other genes and it was therefore not a good candidate. However, when considering the index based on pairwise correlation calculations (i.e. r-coefficients), Y45F10D.4 (0.989), F35G12.2 (0.986), TBA-1(0.980), CDC-42 (0.978), and CSQ-1(0.971) were ranked as the best (Table 4.3). Taking both criteria into consideration, Y45F10D.4 and F35G12.2 had the highest (r-value); however, together with CSQ-1, they had the most variable expression levels among the treatment groups and generations ($SD_{Y45F10D.4=}$0.92, $SD_{F35G12.2}$=0.97, SD_{CSQ-1}=1.11). As a conclusion, the expression levels of TBA-1(SD=0.70) and CDC-42 (SD=0.83) were relatively stable and highly correlated with the BestKeeper index at P=0.001. This result was consistent with results from geNorm and NormFinder. Additionally, TBA-1 was also among the five most stable genes ranked by BestKeeper in a previous study on L4 worms exposed to nanoparticle treatment (Zhang, et al. 2012).

Comprehensive ranking

Taking advantage of the different angles covered by the four different statistical methods, we used RefFinder software (Xie, et al. 2012) that accommodates all the logarithms to finally

provide an overall comprehensive ranking for the stability of the sixteen gene targets. As shown in Table 4.5. TBA-1 (2.51), CDC-42 (2.99), EIF3.C (3.60), ARP-6 (4.24), and Y45F10D.4 (4.36) were the most stable housekeeping genes for reference genes in mutigenerational study. TBA-1 and Y45F10D.4 were also among the top five enlisted genes (Zhang, et al. 2012). On the other hand, the least stable genes were CSQ-1(10.72), AMA-1(10.82), PMP-3(11.31), ACT-2 (11.61), and U18 (13.69). The stability index for CSQ-1 and AMA-1 was consistent with previous results in response to nanoparticle treatment (Zhang, et al. 2012). The radical shift in PMP-3 remained evident in the comprehensive ranking as it was of the least stable genes in our experimental settings.

Discussion

Previous studies involved in choosing reliable reference genes for qRT-PCR normalization have already been conducted in *C. elegans* (Hoogewijs, et al. 2008; Zhang, et al. 2012). However, none has evaluated reference genes in multigenerational investigations as a function of environmental conditions. Choosing a proper reference gene remains one of the golden rules to increase the sensitivity and credibility of data interpretation. Generally, there are two types of approaches to tackle the issue: the top-bottom model is not restricted to a set of genes and starts with a high-throughput investigation from genome-wide background (e.g. microarray). On the other hand, a bottom –top model starts with a handful of genes with conserved basic roles and hypothesized to be of relatively constant expression levels (Hruz, et al. 2011). We were interested in identifying suitable reference genes in *C. elegans* in response to nicotine. Nicotine is one of the major drugs of abuse with high rates of primary and secondary exposures. Here, we evaluated the expression levels of sixteen housekeeping genes, including four small RNA genes, across multiple generations in response to parental nicotine exposure.

We treated *C. elegans* hermaphrodites (N2) with two nicotine concentrations from L1 to the beginning of L4. We collected L4 worms from F0, F1, and F2 generations. All the samples from the three treatment groups (control, and nicotine-treated) were used to investigate the expression levels of sixteen selected genes. Based on our results, particularly from the comprehensive ranking, it appears that TBA-1, CDC-42, EIF3.C, ARP-6 and Y45F10D.4 were the most reliable reference genes among the sixteen gene candidates. Based on outputs from the different methodologies, all except for BestKeeper considered TBA-1, CDC-42, EIF3.C, ARP-6 as the most stable genes. When considering results from all methods, including BestKeeper, TBA-1 and CDC-42 would be the most reliable reference genes to study the transgenerational effect of *C. elegans* exposed to nicotine. Based on results from geNorm, the combination of two reference genes from our list is sufficient for reliable normalization. Thus, we recommend the combination of TBA-1 with any other gene of the top five genes mentioned above. PMP-3, AMA-1, and U18 were the least stable and would not be recommended to be used for normalization.

Our results partially agree with previous studies (Hoogewijs, et al. 2008; Zhang, et al. 2012) where TBA-1, CDC-42 and Y45F10D.4 were the most reliable reference genes. However, other genes, such as PMP-3, were the most reliable reference gene in other reports (Hoogewijs, et al. 2008; Zhang, et al. 2012), but were among the least stable genes in our study. This suggests that housekeeping genes are differentially affected in a context-dependent manner and that assessing potential reference genes should precede expression profile analysis.

Although reference genes related studies are not novel, the replication of such a concept using different treatment conditions and developmental conditions is important for future meta-

analyses. This allows to test whether an ideal universal reference gene exists or to further confirm the concept of condition-specific reference gene selection.

References

Andersen, C. L., J. L. Jensen, and T. F. Orntoft

2004 Normalization of real-time quantitative reverse transcription-PCR data: a model-based variance estimation approach to identify genes suited for normalization, applied to bladder and colon cancer data sets. Cancer Res 64(15):5245-50.

Ashe, A., et al.

2012 piRNAs can trigger a multigenerational epigenetic memory in the germline of C. elegans. Cell 150(1):88-99.

Beitel, G. J., S. G. Clark, and H. R. Horvitz

1990 Caenorhabditis elegans ras gene let-60 acts as a switch in the pathway of vulval induction. Nature 348(6301):503-9.

Braunschweig, Martin, et al.

2012 Investigations on Transgenerational Epigenetic Response Down the Male Line in F2 Pigs. PLoS One 7(2):e30583.

Brenner, S.

1974 The genetics of Caenorhabditis elegans. Genetics 77(1):71-94.

Cappelli, K., et al.

2008 Exercise induced stress in horses: selection of the most stable reference genes for quantitative RT-PCR normalization. BMC Mol Biol 9:49.

CDC

1988 The Health Consequences of Smoking - Nicotine Addiction: A Report of the Surgeon General.

—

2010 The Biology and Behavioral Basis for Smoking-Attributable Disease: A Report of the Surgeon General.

Contreras, Elizabeth Q., et al.

2012 Toxicity of quantum dots and cadmium salt to Caenorhabditis elegans after multigenerational exposure. Environmental Science & Technology.

Ginzinger, D. G.

2002 Gene quantification using real-time quantitative PCR: an emerging technology hits the mainstream. Exp Hematol 30(6):503-12.

Git, A., et al.

2010 Systematic comparison of microarray profiling, real-time PCR, and next-generation sequencing technologies for measuring differential microRNA expression. RNA 16(5):991-1006.

Hoogewijs, D., et al.

2008 Selection and validation of a set of reliable reference genes for quantitative sod gene expression analysis in C. elegans. BMC Mol Biol 9:9.

Hruz, T., et al.

2011 RefGenes: identification of reliable and condition specific reference genes for RT-qPCR data normalization. BMC Genomics 12:156.

Karp, X., et al.

2011 Effect of life history on microRNA expression during C. elegans development. RNA 17(4):639-51.

Kazazian, H. H., Jr.

2004 Mobile elements: drivers of genome evolution. Science 303(5664):1626-32.
Kirienko, N. V., K. Mani, and D. S. Fay
2010 Cancer models in *Caenorhabditis elegans*. Dev Dyn 239(5):1413-48.
Lant, B., and K. B. Storey
2010 An overview of stress response and hypometabolic strategies in Caenorhabditis elegans: conserved and contrasting signals with the mammalian system. Int J Biol Sci 6(1):9-50.
Lefever, S., et al.
2009 RDML: structured language and reporting guidelines for real-time quantitative PCR data. Nucleic Acids Res 37(7):2065-9.
Manikkam, Mohan, et al.
2012 Transgenerational Actions of Environmental Compounds on Reproductive Disease and Identification of Epigenetic Biomarkers of Ancestral Exposures. PLoS One 7(2):e31901.
Matta, S. G., et al.
2007 Guidelines on nicotine dose selection for in vivo research. Psychopharmacology (Berl) 190(3):269-319.
Pertea, M.
2012 The Human Transcriptome: An Unfinished Story. Genes (Basel) 3(3):344-360.
Pfaffl, M. W., et al.
2004 Determination of stable housekeeping genes, differentially regulated target genes and sample integrity: BestKeeper--Excel-based tool using pair-wise correlations. Biotechnol Lett 26(6):509-15.
Pincus, Z., T. Smith-Vikos, and F. J. Slack
2011 MicroRNA predictors of longevity in Caenorhabditis elegans. PLoS Genet 7(9):e1002306.
Silver, N., et al.
2006 Selection of housekeeping genes for gene expression studies in human reticulocytes using real-time PCR. BMC Mol Biol 7:33.
Sulston, J, and J Hodgkin
1988 The Nematode Caenorhabditis elegans, W.B. Wood, ed. New York: Cold Spring Harbor Laboratory Press:p. 587.
Tominaga, N , et al.
2003 A Multi-Generation Sublethal Assay of Phenols Using the Nematode Caenorhabditis elegans. J Health Sci 49(6):459-463.
Vandesompele, J., et al.
2002 Accurate normalization of real-time quantitative RT-PCR data by geometric averaging of multiple internal control genes. Genome Biol 3(7):RESEARCH0034.
Viñuela, Ana, et al.
2010 Genome-Wide Gene Expression Analysis in Response to Organophosphorus Pesticide Chlorpyrifos and Diazinon in C. elegans. PLoS One 5(8):e12145.
WHO
2012 World Health Statistics.Global Health Observatory. World Health Organization. Retrieved from http://www.who.int/gho/publications/world_health_statistics/EN_WHS2012_Full.pdf.
Xie, Fuliang, et al.

2012 miRDeepFinder: a miRNA analysis tool for deep sequencing of plant small RNAs. Plant Molecular Biology 80(1):75-84.

Yu, Z., et al.

2012 Transgenerational effects of heavy metals on L3 larva of Caenorhabditis elegans with greater behavior and growth inhibitions in the progeny. Ecotoxicol Environ Saf.

Zhang, Y., et al.

2012 Selection of reliable reference genes in Caenorhabditis elegans for analysis of nanotoxicity. PLoS One 7(3):e31849.

Table 4.1: Properties of the sixteen candidate genes.

Gene Symbol	Locus tag	Gene description	Forward primer	Reverse primer
CDC-42	R07G3.1	Cell Division Cycle related	AGCCATTCTGGCCGCTCTCG	GCAACCGCTTCTCGTTTGGC
PMP-3	C54G10.3	Peroxisomal Membrane Protein related	TGGCCGGATGATGGTGTCGC	ACGAACAATGCCAAAGGCCAGC
EIF-3.C	T23D8.4	Eukaryotic Initiation Factor	ACACTTGACGAGCCCACCGAC	TGCCGCTCGTTCCTTCCTGG
ARP-6	C08B11.6	Spliceosome-Associated Protein family member (sap-49)	TGGCGGATCGTCGTGCTTCC	ACGAGTCTCCTCGTTCGTCCCA
ACT-2	T04C12.5	ACTin	GCGCAAGTACTCCGTCTGGATCG	GGGTGTGAAAATCCGTAAGGCAGA
CSQ-1	F40E10.3	Calsequestrin	GCCTTGCGCTAGTGGTTGTGC	GCTCTGAGTCGTCCTCTTCCACG
Y45F10D.4	Y45F10D.4	Putative iron-sulfur cluster assembly enzyme	CGAGAACCCGCGAAATGTCGGA	CGGTTGCCAGGGAAGATGAGGC
TBA-1	F26E4.8	TuBulin, Alpha family member	TCAACACTGCCATCGCCGCC	TCCAAGCGAGACCAGGCTTCAG
MDH-2	F20H11.3	Malate DeHydrogenase	TGGAGCTGCCGGAGGAATTGG	TCAGCGTTCTCAACGGCGGC
AMA-1	F36A4.7	AMAnitin resistant family member	CGGATGGAGGAGCATCGCCG	CAGCGGCTGGGGAAGTTGGC
F35G12.2	F35G12.2	ortholog of mitochondrial NAD+-isocitrate dehydrogenase.	ACTGCGTTCATCCGTGCCGC	TGCGGTCCTCGAGCTCCTTC
RBD-1	T23F6.4	RBD(RNA binding domain)protein	GGTCAGATTTCCGATGCGTCGCT	ACTTGCTCCAGGCTCTCGGC
U6	CELE_F35C11.9	snRNA involved in mRNA splicing	CAGAGAAGATTAGCATGGCCC	TTGGAACGCTTCACGAATTTGC
18s rRNA	CELE_F31C3.7	rRNA subunit	TTCTTCCATGTCCGGGATAG	CCCCACTCTTCTCGAATCAG
Ce234.1	DQ789547	C/D box snoRNA	GGTTACGGTAGCCGAGTCAG	GCCATAACTGTTCACCGTCG
U18	Z75111	snoRNA	TGATGATCACAAATCCGTGTTTC	GCTCAGCCGGTTTTCTATCG

Table 4.2: Overall descriptive statistics of the raw Ct values for each candidate gene among all nicotine treatment groups in L4 *C. elegans*.

	N	Minimum	Maximum	Mean	SD	Median
CDC42	56	21.16	24.88	23.02	0.97	23.10
MDH2	56	19.56	23.58	21.52	0.99	21.71
PMP3	56	21.74	24.31	22.83	0.63	22.72
AMA1	56	20.25	24.91	22.04	0.76	22.05
EIF3.C	56	20.14	23.66	21.65	0.83	21.83
F35G12.2	56	20.48	24.17	22.40	1.11	22.55
ARP6	56	23.27	26.76	24.77	0.95	24.77
RBD1	56	22.41	26.10	23.76	0.81	23.79
ACT2	56	18.43	23.05	20.47	1.29	20.39
U6	56	19.17	21.89	20.74	0.61	20.88
CSQ1	56	20.17	24.88	22.59	1.28	22.64
Ce234.1	56	21.01	23.86	22.09	0.64	22.09
Y45F10D.4	56	21.12	25.07	23.05	1.08	23.13
18s rRNA	56	13.01	15.13	14.14	0.49	14.16
TBA1	56	19.17	22.44	20.70	0.84	20.65
U18	56	21.17	27.02	24.56	1.48	25.00

Table 4.3: Ranking of most stable reference genes based on BestKeeper.

Gene	n	GM [CP]	AR [CP]	min [CP]	max [CP]	SD [±CP]	CV [%CP]	[r]	P value	Ranking based on	
										SD	[r]
ARP6	56	24.757	24.774	23.274	26.762	0.793	3.199	0.968	0.001	18s rRNA	Y45F10D.4
18s rRNA	56	14.133	14.141	13.015	15.129	0.397	2.810	0.857	0.001	U6	F35G12.2
CDC42	56	22.999	23.019	21.163	24.883	0.833	3.619	0.978	0.001	EIF3.C	TBA1
CSQ1	56	22.560	22.595	20.165	24.880	1.109	4.907	0.971	0.001	TBA1	CDC42
EIF3.C	56	21.632	21.648	20.135	23.661	0.687	3.172	0.968	0.001	ARP6	CSQ1
F35G12.2	56	22.373	22.400	20.478	24.173	0.971	4.336	0.986	0.001	CDC42	ARP6
MDH2	56	21.496	21.518	19.560	23.585	0.838	3.893	0.966	0.001	MDH2	EIF3.C
TBA1	56	20.688	20.705	19.172	22.444	0.705	3.404	0.980	0.001	Y45F10D.4	MDH2
U6	56	20.731	20.740	19.168	21.887	0.490	2.362	0.799	0.001	F35G12.2	18s rRNA
Y45F10D.4	56	23.022	23.046	21.124	25.067	0.929	4.031	0.989	0.001	CSQ1	U6

Table 4.4: A summary of the pair-wise mean and SD calculations for each of the reference gene candidates. The last column on the left is the average SD for each candidate. The latter was used in the Delta-Ct-based method to identify the most stable genes.

Gene		Pair 1	Pair 2	Pair 3	Pair 4	Pair 5	Pair 6	Pair 7	Pair 8	Pair 9	Pair 10	Pair 11	Pair 12	Pair 13	Pair 14	Pair 15	Avg. SD
TBA1	Mean	-2.31	-0.81	-2.12	-1.33	-0.94	-1.70	-4.07	-3.05	0.23	-0.04	-1.89	-1.39	-2.34	6.56	-3.85	
	SD	0.32	0.37	1.10	1.05	0.27	0.38	0.36	0.67	0.56	0.53	0.54	1.03	0.34	0.48	0.93	0.59
CDC42	Mean	1.50	0.19	0.98	1.37	0.62	-1.76	-0.74	2.55	2.28	0.42	0.93	-0.03	8.88	2.31	-1.54	
	SD	0.34	1.17	1.09	0.29	0.35	0.20	0.65	0.58	0.68	0.42	1.22	0.20	0.66	0.32	0.91	0.61
EIF3.C	Mean	-1.37	0.13	-1.18	-0.39	-0.75	-3.13	-2.11	1.17	0.91	-0.95	-0.44	-1.40	7.51	0.94	-2.91	
	SD	0.29	0.29	1.07	1.01	0.46	0.29	0.65	0.71	0.56	0.60	1.04	0.37	0.54	0.27	0.95	0.61
ARP6	Mean	1.76	3.26	1.95	2.74	3.13	2.37	1.02	4.30	4.03	2.18	2.68	1.73	10.63	4.07	0.22	
	SD	0.20	0.35	1.13	1.02	0.29	0.40	0.62	0.69	0.62	0.55	1.20	0.27	0.65	0.36	0.87	0.61
Y45F10D.4	Mean	0.03	1.53	0.22	1.01	1.40	0.65	-1.73	-0.71	2.57	2.31	0.45	0.96	8.91	2.34	-1.51	
	SD	0.20	0.38	1.29	1.20	0.37	0.25	0.27	0.76	0.46	0.73	0.32	1.30	0.74	0.34	0.86	0.63
MDH2	Mean	-1.50	-1.31	-0.52	-0.13	-0.88	-3.26	-2.24	1.04	0.78	-1.08	-0.57	-1.53	7.38	0.81	-3.04	
	SD	0.34	1.18	1.09	0.29	0.37	0.35	0.69	0.69	0.63	0.55	1.14	0.38	0.66	0.37	0.81	0.64
F35G12.2	Mean	-0.62	0.88	-0.43	0.36	0.75	-2.37	-1.36	1.93	1.66	-0.19	0.31	-0.65	8.26	1.70	-2.16	
	SD	0.35	0.37	1.33	1.22	0.46	0.40	0.77	0.42	0.72	0.34	1.29	0.25	0.75	0.38	0.80	0.66
18s rRNA	Mean	-8.88	-7.38	-8.68	-7.89	-7.51	-8.26	-10.63	-9.61	-6.33	-6.60	-8.45	-7.95	-8.91	-6.56	-10.42	
	SD	0.66	0.66	0.89	0.88	0.54	0.75	0.65	0.64	0.90	0.46	0.92	0.71	0.74	0.48	1.13	0.73
U6	Mean	-2.28	-0.78	-2.09	-1.30	-0.91	-1.66	-4.03	-3.02	0.27	-1.86	-1.35	-2.31	6.60	0.04	-3.82	
	SD	0.68	0.63	0.83	0.82	0.56	0.72	0.62	0.63	0.96	0.97	0.76	0.73	0.46	0.53	1.11	0.73
CSQ1	Mean	-0.42	1.08	-0.23	0.56	0.95	0.19	-2.18	-1.16	2.12	1.86	0.50	-0.45	8.45	1.89	-1.96	
	SD	0.42	0.55	1.52	1.42	0.60	0.34	0.55	0.94	0.33	0.97	1.48	0.32	0.92	0.54	0.91	0.78
RBD1	Mean	0.74	2.24	0.93	1.72	2.11	1.36	-1.02	3.28	3.02	1.16	1.67	0.71	9.61	3.05	-0.80	
	SD	0.65	0.69	1.01	0.89	0.65	0.77	0.62	1.03	0.63	0.94	1.00	0.76	0.64	0.67	1.05	0.80
ACT2	Mean	-2.55	-1.04	-2.35	-1.56	-1.17	-1.93	-4.30	-3.28	-0.27	-2.12	-1.62	-2.57	6.33	-0.23	-4.09	
	SD	0.58	0.69	1.55	1.48	0.71	0.42	0.69	1.03	0.96	0.33	1.43	0.46	0.90	0.56	0.98	0.85
U18	Mean	1.54	3.04	1.73	2.52	2.91	2.16	-0.22	0.80	4.09	3.82	1.96	2.47	1.51	10.42	3.85	
	SD	0.91	0.81	1.65	1.51	0.95	0.80	0.87	1.05	0.98	1.11	0.91	1.50	0.86	1.13	0.93	1.06
AMA1	Mean	-0.98	0.52	-0.79	0.39	-0.36	-2.74	-1.72	1.56	1.30	-0.56	-0.06	-1.01	7.89	1.33	-2.52	
	SD	1.09	1.09	0.82	1.01	1.22	1.02	0.89	1.48	0.82	1.42	0.98	1.20	0.88	1.05	1.51	1.10
Ce234.1	Mean	-0.93	0.57	-0.73	0.06	0.44	-0.31	-2.68	-1.67	1.62	1.35	-0.50	-0.96	7.95	1.39	-2.47	
	SD	1.22	1.14	0.89	0.98	1.04	1.29	1.20	1.00	1.43	0.76	1.48	1.30	0.71	1.03	1.50	1.13
PMP3	Mean	-0.19	1.31	0.79	1.18	0.43	-1.95	-0.93	2.35	2.09	0.23	0.73	-0.22	8.68	2.12	-1.73	
	SD	1.17	1.18	0.82	1.07	1.33	1.13	1.01	1.55	0.83	1.52	0.89	1.29	0.89	1.10	1.65	1.16

Table 4.5: A summary for the different rankings of the 16 candidate genes derived from 5 methods in response to nicotine in L4 *C. elegans*.

Comprehensive ranking		**Delta Ct method**		**BestKeeper**				**NormFinder**		**GeNorm**	
Gene	**Stability value**	**Genes**	**Mean SD**	**Gene**	**SD [Ct]**	**Gene**	**coeff. of corr. [r]**	**Gene**	**Stability value**	**Gene**	**M-value**
TBA1	2.51	TBA1	0.59	18s rRNA	0.40	Y45F10D.4	0.99	TBA1	0.18	CDC42 | Y45F10D.4	0.20
CDC42	2.99	CDC42	0.61	U6	0.49	F35G12.2	0.99	EIF3.C	0.22		
EIF3.C	3.60	EIF3.C	0.61	EIF3.C	0.69	TBA1	0.98	ARP6	0.27	ARP6	0.22
ARP6	4.24	ARP6	0.61	TBA1	0.70	CDC42	0.98	CDC42	0.29	EIF3.C	0.27
Y45F10D.4	4.36	Y45F10D.4	0.63	ARP6	0.79	CSQ1	0.97	MDH2	0.31	TBA1	0.29
18s rRNA	5.03	MDH2	0.64	CDC42	0.83	ARP6	0.97	Y45F10D.4	0.38	MDH2	0.31
U6	6.50	F35G12.2	0.66	MDH2	0.84	EIF3.C	0.97	F35G12.2	0.41	F35G12.2	0.33
MDH2	6.67	18s rRNA	0.73	Y45F10D.4	0.93	MDH2	0.97	18s rRNA	0.42	CSQ1	0.36
F35G12.2	8.17	U6	0.73	F35G12.2	0.97	18s rRNA	0.86	U6	0.42	ACT2	0.41
RBD1	9.43	CSQ1	0.78	CSQ1	1.11	U6	0.80	RBD1	0.53	18s rRNA	0.47
Ce234.1	10.03	RBD1	0.80					CSQ1	0.64	U6	0.51
CSQ1	10.72	ACT2	0.85					ACT2	0.71	RBD1	0.54
AMA1	10.82	U18	1.06					U18	0.93	U18	0.60
PMP3	11.31	AMA1	1.10					AMA1	0.95	AMA1	0.68
ACT2	11.61	Ce234.1	1.13					Ce234.1	1.00	Ce234.1	0.74
U18	13.69	PMP3	1.16					PMP3	1.04	PMP3	0.79

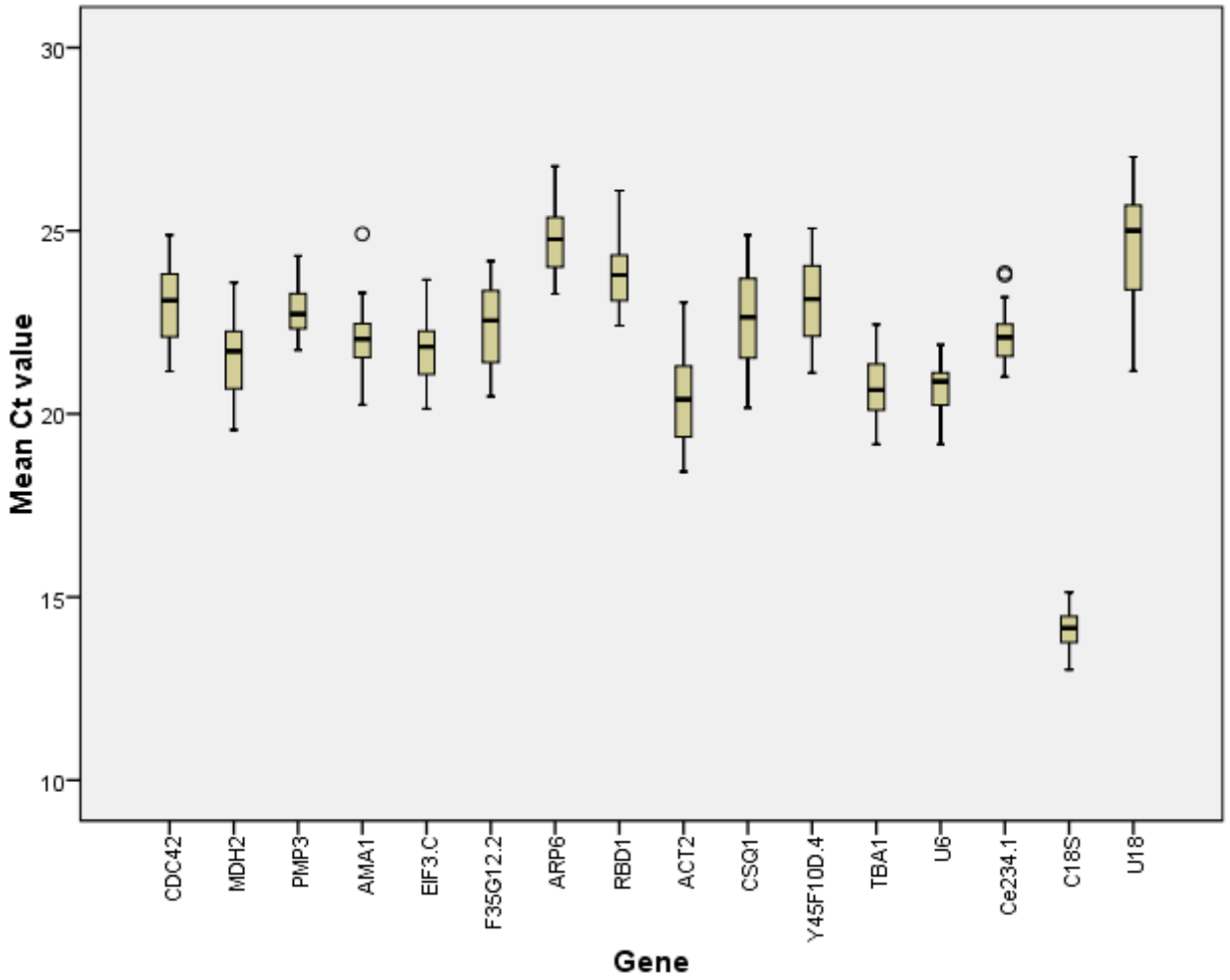

Figure 4.1: The average Ct values calculated from raw qRT-PCR output for the 16 candidate genes in L4 *C. elegans* (N2). 50% of the values are included in the box. The median is represented by the line in the box. The interquartile range is bordered by the upper and lower edges, which indicate the 75th and 25th percentiles, respectively. The whiskers are inclusive of the maximal and minimal values, but exclusive of the outliers, represented as circles.

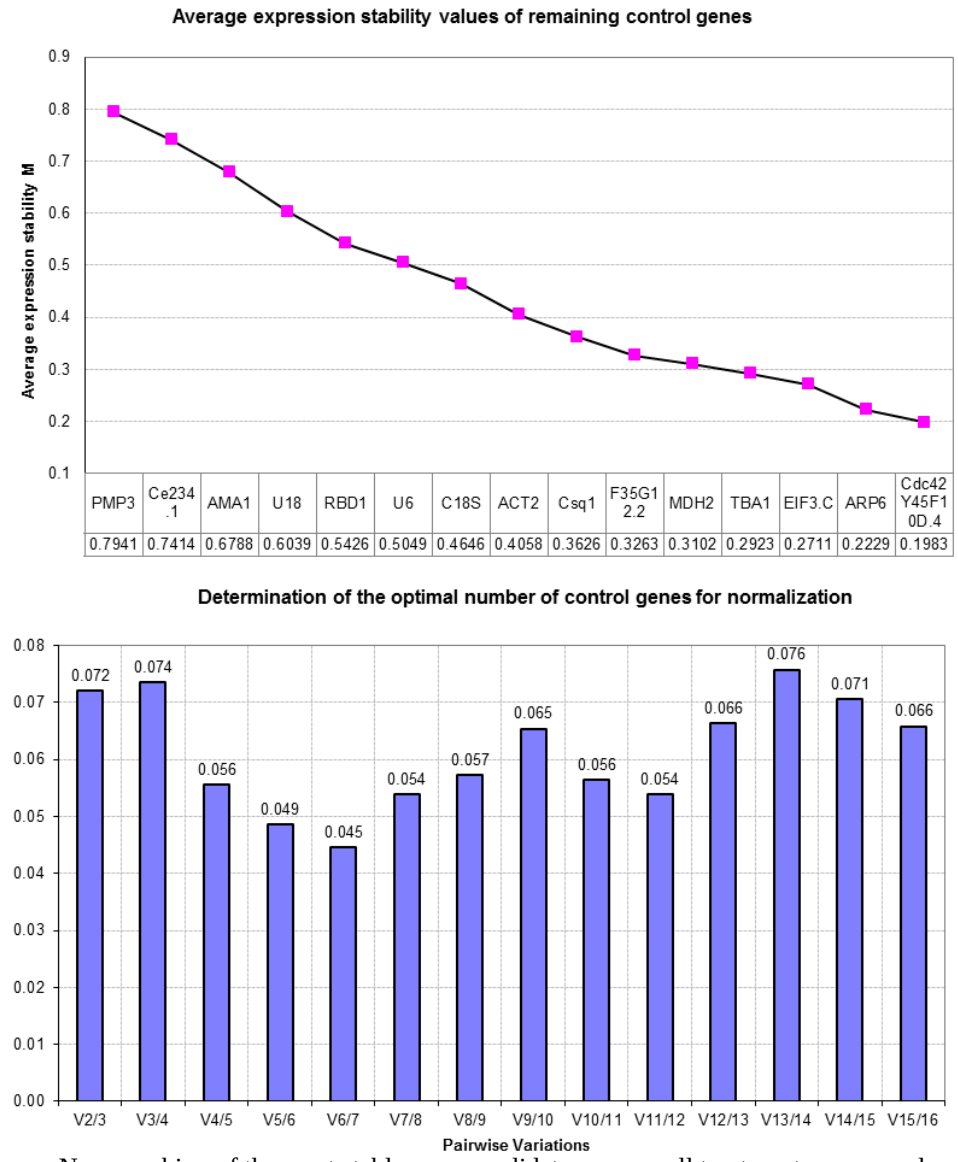

Figure 4.2: Top: geNorm ranking of the most stable gene candidates among all treatment groups and generations. Bottom: GeNorm-based pair-wise variation value (V value) among the candidate genes. The cut-off value being 0.15. All values were below cutoff. Hence, the combination of two reference genes is enough to be used for normalization of qRT-PCR expression levels

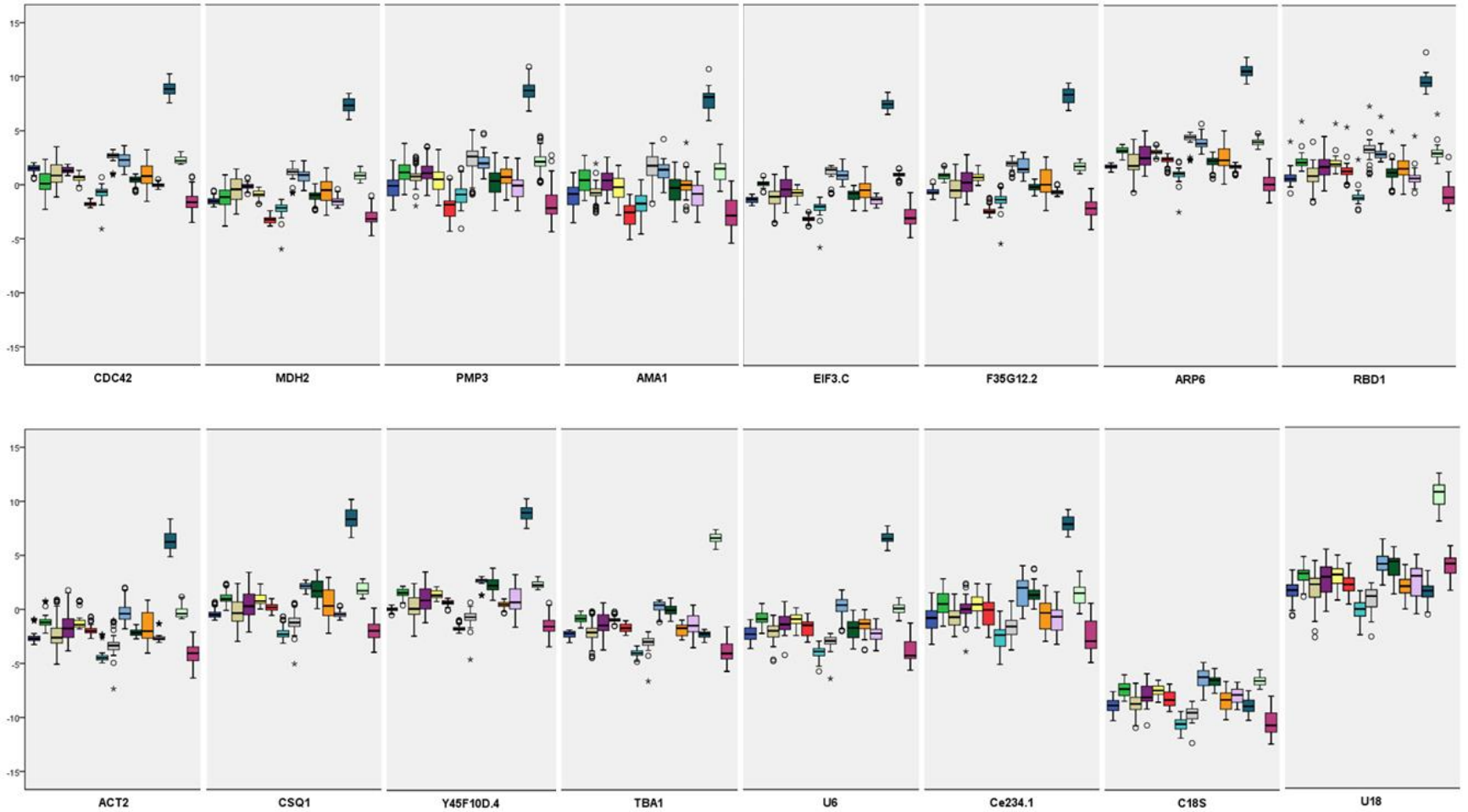

Figure 4.3: A box-plot graph representing the values of pairwise comparisons of the 16 genes based on dCt method. Expression levels were calculated from each "pair of genes" in each group. 50% of the values are included in the box. The median is represented by the line in the box. The interquartile range is bordered by the upper and lower edges, which indicate the 75th and 25th percentiles, respectively. The whiskers are inclusive of the maximal and minimal values, but exclusive of the outliers, represented as circles and asterisks. Different "gene pairs" are shown as different colors. The y-axis represents the ΔCt values between each gene pair/group, while the x-axis shows the 16 reference candidates.